THE JOURNAL
OF
CHEMICAL PHYSICS

VOLUME 13, NUMBER 6 JUNE, 1945

Distribution of Chain Lengths and Compositions in Copolymers*

W. H. STOCKMAYER
Research Laboratory of Physical Chemistry, Massachusetts Institute of Technology, Cambridge, Massachusetts

(Received March 6, 1945)

The instantaneous distribution of chain compositions and chain lengths in vinyl copolymers is obtained in a simple form valid for long chains. The compositions of chains of a given length are normally distributed about the mean value, with a standard deviation which can be calculated from experimentally observable quantities. The distribution of chain lengths intimately resembles that for simple polymers.

I. INTRODUCTION

RECENTLY several authors[1–3] have independently derived a simple differential equation[4] relating the over-all composition of a long-chain vinyl copolymer to that of its parent monomer solution, and this relation has been found to agree well with experimental data.[2] The distribution of sequences of like monomer units along the chains was also readily obtained.[1,3]

Since the molecular weight of a copolymer is finite, the compositions, as well as the lengths, of the individual molecules cannot all be identical; even in the copolymer formed during a very small time interval, there exists a distribution of chain lengths and compositions. Although one could reasonably expect the fluctuations of composition to be quite small for long molecules, it seems worth while to obtain a quantitative estimate of their magnitude. A general theory of copolymerization which embraces this problem has been formulated by Simha and Branson,[5] but the equations given by them are unfortunately too complex for convenient use.[6] With the aid of further approximations (but no new assumptions) valid for long chains, the distribution of chain compositions and lengths can be expressed in a simple and tractable form. In this paper, the simplified result is derived, discussed, and illustrated.

II. MEAN COMPOSITION AND CHAIN LENGTH

In describing the mechanistic assumptions and the symbolism to be employed, some repetition of the discussion in previous papers[1–5] inevitably occurs. We consider a binary system with monomer concentrations A and B. The growing free-radical[7] chains present during polymeriza-

* Contribution No. 513 from the Research Laboratory of Physical Chemistry, Massachusetts Institute of Technology.

[1] T. Alfrey and G. Goldfinger, J. Chem. Phys. 12, 205 and 322 (1944).

[2] F. R. Mayo and F. M. Lewis, J. Am. Chem. Soc. 66, 1594 (1944).

[3] F. T. Wall, J. Am. Chem. Soc. 66, 2050 (1944).

[4] See Eq. (5).

[5] R. Simha and H. Branson, J. Chem. Phys. 12, 253 (1944).

[6] Some of the equations and all of the numerical examples in the paper of Simha and Branson pertain to a special case which rarely, if ever, is found experimentally.

[7] The expression "free radical" is used advisedly, in conformity with present ideas regarding the most common polymerization mechanism. Actually the equations to be derived are valid for any mechanism in which the concen-

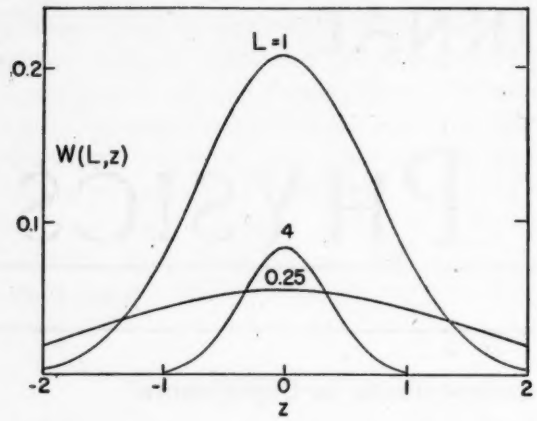

FIG. 1. Reduced composition distribution according to Eq. (17). Weight fractions are plotted against the reduced composition-deviation at relative lengths of 0.25, 1, and 4.

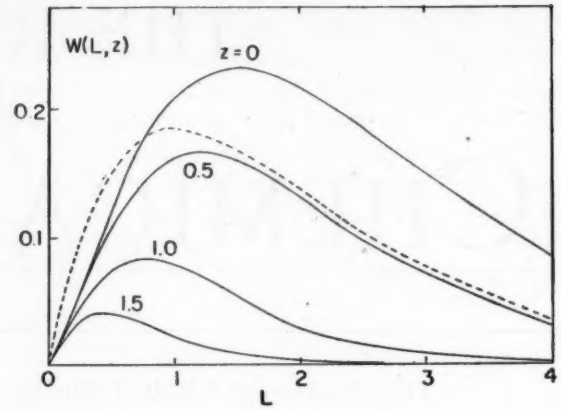

FIG. 2. Reduced chain-length distribution according to Eq. (17). Weight fractions are plotted against relative length at reduced composition-deviations of 0, 0.5, 1, and 1.5. The dashed curve is the distribution summed over all compositions, divided by two to facilitate comparison.

tion are called either A-radicals or B-radicals, according to the identity of the monomer unit at the active end. The total concentrations of A- and B-radicals of all lengths and compositions will be written m and n, respectively, while the symbols m_{rs} and n_{rs} denote the concentrations of such radicals composed specifically of r A-units and s B-units. If, as is usually assumed, the reactivity of a radical depends only on the nature of its active end (and not on its length or composition), just four different propagation (growth) reactions must be considered,[8] as set forth in the following scheme:

$$\begin{aligned} m_{rs}+A &\rightarrow m_{r+1,\,s} \quad (k_{aa}m_{rs}A), \\ m_{rs}+B &\rightarrow n_{r,\,s+1} \quad (k_{ab}m_{rs}B), \\ n_{rs}+A &\rightarrow m_{r+1,\,s} \quad (k_{ba}n_{rs}A), \\ n_{rs}+B &\rightarrow n_{r,\,s+1} \quad (k_{bb}n_{rs}B). \end{aligned} \tag{1}$$

The expressions in parentheses following each equation denote the reaction rates. The bimolecular character of these propagation steps may be regarded as experimentally confirmed,[2] and no other specific kinetic assumptions are required.

The rates of formation of the two kinds of radicals by other than propagation steps will be denoted simply by i_aA and i_bB. These rates thus include not only true initiation processes, but also the possible formation of A- and B-radicals by addition of monomers to other types of radicals produced in chain transfer. Obviously, i_a and i_b are therefore usually not constants, but are functions of monomer, solvent, and catalyst concentrations.[9] Similarly, the rates at which the

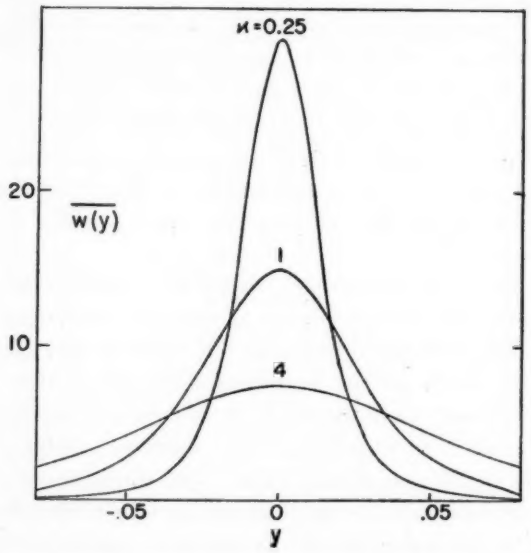

FIG. 3. Over-all distribution of compositions, according to Eq. (14), for copolymers with $\lambda/2p_0q_0=400$, showing the effect of the parameter κ.

tration of active growing chains (whether free radicals, ions, or excited molecules) is limited by some termination reaction to such small values that the steady-state assumption is valid.

[8] See the aforementioned articles, references 1–5, or earlier papers by R. G. W. Norrish and E. F. Brookman, Proc. Roy. Soc. (London) **A171**, 147 (1939) and E. Jenckel, Zeits. f. physik. Chemie **A190**, 24 (1941).

[9] For example, for the simple case of a peroxide-activated polymerization in which chain transfer is negligible, one might expect the following expressions to hold: $i_aA=k_{1a}CA$, $i_bB=k_{1b}CB$, $\tau_am=k_{3m}m^2+k_{3x}mn$, $\tau_bn=k_{3x}mn+k_{3n}n^2$, in which C is the peroxide concentration and the various k's are rate constants.

two kinds of radicals are converted into stable polymer (including chain-transfer processes) will be written $\tau_a m$ and $\tau_b n$, where the quantities τ_a and τ_b are certainly not constants.[9]

With these definitions, the total radical concentrations are governed by the equations

$$\begin{aligned} dm/dt &= i_a A - k_{ab} m B + k_{ba} n A - \tau_a m, \\ dn/dt &= i_b B - k_{ba} n A + k_{ab} m B - \tau_b n. \end{aligned} \tag{2}$$

In practical cases, the chains are so long that propagation must be much more rapid than initiation or termination. With the neglect of these latter, the assumption of a steady state[10] ($dm/dt = dn/dt = 0$) then gives the important approximate equality

$$k_{ab} m B = k_{ba} n A, \tag{3}$$

which, together with the rates of monomer consumption,

$$\begin{aligned} -dA/dt &= k_{aa} m A + k_{ba} n A, \\ -dB/dt &= k_{bb} n B + k_{ab} n B, \end{aligned} \tag{4}$$

leads to the previously mentioned expression[1-3] for the over-all composition of the copolymer which is forming at any chosen time:

$$dA/dB = A(\alpha A + B)/B(A + \beta B) = p_0/q_0, \tag{5}$$

where

$$\alpha = k_{aa}/k_{ab}, \quad \beta = k_{bb}/k_{ba}.$$

For later use, we have here introduced the symbol $p_0 = 1 - q_0$ for the over-all mole fraction of A in the copolymer chains produced during the (infinitesimal) time interval when the monomer concentrations are A and B. The convenience of dealing with symmetrical equations leads us to retain a separate symbol q_0 for the over-all mole fraction of B. The "monomer reactivity ratios"[2] α and β, which with the aid of Eq. (5) may be obtained from experimental studies of copolymer compositions, also play a role in determining the distribution of chain compositions.

The number-average length (polymerization degree) λ of the growing radical chains is simply the total rate of monomer consumption, $-d(A+B)/dt$, divided by the rate either of radical production or of radical termination;[11] thus,

$$\lambda = \frac{-d(A+B)dt}{\tau_a m + \tau_b n} = \frac{\alpha A^2 + 2AB + \beta B^2}{(\tau_a A/k_{ab}) + (\tau_b B/k_{ba})}, \tag{6}$$

with the aid of Eqs. (3) and (4). If all the chains terminate by disproportionation of radicals, the number-average length of the stable polymer chains is also λ; if all the chains combine in pairs when mutually terminating, it is 2λ. In view of the unspecified concentration-dependence of the termination parameters τ_a and τ_b, Eq. (6) is of no direct use as it stands. We shall employ it only to express the chain-length distribution conveniently in terms of the mean chain length.

III. DISTRIBUTION OF COMPOSITIONS AND LENGTHS

When the steady-state condition is applied separately to radicals of each length and composition, the following recursion formulae result:

$$\begin{aligned} \frac{dm_{rs}}{dt} &= k_{aa} A m_{r-1,\,s} + k_{ba} A n_{r-1,\,s} - (k_{aa} A + k_{ab} B + \tau_a) m_{rs} = 0, \\ \frac{dn_{rs}}{dt} &= k_{bb} B n_{r,\,s-1} + k_{ab} B m_{r,\,s-1} - (k_{bb} B + k_{ba} A + \tau_b) n_{rs} = 0. \end{aligned} \tag{7}$$

The species m_{10} and n_{01}, of course, follow different equations, involving $i_a A$ and $i_b B$, respectively. The solution of Eqs. (7) is[5]

$$\begin{aligned} m_{rs} &= \omega_a{}^r \omega_b{}^s \left[\frac{i_a}{k_{aa}} \sum_{j \geq 1} \binom{r-1}{j} \binom{s-1}{j-1} x^j + \frac{i_b}{k_{ab}} \sum_{j \geq 1} \binom{r-1}{j-1} \binom{s-1}{j-1} x^j \right], \\ n_{rs} &= \omega_a{}^r \omega_b{}^s \left[\frac{i_a}{k_{ba}} \sum_{j \geq 1} \binom{r-1}{j-1} \binom{s-1}{j-1} x^j + \frac{i_b}{k_{bb}} \sum_{j \geq 1} \binom{r-1}{j-1} \binom{s-1}{j} x^j \right], \end{aligned} \tag{8}$$

[10] For a brief discussion of the conditions of validity of this assumption, see W. H. Stockmayer, J. Chem. Phys. 12, 143 (1944).

[11] On the steady-state assumption, radicals are made and destroyed at equal rates, so that $i_a A + i_b B = \tau_a m + \tau_b n$.

where

$$\omega_a = k_{aa}A/(k_{aa}A + k_{ab}B + \tau_a), \quad \omega_b = k_{bb}B/(k_{bb}B + k_{ba}A + \tau_b), \quad x = k_{ab}k_{ba}/k_{aa}k_{bb} = 1/\alpha\beta.$$

For the pure radical species m_{r0} and n_{0s} the equations are simpler, but they need not be considered here.

A physical interpretation of Eqs. (8) is not difficult.[5] Each expression falls into two sums, the first describing chains which began with an A-unit and the second those which began with a B-unit. A single term within a sum denotes radicals in which j cross-additions of one kind (A to B in the first equation and B to A in the second) have occurred, and the combinatory factor gives the number of ways (sequences of addition) in which such radicals can be built up. The fractions ω_a and ω_b are propagation probabilities for homogeneous addition (A to A and B to B), while x is a measure of the relative probability of cross-addition.

The procedure followed in simplifying Eqs. (8) is described in some detail in the Appendix. In brief, the sums over j are approximated by integrals and evaluated with the aid of Stirling's formula. The logarithm of m_{rs} can then be expanded as a power series in the composition-deviation y, defined by

$$y = p - p_0 = q_0 - q, \tag{9}$$

where $p = 1 - q = r/(r+s)$ is the composition of an individual chain and $p_0 = 1 - q_0$ is the over-all composition. This procedure leads naturally to a Gaussian distribution[12] of chain compositions about the mean value. To this approximation, the distributions for A- and B-radicals are identical.

The final result is most compactly expressed as a continuous weight distribution, in which equal weights are assigned to the two types of monomer unit. The weight fraction of radicals with lengths (polymerization degrees) between l and $l+dl$ and composition-deviations between y and $y+dy$ is then given by

$$w(l, y)dldy = [\exp(-l/\lambda)ldl/\lambda^2][(l/2\pi p_0 q_0 \kappa)^{\frac{1}{2}} \exp(-ly^2/2p_0q_0\kappa)dy], \tag{10}$$

where

$$\kappa = [1 - 4p_0q_0(1-\alpha\beta)]^{\frac{1}{2}} = \frac{\alpha A^2 + 2\alpha\beta AB + \beta B^2}{\alpha A^2 + 2AB + \beta B^2},$$

and λ is the number-average length of the radicals given in Eq. (6).

If the termination step is entirely one of disproportionation, Eq. (10) also describes the distribution of the stable polymer forming at any instant, for then the concentration N_{rs} of stable chains of the indicated length and composition is determined by the equation

$$dN_{rs}/dt = \tau_a m_{rs} + \tau_b n_{rs}. \tag{11}$$

More generally, if a fraction ρ of the radical chains were terminated by combination, the stable polymer distribution would be

$$w(l, y)dldy = [\exp(-l/\lambda)(1 - \rho + \rho l/2\lambda)ldl/\lambda^2] \times [(l/2\pi p_0 q_0 \kappa)^{\frac{1}{2}} \exp(-ly^2/2p_0q_0\kappa)dy], \tag{12}$$

in which λ still denotes the number-average length of the *radicals*. This result is in complete analogy with the size distribution for pure polymers.[13] The radical distribution, of course, is unaffected by the nature of the termination process, being always given by Eq. (10).

It should be emphasized that the distribution equations are as generally applicable as the experimentally confirmed Eq. (5), for no additional assumptions are required for their derivation. Only

---

[12] For copolymers with a very small percentage of one component ($p_0 \ll q_0$), an equivalent Poisson distribution could be obtained if desired.

[13] E. F. G. Herington and A. Robertson, Trans. Faraday Soc. **38**, 490 (1942).

the uncertainty with respect to the termination process mars their quantitative utility, and this can be seen to affect only the distribution of lengths. It may be concluded that Eqs. (10) and (12) are no less valid than the theoretical distributions heretofore derived for pure polymers. In the paragraphs to follow, we shall for simplicity use Eq. (10) as it stands.

To find the chain-length distribution irrespective of composition, Eq. (10) must be integrated over y. The limits of integration may be taken as infinite because the distribution of compositions is narrow, and in fact the equation is already normalized to these limits. The result is therefore simply

$$\langle w(l)\rangle dl = \exp(-l/\lambda) l dl/\lambda^2, \tag{13}$$

which is exactly the equation for pure polymers terminating entirely by disproportionation.[13]

The over-all distribution of compositions irrespective of chain length is found in similar fashion by integrating over l, the result being

$$\langle w(y)\rangle dy = \frac{3dz}{4(1+z^2)^{5/2}}, \tag{14}$$

with

$$z^2 = \lambda y^2/2p_0q_0\kappa.$$

It is interesting to express the parameter κ, which controls the spread of chain compositions, in somewhat different terms. For sufficiently long chains, the number-average lengths of sequences of like monomer units are given[1,3] by

$$\bar{l}_A = 1+(\alpha A/B), \quad \bar{l}_B = 1+(\beta B/A). \tag{15}$$

Employing these relations together with Eq. (5), one obtains

$$\kappa = p_0(\bar{l}_B - 1)+q_0(\bar{l}_A - 1), \tag{16}$$

identifying κ as a certain kind of average sequence length. Thus longer sequences correspond to a broader distribution of compositions, as would be expected.

For the special case $\alpha\beta = 1$, which corresponds to an earlier theory of Wall,[14] and which also was given great prominence in the work of Simha and Branson,[5] Eq. (10) shows that $\kappa = 1$. In fact, for this case the distribution of compositions could have been written down directly, for if $\alpha\beta = 1$ the probability of chain growth depends solely on the nature and concentration of the monomers, and not at all on the type of active end possessed by the growing chain.

The distribution may be more compactly expressed in terms of the relative length, $L = l/\lambda$, and the reduced composition-deviation, $z = (\lambda/2p_0q_0\kappa)^{\frac{1}{2}}y$, which has already been introduced in Eq. (14). With these substitutions, Eq. (10) becomes

$$w(l, y)dldy = W(L, z)dLdz = \pi^{-\frac{1}{2}}L^{\frac{1}{2}}\exp[-L(1+z^2)]dLdz. \tag{17}$$

The shape of the $W(L, z)$ surface thus defined can be visualized from Figs. 1 and 2, in which $W(L, z)$ is plotted against z for several values of L, and against L for several values of z. It is seen that greater deviations of composition occur in the shorter chains, and conversely that chains with the average composition are the longest.

The magnitude of the effect produced by a change in κ may be judged from Fig. 3, in which the over-all distribution of chain compositions, given by Eq. (14), is plotted for several systems with an arbitrarily chosen value of $\lambda/2p_0q_0 = 400$. The abscissa scale is seen to be proportional to the quantity $(2p_0q_0\kappa/\lambda)^{\frac{1}{2}}$, which is a convenient measure of the breadth of the distribution, for integration of Eq. (14) shows that 88.4 percent by weight of the copolymer falls in the range $|y| < (2p_0q_0\kappa/\lambda)^{\frac{1}{2}}$.

It must be emphasized that the practical utility of Eq. (10) and its corollaries is severely limited, in that only the distribution for the copolymer forming at any instant is described. Since the

[14] F. T. Wall, J. Am. Chem. Soc. **63**, 1862 (1941).

parameters p_0, q_0, κ, and λ will in general change as the reaction proceeds,[15] these equations may safely be used only for copolymers of very low conversion. For higher conversions, the instantaneous spread of compositions will often be quite insignificant in comparison with the steady change of the mean composition, governed by Eq. (5), as the reaction progresses. In principle, the complete distribution for a high-conversion copolymer could be found by integration from Eqs. (5) and (10) and a detailed knowledge of the dependence of λ on concentration and conversion. In the absence of the latter information, such an effort would at present necessarily be speculative and scarcely worthwhile.

It should be possible to subject the distribution formulae to experimental test, preferably by fractionating "azeotropic" copolymers of low conversion, These should have rather low average molecular weights, in order to secure a sufficiently broad distribution of compositions.

Because of their simplicity of form and interpretation, these distribution equations should be of at least qualitative assistance to a better understanding of the relationship between structure and properties of copolymers.

APPENDIX

Since the symmetry of Eqs. (8) is obvious, it will be sufficient to consider the expression for m_{rs}' which can be rewritten in the form

$$m_{rs}=(\omega_a{}^p\omega_b{}^q)^l[(i_a/k_{aa})(S_0/q-S_1/pq)+(i_b/k_{ab})(S_1/pq)], \tag{A1}$$

where

$$l=r+s, \quad p=r/l, \quad q=s/l=1-p;$$

and

$$S_n=\sum_j (j/l)^n T_j,$$

with

$$T_j=(j/l)x^j\binom{lp}{j}\binom{lq}{j}.$$

For reasons of symmetry, it is convenient to retain both p and q as symbols.

For large l, Stirling's formula may be used to evaluate the combinatory factors. Putting $j=lw$, we have

$$T_j=wx^{lw}\binom{lp}{lw}\binom{lq}{lw}, \tag{A2}$$

and hence

$$\ln T_j \doteqdot -\ln(2\pi l)-\tfrac{1}{2}\ln[(p-w)(q-w)/pq] + l[w\ln x-2w\ln w-(p-w)\ln(p-w)-(q-w)\ln(q-w)]. \tag{A3}$$

By differentiating this expression, we obtain

$$\partial \ln T_j/\partial w=\tfrac{1}{2}\left(\frac{1}{p-w}+\frac{1}{q-w}\right)+l\ln\left[\frac{x(p-w)(q-w)}{w^2}\right], \tag{A4}$$

from which it is seen that T_j passes through a maximum at a certain value of w. For large l, only the last term in Eq. (A4) need be retained. Setting $w_{\max}=u$, we therefore have

$$u^2=x(p-u)(q-u), \tag{A5}$$

or

$$u=\{1-[1-4pq(1-1/x)]^{\frac{1}{2}}\}/2(1-1/x), \tag{A6}$$

where the negative root is necessary because $u(=w_{\max}=j_{\max}/l)$ may not exceed unity.

---

[15] In the special case of an "azeotropic" copolymerization, reference 3, p_0 and κ remain constant, but λ may still change.

We may pause to recall that j is the number of cross-additions of one kind (actually, A to B) in the chain. Hence $u(=j_{\max}/l)$ is the most probable fraction of such bonds in a chain of length l and composition p. For chains with the mean composition p_0, the use of Eq. (5) of the text, together with the relation $x=1/\alpha\beta$, gives, from Eq. (A6), the result

$$u_0=AB/(\alpha A^2+2AB+\beta B^2), \tag{A7}$$

which is readily shown[3] to be the fraction of $A-$ to $-B$ additions taken over all the chains.

The value of a general term T_j may now be found in relation to the maximum term T_m by setting $w=u+v$ and expanding in powers of v. With the aid of Eq. (A5) to effect cancellation, we find

$$(1/l)\ln(T_j/T_m)=-\mu^2v^2+O(v^3, 1/l), \tag{A8}$$

with $\mu^2=(1/u)+(1-2u)/2(p-u)(q-u)$.

The Euler-Maclaurin sum formula shows that, for large l, the sums defining S_0 and S_1 may be replaced by integrals with little error. Furthermore, the limits of integration may be extended to infinity, because the maximum in T_j is sharp; in fact, as is usual in such problems, the use of infinite limits is consistent with the previous approximations. We therefore may write

$$S_0=\sum_j T_j \cong \int T_j dj = lT_m\int_{-\infty}^{+\infty}\exp(-l\mu^2v^2)dv=(\pi l)^{\frac{1}{2}}T_m/\mu. \tag{A9}$$

Since the maximum term in S_1 occurs at practically the identical value of j, we also have

$$S_1=\sum_j wT_j \cong lT_m\int_{-\infty}^{+\infty}(u+v)\exp(-l\mu^2v^2)dv=uS_0. \tag{A10}$$

At this stage, Eq. (A1) can be rewritten to read

$$m_{rs}=(\omega_a{}^p\omega_b{}^q)^l S_0\left[(i_a/k_{aa})\left(\frac{p-u}{pq}\right)+(i_b/k_{ab})(u/pq)\right], \tag{A11}$$

but the dependence of S_0 on l and p, q must be more explicitly stated. By substitution for T_m and μ in Eq. (A9), with the aid of Eqs. (A3), (A5), and (A8), there is obtained

$$\ln S_0=-\tfrac{1}{2}\ln(2\pi l)+\tfrac{1}{2}\ln\frac{pq}{(p-u)(q-u)}-\tfrac{1}{2}\ln\left[\frac{2}{u}+\frac{1-2u}{(p-u)(q-u)}\right]$$
$$+l\left[p\ln\left(\frac{p}{p-u}\right)+q\ln\left(\frac{q}{q-u}\right)\right], \tag{A12}$$

for chains of length l and composition p, q.

We next proceed to expand $\ln S_0$ about its value for chains having a composition p_0, q_0 which equals the over-all composition as given by Eq. (5) of the text. The deviation from this mean composition will be defined as

$$y=p-p_0=q_0-q. \tag{A13}$$

Before attacking Eq. (A12), we require an expansion for u. Eq. (6) leads to

$$u-u_0=y(q_0-p_0)/\kappa+y^2[(q_0-p_0)^2(1-1/x)-\kappa^2]/\kappa^3+O(y^3), \tag{A14}$$

where the important new quantity κ, which persists in the final equations, is defined by

$$\kappa=[1-4p_0q_0(1-1/x)]^{\frac{1}{2}}$$
$$=(\alpha A^2+2\alpha\beta AB+\beta B^2)/(\alpha A^2+2AB+\beta B^2). \tag{A15}$$

Now, upon entering Eq. (A12) with Eqs. (A13) and (A14), there is obtained, after a lengthy but straightforward expansion and collection of terms, the result

$$S_0=\left(\frac{p_0q_0}{2\pi l\kappa}\right)^{\frac{1}{2}}\left(\frac{p_0}{p_0-u_0}\right)^{pl}\left(\frac{q_0}{q_0-u_0}\right)^{ql}\exp\left(-ly^2/2p_0q_0\kappa\right), \tag{A16}$$

in which terms of $O(y^3)$ in $\ln S_0$ have been neglected.

Before inserting this expression into Eq. (A11), we note the equalities

$$\begin{aligned} p_0/(p_0-u_0)&=(\alpha A+B)/\alpha A=(k_{aa}A+k_{ab}B)/k_{aa}A,\\ q_0/(q_0-u_0)&=(\beta B+A)/\beta B=(k_{bb}B+k_{ba}A)/k_{bb}B, \end{aligned} \tag{A17}$$

which may be obtained from Eqs. (5) and (A7). Also, the dependence on composition is so overwhelmingly dictated by the last factor in Eq. (A16) that everywhere else the arbitrary composition p, q may be replaced by the mean composition p_0, q_0 without appreciable error. It can be shown that this maneuver amounts to neglecting a skewness in the distribution which becomes negligible for long chains. With the aid of the definitions of ω_a and ω_b given in Eq. (8) of the text, Eq. (A11) then yields

$$m_{rs}=\frac{A(i_aA+i_bB)}{k_{ab}(\alpha A^2+2AB+\beta B^2)}\xi^l(2\pi p_0q_0\kappa l)^{-\frac{1}{2}}\exp\left(-ly^2/2p_0q_0\kappa\right) \tag{A18}$$

where

$$\xi=\left(\frac{k_{aa}A+k_{ab}B}{k_{aa}A+k_{ab}B+\tau_a}\right)^{p_0}\left(\frac{k_{bb}B+k_{ba}A}{k_{bb}B+k_{ba}A+\tau_b}\right)^{q_0}.$$

The significance of the two factors in ξ as propagation probabilities, for $A-$ and $B-$ radicals respectively, is clear.

To obtain the total concentration of radical chains, summation over all compositions and lengths is required, but the approximations previously introduced are obviously consistent with integration over ly, followed by summation over l. Eq. (A18) is therefore more conveniently used in the form

$$m_l(y)dy=\frac{A(i_aA+i_bB)}{k_{ab}(\alpha A^2+2AB+\beta B^2)}\xi^l\left(\frac{l}{2\pi p_0q_0\kappa}\right)^{\frac{1}{2}}\exp\left(-ly^2/2p_0q_0\kappa\right)dy, \tag{A19}$$

where $m_l(y)dy$ is the concentration of A-radicals with length l and compositions lying between (p_0+y) and (p_0+y+dy). From the symmetry of Eqs. (8), a similar equation obviously applied to the B-radicals, $n_l(y)dy$ being given by Eq. (A19) with the factor A/k_{ab} replaced by B/k_{ba}. Thus the steady-state condition of Eq. (3) is seen to hold not only for the total radical concentrations, but also separately for radicals of each length and composition.

The concentration of radicals of length l but of all compositions is found by integration of Eq. (A19) to be

$$m_l=\int_{-\infty}^{+\infty}m_l(y)dy=A(i_aA+i_bB)\xi^l/k_{ab}(\alpha A^2+2AB+\beta B^2). \tag{A20}$$

Summation over l then gives the total concentration of A-radicals, yielding

$$m=\sum_{l\geq 1}m_l=\left[A(i_aA+i_bB)/k_{ab}(\alpha A^2+2AB+\beta B^2)\right]\left[\xi/(1-\xi)\right]. \tag{A21}$$

For long chains, ξ must be nearly unity, and a sufficient approximation may be found by expanding:

$$\begin{aligned}\xi&=[1+\tau_a/(k_{aa}A+k_{ab}B)]^{-p_0}[1+\tau_b/(k_{bb}B+k_{ba}A)]^{-q_0}\\&=1-[p_0\tau_a/(k_{aa}A+k_{ab}B)]-[q_0\tau_b/(k_{bb}B+k_{ba}A)]+\cdots\\&=1-[(\tau_aA/k_{ab})+(\tau_bB/k_{ba})]/(\alpha A^2+2AB+\beta B^2)+\cdots.\end{aligned}\tag{A22}$$

Using this relation in Eq. (A21), we obtain

$$m=(A/k_{ab})((i_aA+i_bB)/[(\tau_aA/k_{ab})+(\tau_bB/k_{ba})]),\tag{A23}$$

and similarly

$$n=(B/k_{ba})((i_aA+i_bB)/[(\tau_aA/k_{ab})+(\tau_bB/k_{ba})]).\tag{A24}$$

These results are seen to be consistent with the steady-state requirement that

$$i_aA+i_bB=\tau_am+\tau_bn.\tag{A25}$$

The number-average length of the radicals is at once found to be

$$\begin{aligned}\lambda&=\sum lm_l/\sum m_l=\sum ln_l/\sum n_l=1/(1-\xi)\\&=(\alpha A^2+2AB+\beta B^2)/[(\tau_aA/k_{ab})+(\tau_bB/k_{ba})],\end{aligned}\tag{A26}$$

as previously found more directly in Eq. (6) of the text.

We finally convert Eq. (A19) into a weight distribution. If equal weights are assigned to A- and B-monomers, the weight fraction $w_l(y)dy$ of chains of length l and compositions between (p_0+y) and (p_0+y+dy) is given by

$$\begin{aligned}w_l(y)dy&=lm_l(y)dy/\sum lm_l\\&=l(1-\xi)^2\xi^{l-1}(l/2\pi p_0q_0\kappa)^{\frac{1}{2}}\exp(-ly^2/2p_0q_0\kappa)dy.\end{aligned}\tag{A27}$$

Since long chains have been assumed, the distribution of chain lengths can also be conveniently made continuous. With the substitution $\lambda=(1-\xi)^{-1}$ from Eq. (A26), the result is

$$w(l,y)dldy=[\exp(-l/\lambda)ldl/\lambda^2][(l/2\pi p_0q_0\kappa)^{\frac{1}{2}}\exp(-ly^2/2p_0q_0\kappa)dy],\tag{A28}$$

which is Eq. (10) of the text.

Target Chemistry of Zirconium and Yttrium; Isolation of Zr^{89} in Pure State

M. H. KURBATOV AND J. D. KURBATOV
The Ohio State University, Columbus, Ohio

(Received January 16, 1945)

Radioactive Zr^{89} obtained by bombardment of Y_2O_3 with deuterons, was separated without addition of stable zirconium in quantities $\sim 10^{-10}$ gram. Oxychloride solutions of Zr^{89} mixed with inactive Zr were used for coagulation studies in the concentration range 1.5×10^{-4}—1.5×10^{-11} gA/l. It was found that the fraction coagulated increased with dilution under the constant conditions used (pH-4.0; NaCl$-2.5\times10^{-2}N$; $T-25°$), to 2.7×10^{-6} gA/l. The log-log plot of zirconium concentration (C) in solution against coagulated part (c) closely approaches a straight line with exponent $n=1.50$ and $k=490$. At 1.5×10^{-6} gA/l and lower concentrations the coagulated fraction reaches a maximum and becomes constant, $k=C/c=.45$. Within the range studied salt increases coagulation of zirconium above 10^{-5} gA/l; but below 10^{-6} gA/l the salt effect is reversed. Increase in pH results in increase in the fraction coagulated (r) in all concentrations studied. At a minute concentration $r=(p\text{H}-K)/m$, K being 1.85 with NaCl, 0.05N and 1.58 with NaCl, 0.005N and m being 3.15. The separation of Zr^{89} in minute quantities without addition of stable zirconium is plausible if a Nernst distribution of zirconium between coagulated part and solution is postulated. The concept of the solubility of the hydrous oxide of zirconium as a constant quantity remaining in solution under specified conditions was not verified.

I. INTRODUCTION

ISOLATION of artificial radioactive isotopes without dilution by inactive isotopes of the same charge number is pertinent to the solution of some problems in nuclear physics. Isotopes of a different charge number ($Z\pm1$, 2) than those bombarded (Z) are produced by several nuclear reactions. However, the yields are minute quantities so their separation involves unconventional procedure and the little known behavior of elements in extreme dilution.

For instance, it has been shown in the past[1–6] that some natural radioactive isotopes which form slightly soluble hydrous oxides can be agglomerated at very low concentrations even when the amounts in solution are much below their solubilities. These agglomerates were termed radio-colloids while the phenomenon was treated mainly as adsorption in order to avoid conflict with the solubility product principle.[7]

In the field of artificial radioactivity the formation of radio-colloids has been used in the separation of yttrium isotopes ($Y^{87,88}$) obtained by the reactions, $Sr^{86,88,87}(d, n \text{ and } d, 2n)Y^{87,88}$, without addition of inactive yttrium as carrier.[8] It was found that partial agglomeration of yttrium takes place in solutions of minute* concentrations and its extent depends primarily upon two factors, the pH of the solution and the salt concentration. These two factors act in opposite directions and affect the splitting of yttrium between the solution and the radio-colloid.

The experiments showed furthermore, that with very dilute solutions the fraction coagulated at a given pH and salt concentration, increases with dilution to some limit. This, of course, is contrary to the behavior of yttrium in conventional concentrations.

The present work on the tetravalent element zirconium was undertaken as an extension of the previous studies of yttrium to confirm the basic

[1] Blau and Rona, Akad. Wiss. Wien **139**, 275 (1930).
[2] Chamie, J. Phys. Rad. **10**, 44 (1929).
[3] Chamie and Guillot, Comptes rendus **190**, 1187 (1930).
[4] Hahn, *Applied Radiochemistry* (Cornell University Press, Ithaca, New York, 1936).
[5] Hahn and Werner, Naturwiss. **17**, 961 (1929).
[6] Werner, Zeits. f. physik. Chemie **A156**, 89 (1931).
[7] In the literature there is considerable controversy on radio-colloid formation. One school of thought admits only an adsorption grouping while another supports independent coagulation. An example which has had contradictory explanations is the formation of radio-colloids of thorium B, an isotope of lead, agglomeration of which has been observed in concentrations as low as 10^{-11} gA/liter while the solubility under the conditions of the experiment was 5×10^{-5} gA/liter. Paneth, Mitt. Rad. Inst. Wien **34**, 47, 55 (1913); Zeits. f. Electrochemie **31**, 5 (1925).
[8] J. D. Kurbatov and M. H. Kurbatov, J. Phys. Chem. **46**, 441 (1942).
* Minute quantities are accepted arbitrarily as those less than 10^{-9} gram.

observation of increased coagulation with dilution, within certain limits. The radioactive isotopes of zirconium were selected mainly because of the convenient half-lives and strong radiation intensities of Zr^{89} and Zr^{93}.

Of these, Zr^{93} has characteristics which make it advantageous for studies of dilute solutions (10^{-6} to 10^{-3} gram atom per liter) and Zr^{89} for concentrations below 10^{-6} gram atom per liter.

The interrelation of the isotopes of yttrium, zirconium and columbium is shown in Fig. 1.

The half-lives (T) and upper limits of radiation energies in Mev are given according to latest data.[9,10] The radioactive isotopes used in the present work are shown in heavy lines.

II. TARGET CHEMISTRY OF ZIRCONIUM

By activation of metallic zirconium with deuterons in the Ohio State University cyclotron, the radioactive isotope Zr^{93} of $T-65.5$ days was secured for studies of dilute solutions.

In spite of the convenient half-life and strong radiation intensity Zr^{93} has the disadvantage of chain disintegration into Cb^{93}, $T-38.7$ days, the latter an isomer of stable Cb. Therefore, a separation of Cb from Zr is required just prior

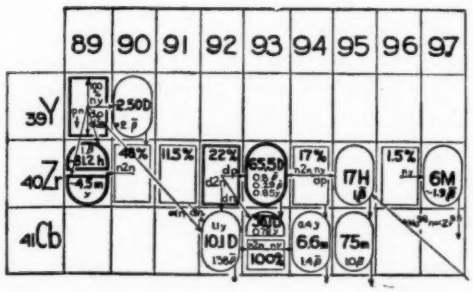

FIG. 1. Region of yttrium, zirconium, and columbium isotopes. Stable isotopes are shown in rectangles and radioactive in ovals.

to each series of experiments with dilute solutions of zirconium.

The target chemistry of the metallic zirconium (*ca.* 0.1 g) bombarded with deuterons consisted in dissolving the metal, separating the isotopes of columbium (d, n and d, $2n$ reactions) and yttrium (d, α reaction) and removing from the zirconium the usual active impurities Cu, Ni, Co, Na, etc.

After only the surface of the zirconium was dissolved in acids, stable yttrium was added and

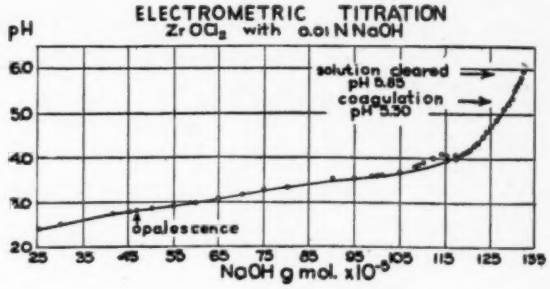

FIG. 2. Electrometric titration; final concentration of zirconium 4.4×10^{-3} gA/l.

later separated by the hydrofluoric acid procedure.

The columbium isotopes were first separated, without addition of stable columbium, by means of the potassium carbonate procedure. The minute quantities of potassium hexacolumbate so obtained were used later as tracer for repeated purification of zirconium from accumulated Cb^{93} since the minute Cb^{92} has a strong radiation intensity.

The final separation of yttrium from the experimental solution of zirconium was made by partial and repeated coagulation of zirconium at *p*H, 4.0.

The common impurities were removed by the ammoniacal procedure.[11]

By direct dilution of the active zirconium obtained, as little as 0.06 mg could be used per experiment since it had sufficient activity for accurate measurement. However, since Zr is secured already mixed with stable isotopes the ratio of active to stable cannot be increased. Therefore, the properties of very dilute solutions could be studied only after separation of Zr^{89} without carrier, from yttrium bombardment.

Since the target chemistry in this case is unconventional the properties of zirconium in dilute solution will be treated first, returning later to the isolation of Zr^{89}.

[9] M. L. Pool and J. E. Edwards, Bull. Am. Phys. Soc. **19**, 7 (1944).
[10] G. T. Seaborg, Rev. Mod. Phys. **16**, 13 (1944).
[11] Allen, Pool, Kurbatov, and Quill, Phys. Rev. **60**, 425 (1941).

III. EXPERIMENTAL PROCEDURE

When ten milliliters of a solution containing 6×10^{-4} g of zirconium as oxychloride is titrated with sodium hydroxide ($0.01N$) opalescence appears at a *p*H as low as 2.8. The solution becomes increasingly cloudy as the *p*H rises then clears at a much higher *p*H than that at which coagulation started (Fig. 2). A continuous coagulation process is evident during the titration.

On the basis of these data a *p*H range well below that of quantitative precipitation was selected for studies of the behavior of more dilute solutions.

The method used for coagulation and separation of precipitate and filtrate was as follows: Samples of 20 to 40 ml of known zirconium concentration in known acid concentration were titrated to a desired *p*H with standardized sodium hydroxide solutions of various strengths depending upon the final concentration of zirconium and salt desired in the particular experiment. These titrations were carried out at 25° using a Leeds and Northrup *p*H meter. Then the samples were allowed to stand for an agglomeration period before removal of the coagulated part.

Since the quality of water is of primary significance in securing reproduceable results the following standardized conditions were used throughout: Portions of the freshly redistilled water to be used for a series of experiments were electrometrically titrated with sodium hydroxide to *p*H 9 and back titrated with hydrochloric acid of known normality to *p*H 2 to be certain that no buffering compounds were present. The initial *p*H of the water was regularly found to be not less than 6.6.*

The requirement of maintaining *p*H without change during the agglomeration period was met by performing the experiments in a room free from other chemical work using a separate enclosed space having open vessels of soda-lime and provision for air exchange through filters with sodium hydroxide. A facilitating circumstance in avoiding carbon dioxide effect is the *p*H range of 3 to 4.5 when the admixture of sodium carbonate owing to the initial *p*H of the water constitutes less than 0.1 percent of the total salt (NaCl) concentration present in the experiment.

With the higher concentrations of zirconium, 10^{-5} gA/l and with the higher *p*H, 4.5, it was observed that on standing within the first half hour the *p*H drops to the extent of 0.1 to 0.2. On the contrary, no experimentally observable change in *p*H takes place during the agglomeration period with the very dilute solutions of zirconium. The observation of *p*H lowering on standing only with higher concentrations of zirconium was attributed to the fact that the agglomeration process requires some time. The duration of agglomeration was standardized at six hours, this period having been selected upon evaluation of the attainment of full agglomeration after titration of a sample to a definite *p*H. Separations were made after six hours and fourteen hours with 2.78×10^{-4} gAZr/l giving the following results:

*p*H	Percent coagulated 6 hr.	Percent coagulated 14 hr.
3.5	13.0	12.8
4.5	26.3	25.4

Since radioactivity measurements, owing to the geometry of samples relative to the G-M counter tube or ionization chamber, vary to the extent of ±3 percent of the activity measured the above figures indicate that extension of agglomeration time beyond six hours is not required if there is no removal of coagulated fraction and no distortion of other conditions. It was found that an hour and a half was insufficient since the results vary especially at high concentrations.

After the six-hour agglomeration period the solutions were filtered through Schleicher and Schull blue ribbon paper, and the deposits on

* Agglomeration of radio-colloids has been previously reported in the literature as attributable entirely to the purity of the water used and experiments were described using water prepared by centrifuging. In the present work, accordingly, centrifuged water was tested in control experiments with minute concentrations. However, no observable effect was found with the centrifuged water as compared to the redistilled water maintained free from carbon dioxide. (Table II.) In addition, the formation of radio-colloids was described previously without reference to control of the *p*H of the solutions or the salts present. Consequently the observations made were found to be inconclusive. O. Werner, Zeits. f. physik Chemie **A156**, 89 (1931).

the paper subsequently dissolved by washing first with $2N$ hydrochloric acid and then several times with $0.1N$ hydrochloric acid until the papers were inactive.

The method of removing the coagulated part by means of filter paper was chosen after a comparison of data obtained on agglomeration of yttrium,[8] cerium,[12] and zirconium.* Filter papers were washed before using with salt and hydrochloric acid solutions of pH corresponding to that of the experimental series of zirconium. No washing, in the analytical sense, can be done on the agglomerated fraction on the papers even with wash water of corresponding pH and salt concentration, therefore, the volume of solution left on the filter paper was reduced to an amount not exceeding 2 percent by use of 6-cm filter papers.

The effect of filter paper on agglomeration was evaluated by arranging consecutive filtrations, that is, the filtrate from one funnel immediately filling a second paper placed below the first funnel. It was found that in minute concentrations the amount of coagulation on the second paper does not exceed 5 percent of the agglomerated fraction on the first paper.

While the effect of the filter paper undoubtedly cannot be excluded as a part of the process of separation, the experimental data suggest that the agglomeration of radio-colloids begins with adjustment of pH and after a period of time the filtration facilitates the removal of coagulated particles by localizing their accumulation on the paper.

With concentrations of 10^{-5} gA/l of zirconium and less no coagulated fraction is visible. Consequently the experimental procedure cannot be followed by common analytical methods. The complete transfer of agglomerated phase to filter paper and complete solution from the filter paper into a vessel for measuring on the G-M counter was controlled by means of activity determinations. Secondary treatment was made of the beakers and filter papers with weighable quantities of zirconium. When zero activity was found on the beakers and papers the procedure with very dilute solutions was considered to have been adequately performed. Careful performance of a standardized technique which is entirely controlled by instruments is required instead of the visual judgment of the experimenter, when working with concentrations below 10^{-5} gAZr/l.

The activities of the solutions so obtained and the original filtrates were determined either (a) directly by means of a Geiger-Mueller counter with immersion tube for liquids or (b) by means of a Wolf unifilar electrometer. In the latter case the solutions were evaporated to dryness in Petri dishes of 4-cm diameter and the activities measured with an ionization chamber filled with freon at 20-lb. pressure.

Both methods have certain disadvantages. Zirconium can be kept in solution only in strong acid and the very thin glass of the G-M counter immersion tube cannot be used long. The electrometer measurements require preparation of solid samples of uniform geometry and there is a loss in total activity owing to the depth of the measured material.

In all cases where the ratio of beta- and gamma-radiation intensities was required to establish the purity of an isotope the electrometer was used.

IV. SOME PROPERTIES OF ZIRCONIUM IN DILUTE SOLUTION AT pH 4.0 AND 4.5

After purification, the oxychloride solutions of bombarded zirconium were diluted as previously mentioned so that 20 ml of solution had an activity of approximately 400 counts per minute, measured on the G-M counter.*

The concentration of such a solution was found by usual analysis of undiluted zirconium to be 1.23×10^{-5} gA/l. The more concentrated solutions were obtained then by adding the desired amount of stable zirconium; the actual quantities

[12] J. D. Kurbatov and M. L. Pool, Phys. Rev. **65**, 61 (1944).

* It was found that agglomeration and settling of radio-colloids takes place even in concentrations below 10^{-6} gA/l without filtration. Samples were titrated to the desired pH values and allowed to stand for eight days in stoppered graduated cylinders. A top portion (about 25 percent) of the liquid was slowly pipetted, and the quantity of material found in the upper liquid phase was always lower than that of the original. However, the concentration of the liquid separated by pipette, without filtration, varied considerably (±16 percent). Similar observations were made by centrifuging samples after elapse of an agglomeration period.

* The activity of these solutions, expressed in counts, was correlated with electrometer measurements expressed in units of a constant source of activity.

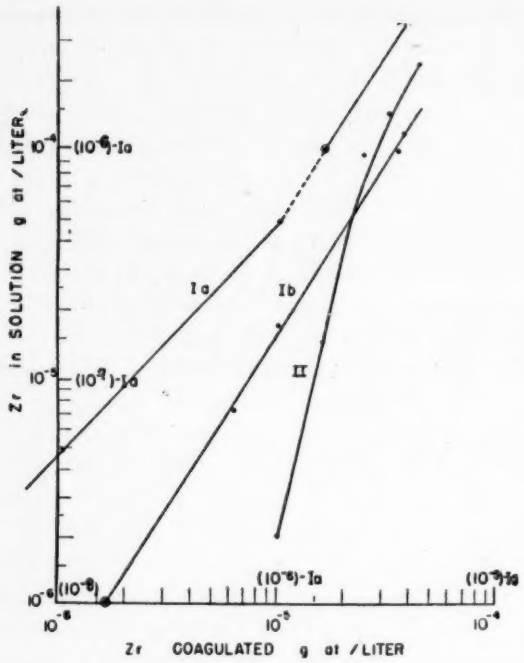

FIG. 3. Coagulation of zirconium at pH, 4.0.

Curve No.	NaCl conc. N	Final conc. Zr gA/l	Zr Coagulated gA/l
Ia	.025	10^{-8} to 10^{-6}	10^{-7} to 10^{-6}
Ib	.025	10^{-6} to 10^{-4}	10^{-6} to 10^{-5}
II	.005	10^{-6} to 10^{-4}	10^{-5}

(Curve Ib is a continuation of Curve Ia).

of zirconium used in this series of experiments being from 4.1×10^{-5} to 1.0×10^{-3} g.

Agglomeration was obtained in the two pH regions, 4.0 and 4.5 while the sodium chloride concentration was maintained approximately $0.005N$.

The deviations in measurements of the activities of filtrates and solutions of coagulated part did not exceed ±2 percent of the total counts taken for experiment.

In Table I the results are given for the coagulate. The log-log plot of coagulated Zr and final concentration (Fig. 3, Curve II) approaches a straight line only below 1.2×10^{-4} gAZr/l. If the distribution of zirconium between solution and coagulate in this region is expressed as

$$C/c^n=K,$$

where c is the amount coagulated per liter of solution and C is the final concentration, the value of n is 4.1 at 25° with sodium chloride concentration $\sim0.005N$ and pH 4.0.

At higher concentrations than 1.2×10^{-4} gA/l at pH 4.0 and 4.5 the log-log plot of coagulate against final concentration does not hold as a straight line. However, the log-log plot of coagulate against initial concentration (shown in Fig. 4) gives a straight line with exponent $n=0.48$ (pH=4.0) and 0.58 (pH=4.5) and proportionately constant, $k=2.2\times10^{-3}$ and 8.0×10^{-3} respectively.

Thus the interpretation of zirconium coagulation as a distribution phenomenon with the above dilutions and under the condition that the duration of the experiments be maintained constant is limited to the lower concentrations. The time allowed for coagulation was found to be significant so, to make results comparable, these and following separations of the coagulated fraction were performed six hours after titration.

From the tabulated data it is evident that (a) the coagulated fraction increases with dilution in this zirconium concentration range, at a given salt, pH, and temperature and (b) that the fraction of zirconium removed depends on pH at this temperature and salt concentration.

These results were used as a basis for the separation of pure Zr^{89} from bombarded yttrium.

V. TARGET CHEMISTRY OF YTTRIUM AND SEPARATION OF Zr^{89} WITHOUT CARRIER

Yttrium oxide, Hilger's spectroscopically pure, was bombarded with deuterons for four and a half hours in the Ohio State University cyclotron. The main nuclear reactions are: $Y^{89}(d, p)Y^{90}$, $Y^{89}(d, 2n)Zr^{89}$, and $Y^{89}(d, \alpha)Sr^{87}$ and owing to the

Table I. Coagulation of zirconium from dilute solutions at 25°. (Final volume approximately 40 ml per experiment.)

Initial conc. Zr gA/l $\times10^4$	pH	NaCl normality $\times10^3$	Zr coagulated gA/l $\times10^4$	Zr coagulated Percent
		pH 4		
.124	3.90	4.9	.103	83
.305	4.01	5.0	.162	53
.612	4.02	5.0	.220	36
1.20	3.97	5.1	.252	21
1.74	4.04	5.2	.331	19
2.78	3.88	5.4	.445	16
		pH.4.5		
.306	4.43	5.0	.211	69
.606	4.53	5.0	.285	47
1.18	4.44	5.1	.413	35
1.74	4.53	5.2	.574	33
2.76	4.34	5.5	.690	25

presence of fast neutrons $Y^{89}(n, 2n)Y^{88}$, and $Y^{89}(n, p)Sr^{89}$ may occur.

Since Zr^{89} disintegrates with emission of positrons and gamma-radiation and Y^{90} by emission of electrons and no gamma-rays, the extent of separation of zirconium from yttrium without the addition of stable yttrium can be observed from the beta-gamma ratio in Zr^{89} and the presence or absence of gamma-radiation in Y^{90}.*

In Fig. 5 is a condensed outline of the procedure used in the isolation of Zr^{89}. It may be noted that after solution and purification of yttrium by the ammonia procedure (not shown on chart) yttrium was again purified by solution in hydrochloric acid and precipitation with sodium hydroxide and finally electrometrically titrated to *p*H 4.0. Because of the high salt concentration and large quantity of yttrium, Zr^{89} was coagulated to the extent of 58.7 percent; 41.3 percent remaining in solution with the yttrium. All the yttrium, within the limits of the experimental procedure, was found to be left in solution.

On the right side of the chart are shown the results on the purification of zirconium. At the lower salt concentration 94.2 percent of zirconium was coagulated. The beta-gamma ratio remained constant and was not decreased by all subsequent coagulations. The purity of the zirconium was also confirmed by following its disintegration for several half-lives.

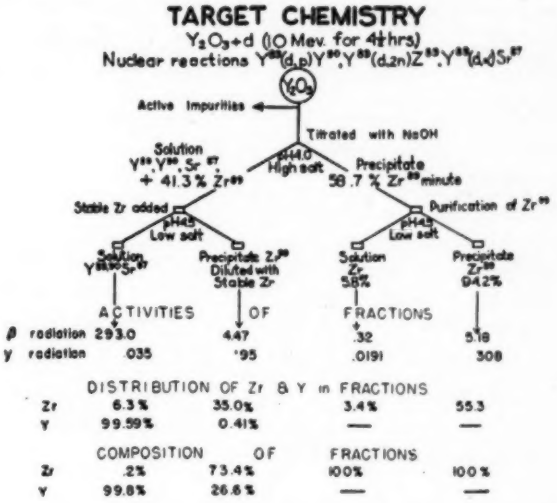

FIG. 5. Scheme of purification of bombarded yttrium and isolation of Zr^{89} in pure state.

During this work an evaluation of the half-life of Zr^{89} was made and found to be slightly longer than previously reported owing mainly to better removal of yttrium from the zirconium fraction. In addition, the nuclear reaction $Y^{89}(d, 2n)Zr^{89}$ was established.

On the left-hand side of the chart are the results on separation of yttrium and zirconium with zirconium carrier added in quantity equivalent to the yttrium. The yttrium left in solution in this case was uncontaminated by zirconium but the precipitate of zirconium (41.3 percent of total) contained 26.6 percent of yttrium.

At the bottom of the chart are shown relative beta- and gamma-intensities for each fraction and the percentages of zirconium and yttrium as deduced from these measurements.

The precision of common gravimetric separation of two substances is usually determined by a comparison of weights found and known weights originally mixed in the sample. In case some of each constituent appears mixed with the other there is no measure of the purity of the fractions. However, with the aid of tracer procedure it can be seen that by means of electro-

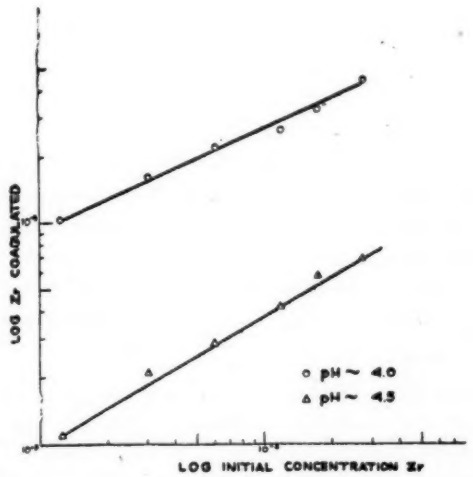

FIG. 4. Coagulation of zirconium in the region of concentrations from 2.8 to 0.12×10^{-4} gA/l with NaCl concentration 0.005*N*. (Plot against initial concentration of Zr.)

* Identical geometry of samples and thickness of precipitates were easily maintained due to the small quantities of material. Radiation contributed by x-rays was included in the ratio of beta- and gamma-intensities no separation of x-ray intensities being necessary for observation of purity of fractions.

TABLE II. Coagulation of zirconium from dilute and minute concentrations at 25° and pH = 4.

Zr conc. gA/l	pH	NaCl normality $\times 10^2$	Zr coagulated gA/l	Zr coagulated Percent
Minute	4.01	2.38	—	69*
1.54×10^{-7}	4.00	2.41	1.06×10^{-7}	69**
1.54×10^{-6}	4.00	2.46	1.06×10^{-6}	69
2.69×10^{-6}	4.00	2.54	1.67×10^{-6}	62
1.35×10^{-5}	4.00	2.53	6.35×10^{-6}	47
2.69×10^{-5}	4.00	2.51	1.02×10^{-5}	38
1.34×10^{-4}	4.01	2.54	3.62×10^{-5}	27
1.54×10^{-4}	4.00	2.40	3.85×10^{-5}	25

* Centrifuged water.
** Water not centrifuged: freshly redistilled.

metric titration pure zirconium can be secured even in minute concentration but part will remain in the yttrium fraction. An yttrium fraction free of zirconium can be obtained if part of the yttrium is left in the zirconium. This is caused by the overlapping of the pH ranges of coagulation of these two elements.

VI. PROPERTIES OF ZIRCONIUM IN CONCENTRATIONS BELOW 10^{-6} gA/l

Using the radioactive Zr^{89}, a series of solutions was prepared by adding stable zirconium in known quantities, and in order to link these experiments with those previously described the highest concentration prepared was 1.54×10^{-4} gA/l. The lowest concentration of Zr^{89} was approximately 10^{-11} gA/l. This did not contain common zirconium and is referred to later as minute.*

The same standardized procedure used on zirconium concentrations above 10^{-6} gA/l was followed with the lower concentrations. This included the precautions as to the purity of the water and reagents as described above; prevention of change in pH during the agglomeration by maintaining the samples in an enclosed space free from carbon dioxide, other gas impurities and laboratory dust and especially care with regard to the temperature of experiments and duration of agglomeration time. The variation in temperature allowed in a complete series of experiments did not exceed $\pm0.5°$ from the 25° selected.

* The total yield of purified Zr^{89} was estimated by comparison of activity with known natural sources to be of the order of magnitude of 10^{-10} g.

Coagulations were carried out at pH 4 with a salt concentration of $\sim0.025N$ giving the results shown in Table II. It can be seen that the fraction coagulated increases with dilution to a certain limit, in this case, 1.54×10^{-6} gA/l. Below this concentration the percent of zirconium coagulated remains constant.

The log-log plot of coagulated and final concentration of zirconium from 1.5×10^{-4} to 2.7×10^{-6} gA/l approaches a straight line (Fig. 3, Curve Ib). The constant, n, for this curve at pH 4 and $0.025N$ salt concentrations is 1.5.

These values can be compared with those given previously for pH 4: the fivefold increase in salt concentration resulting in less increase in coagulation with dilution.

Within a narrow range of concentrations 2.6 to 1.54×10^{-6} gA/l the slope, n, decreases to unity and becomes constant and k decreases to 0.45 (Curve Ia, Fig. 3).

It is well known that electrolytes aid in the coagulation of colloids and this is true in the case of zirconium in concentrations greater than 10^{-5} gA/l. In Table III are given the results on coagulation at three different pH values and two salt concentrations and it can be seen that the higher salt results in consistently higher fractions coagulated.

However, with minute concentrations the effect of salt is reversed. In Table IV it is shown that at a given pH a tenfold increase in salt results in a smaller fraction coagulated.

It should be expected therefore, that at some intermediate concentration of zirconium and at a certain pH a change in salt concentration would be without apparent effect. This is found in the zirconium concentration range of 7×10^{-5} and 10^{-6} gA/l at pH 4 when the salt concentrations are as shown:

Zr conc. gA/l	NaCl N	Percent coag.	NaCl N	Percent coag.
1.54×10^{-6}	.0246	69	.503	70
7.25×10^{-5}	.025	31	.005	31*

* Data read from crossing of curves Ib and II, Fig. 3.

The curves in Fig. 6 show that at the same minute concentration the fraction coagulated within the limits of the experiments is directly proportional to the pH, that is, $r=(p\mathrm{H}-K)/m$,

r being the coagulated fraction, m, the slope and k the intercept. The constants are $m=3.15$ for both curves and $k=1.85$ and 1.58 for 0.05 and $0.005N$ salt respectively.

The effect of pH on coagulation of zirconium throughout the range of concentrations studied, has been observed to be in the same direction in all cases, that is, increase in pH increase coagulation, salt being constant.

The basic observation on the coagulation of zirconium from very dilute solutions which is in line with the results previously observed with yttrium, is that this hydrous oxide does not exhibit a constant solubility value.

This has been confirmed by experiments extended for eight days. Two different concentrations of zirconium were coagulated at three different pH values. The results are shown in the left column of Table V. After eight days the pH was redetermined and a second coagulated part

TABLE III. Effect of salt concentration and pH on dilute solutions of zirconium. (Final volume ~45 ml/experiment.)

Zr conc. gA/l $\times 10^4$	NaCl conc. $N\times 10^3$	pH	Percent coag.	Zr conc. gA/l $\times 10^4$	NaCl $N\times 10^2$	pH	Percent coag.
2.86	5.3	3.43	13	2.55	1.91	3.47	17
2.78	5.4	3.92	16	2.50	1.88	4.00	28
2.76	5.5	4.47	25	2.44	1.82	4.43	98

TABLE IV. Effect of salt and pH on coagulation of minute concentrations of zirconium.

NaCl conc. $N\times 10^3$	pH	Percent coag.	NaCl conc. $N\times 10^2$	pH	Percent coag.
4.57	2.50	29	5.01	2.50	20
5.53	3.01	47	5.35	3.00	35
5.85	3.51	60	5.40	3.52	53
5.93	4.00	77	5.43	4.02	63
			5.43	4.25	76

TABLE V. Two successive coagulations of zirconium.

First coagulation separation after 6 hours				Second coagulation from filtrate. Separation after 8 days			
Conc. Zr gA/l $\times 10^4$	pH	Percent coag.	NaCl conc. $N\times 10^3$	Conc. Zr gA/l $\times 10^4$	pH	Percent coag.	NaCl conc. $N\times 10^2$
.622	3.48	24	4.9	1.29	3.25	11	1.18
.612	4.02	36	5.0	.950	3.62	37	1.06
.606	4.53	47	5.0	*.795*(1)	*3.97*	*73*	*1.07*
1.80	3.52	8	5.1	4.07	3.34	7	1.1
1.74	4.04	19	5.2	3.46	3.73	14	1.1
1.74	4.53	33	5.2	*2.86*(2)	*3.98*	*77*	*1.1*

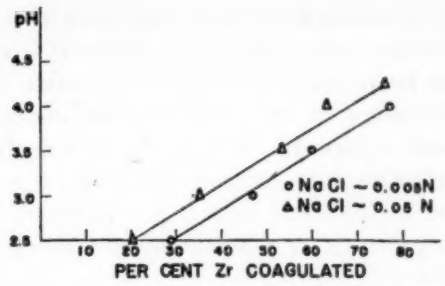

FIG. 6. Effect of salt and pH on a minute concentration of zirconium at 25°.

removed from which it can be seen that at essentially identical salt concentration and pH (pH -3.97:NaCl$-.011N$) a three and a half-fold increase in concentration of zirconium in solution has negligible effect on coagulation.*

The experiments described may be partially interpreted if the phenomenon of distribution of zirconium between solution and coagulate be accepted as a Nernst distribution. The law holds well for concentrations below 10^{-6} gA/l and up to 1×10^{-4} gA/l if the salt concentration is as high as $2.5\times 10^{-2}N$.

It has been pointed out that in heterogeneous systems the distribution law holds well only for dilute conditions. With the lowest concentrations of zirconium studied, it was found that the amount coagulated is directly proportional to the amount left in solution. In the light of classical concepts of distribution this would mean only one molecular species of zirconium in such dilute solutions under the conditions specified.

In the region of 10^{-6} to 10^{-4} gAZr/l in which the log-log plot of zirconium in solution against zirconium coagulated closely approaches a straight line the exponent n, is 1.5 with $0.025N$ salt and 4.1 with $0.005N$ salt. This may indicate that the zirconium left in solution exists in more than one form in this range or that the coagulated part is more associated.

The log-log plot of coagulated Zr against final concentration of Zr does not give a straight line for concentrations $>10^{-4}$ gA/l. This indicates a more rapid change in the composition of zir-

* If the solubility were constant and these solutions saturated the coagulated fraction, for example, from the solution numbered (2) should be 92 percent instead of 77 percent if the solution numbered (1) were considered saturated.

conium in solution or coagulate than that observed in the range immediately above 10^{-6} gA/l.

It has been established that coagulation of Zr will take place at any concentration under the conditions described. Accordingly, it was shown above that for consecutive coagulations a second addition of hydroxyl ions is not required. The process proceeds at somewhat lower *p*H values but extremely slowly.

The observation that the fraction coagulated increases with dilution to some limit is well supported by the effect of hydroxyl ions on hydrolysis.

Below 10^{-6} gA/l the coagulation of zirconium reaches a maximum and the fraction remains constant consequently the separation of Zr^{89} in pure state, in quantities of the order of 10^{-10} g, was possible.

ACKNOWLEDGMENT

It is a pleasure to express our gratitude to Dr. M. L. Pool for activation of research material in the Ohio State University cyclotron and our indebtedness to Dr. A. B. Garrett for his continuing support facilitating research work.

The grant of the Ohio State University Development Fund for research equipment is greatly appreciated by the authors.

THE JOURNAL OF CHEMICAL PHYSICS VOLUME 13, NUMBER 6 JUNE, 1945

The Elastic Scattering and Neutralization of Low Velocity Hydrogen Ions in Methane

J. H. SIMONS AND G. C. FRYBURG
School of Chemistry and Physics, The Pennsylvania State College, State College, Pennsylvania

(Received February 16, 1945)

The low velocity scattering of H^+, H_2^+, and H_3^+ in methane was measured at voltages between about 1 and 150. Neutralization is found in all three cases, being much greater for H_2^+ and H^+ than for H_3^+. The elastic scattering is also relatively high compared to hydrogen and helium. It was found that there was an effect of pressure at constant voltage on the experimental determination of effective cross section for elastic scattering. This has been explained on the basis of multiple scattering. Approximate potential laws for the interactions have been evaluated.

THE experience gained in previous experimental[1] work on the measurement of low velocity ion scattering and the techniques developed in this work enabled the measurements of the scattering of low velocity hydrogen ions in hydrocarbons to be approached with confidence. In particular, the techniques of the determination of neutralization[1(d)] and of the removal of carbonaceous films[1(e)] provided procedures which enabled such measurements to be made. Methane was the choice for the first hydrocarbon to be studied because of its simplicity and gaseous nature.

In the same apparatus and using the same experimental methods and analytical correlations as have been previously described,[1] the elastic scattering and neutralization in methane of all three hydrogen ions, H^+, H_2^+, and H_3^+, have been measured from approximately 1 to 150 volts. The formation of carbonaceous films from the methane required their frequent removal (between every several experiments) by the method of a discharge in oxygen. The results are given in Table I and shown graphically in Figs. 1–3.

In the text, R_T represents the ratio of the unscattered current to the total ion current entering the scattering chamber; and R_S represents the ratio of the unscattered current to the total current minus that deflected by neutraliza-

[1] (a) A. S. Russell, C. M. Fontana, and J. H. Simons, J. Chem. Phys. **9**, 381 (1941). (b) J. H. Simons, H. T. Francis, C. M. Fontana, and S. R. Jackson, Rev. Sci. Inst. **13**, 419 (1942). (c) J. H. Simons, C. M. Fontana, E. E. Muschlitz, Jr., and S. R. Jackson, J. Chem. Phys. **11**, 307 (1943). (d) J. H. Simons, C. M. Fontana, H. T. Francis, and L. G. Unger, J. Chem. Phys. **11**, 312 (1943). (e) J. H. Simons, H. T. Francis, E. E. Muschlitz, Jr., and G. C. Fryburg, J. Chem. Phys. **11**, 316 (1943). (f) J. H. Simons, E. E. Muschlitz, Jr., and L. G. Unger, J. Chem. Phys. **11**, 322 (1943).

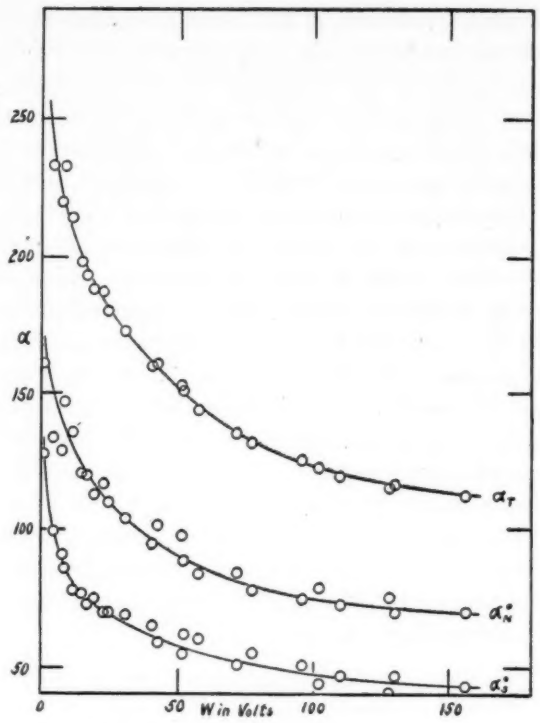

FIG. 1. Scattering of H^+ in methane.

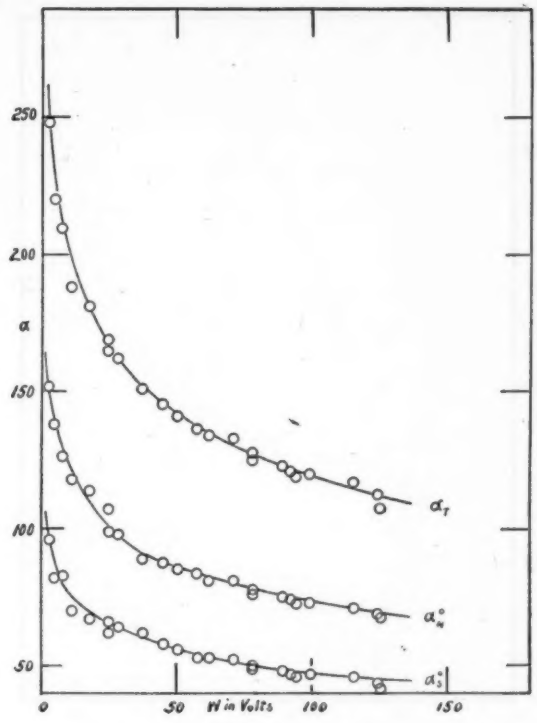

FIG. 2. Scattering of H_2^+ in methane.

TABLE I. Scattering of hydrogen ions in methane.

H^+			H_2^+			H_3^+		
Velocity in Volts	α_T	α_s^0	Velocity in Volts	α_T	α_s^0	Velocity in Volts	α_T	α_s^0
156.0	113.0	43	125.0	110.8	42	152.0	35.0	24
130.0	117.0	47	125.0	109.6	41	130.0	35.1	25
128.0	116.0	40.5	124.0	112.8	44	128.0	36.4	24.4
110.0	120.0	47	115.0	117.0	46	125.0	34.0	25
102.0	123.0	44	99.0	120.0	47	116.0	38.2	25.2
96.0	126.0	51	96.0	118.8	46	108.0	36.6	28
77.5	132.0	55	92.0	121.0	47	103.0	39.5	26.7
72.0	135.5	51	89.0	123.0	48	101.0	39.2	27.7
58.0	144.0	60	78.0	128.0	50	80.3	41.2	27
52.5	151.0	62	78.0	125.1	49	78.0	40.9	31.5
52.0	153.0	55	71.0	133.0	52	74.0	42.6	30.1
42.8	161.0	59	62.0	134.0	53	66.0	43.5	32.3
40.9	160.0	65	57.5	136.6	53	63.5	46.0	31
31.0	173.0	69	50.5	141.0	56	56.0	45.0	34.5
24.6	180.0	70	45.0	145.5	58	49.0	49.7	35.5
23.0	187.0	70	37.5	151.0	62	49.0	50.4	33.3
19.5	188.0	75	28.5	162.0	64	47.0	52.6	37
17.0	193.0	73	25.0	165.0	66	44.0	50.8	35
15.0	198.0	77	25.0	169.0	62	34.5	55.1	38
11.6	214.0	78	18.0	181.0	67	32.0	57.2	42
8.7	233.0	86	11.5	188.0	70	30.5	58.8	43
7.8	220.0	91	8.1	209.5	83	28.0	62.9	42
4.4	233.0	99	5.1	220.0	82	26.5	62.1	42.4
1.1	289.0	128	3.0	248.0	96	20.5	68.2	48
						13.6	88.3	61.5
						13.6	87.2	61.5
						12.0	90.9	62
						11.5	86.8	60
						11.5	95.3	65
						9.5	98.7	69
						8.5	108.3	78
						7.8	113.0	82
						3.9	157.0	112
						3.0	160.0	111
						1.5	185.0	148

Gas pressures of the order of magnitude of 1×10^{-3} mm were used for H^+ and H_2^+ and 2 to 3×10^{-3} for H_3^+. Empty tube pressure was 1×10^{-5} mm or less. Temperature was 25 to 30°C. $\alpha_N^0=\alpha_T-\alpha_s^0$.

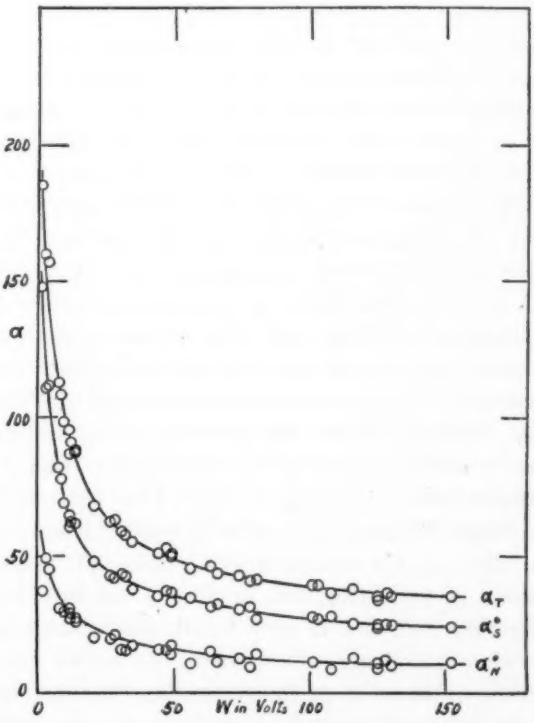

FIG. 3. Scattering of H_3^+ in methane.

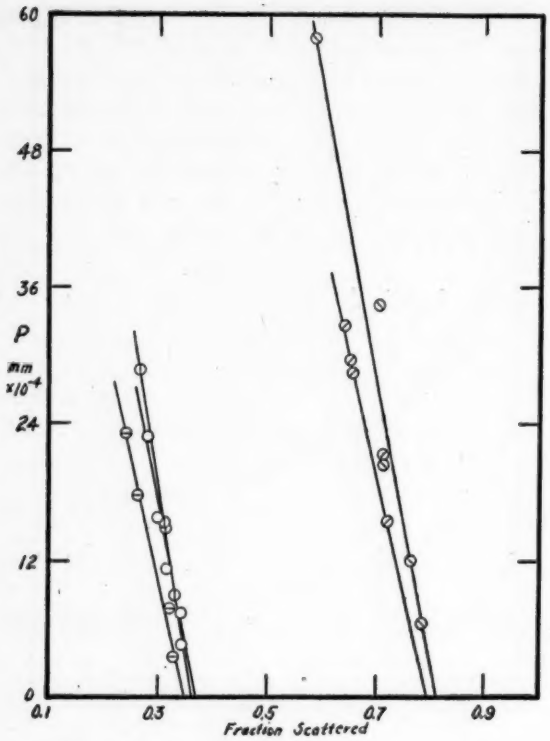

FIG. 4. Effect of pressure on elastic scattering.

For scattering in methane of 56 volt H^+(⊖), 56 volt H_3^+(○), 125 volt H_2^+(◫), 56 volt H_3^+(⊘), and 125 volt H_2^+(⊘).

tion. R_T^0 and R_S^0 are the same ratios taken at some very low pressure in the measuring tube to correct for tube alinement, etc. α_N, α_S, and α_T are the experimental effective cross sections for neutralization, elastic scattering, and total scattering, respectively, obtained without correction from the measured ratios. α_S^0 and α_N^0 are the corrected values of α_S and α_N. $\alpha_N^0=\alpha_T-\alpha_S^0$.

A further difficulty was encountered in these measurements. This had been theoretically anticipated previously but not experimentally experienced. There is a possibility of an ion that has been deflected from the primary beam by an elastic scattering collision to suffer a further collision before reaching the wall of the scattering chamber. If this second collision is an elastic one, the effect on the measurement will be nil, as the chance of deflecting this scattered ion into the collecting chamber is very small. The chance of the elastic collision changing its direction sufficiently to direct it to the scattering chamber lid is also extremely small, and these are the only two possibilities that would influence the measurement. However, if the second collision is an inelastic one (neutralization), then the ion already scattered will be collected on the scattering chamber lid and so instead of being counted as elastically scattered, it is counted as neutralized. The total scattering would be almost unaffected by this process but the relative amounts of elastic scattering and neutralization would be affected. This effect would be most marked for substances having relatively large values of neutralization, and it would also be a function of the pressure, increasing with increasing pressure. As the pressure increased, the experimentally determined elastic scattering would be too low and the neutralization too high. To obtain more accurate measurements of elastic scattering for any substance experiencing considerable neutralization, measurements at any one voltage could be made over a range of pressures and these extrapolated to zero pressure. As

$$\alpha_S=\frac{(R_S^0/R_S)-1}{(R_T^0/R_T)-1}\alpha_T,$$

TABLE II. Variation of elastic scattering with pressure.

Particle	$P\times10^4$ (mm)	Fract. Scatt.	α_T	α_s	α_s^0	α_N^0
125 volt	32.53	0.645	35.1	22.6	24	11.1
	29.53	0.655	33.8	22.1	23.5	10.3
H_3^+	28.43	0.658	33.0	21.7	23	10
	21.20	0.716	34.0	24.4	25	9
	15.38	0.722	33.0	23.8	24.5	8.5
	Extrap	0.795	33.9		27	6.9
56 volt	57.83	0.592	44.9	26.6	31	13.9
	34.33	0.710	44.1	31.3	33.7	10.4
H_3^+	20.29	0.717	43.9	31.5	33	10.9
	11.95	0.764	43.9	33.5	34.2	9.7
	6.47	0.785	43.2	33.9	34.2	9.0
	Extrap	0.790	44.0		34.7	9.3
125 volt	28.72	0.269	108.8	29.3	42.5	66.3
	15.38	0.312	109.6	34.2	42	67.6
H_2^+	14.83	0.314	110.8	34.7	42.6	68.2
	8.86	0.330	109.6	36.2	41	68.6
	Extrap	0.360	109.7		39.5	70.2
56 volt	22.89	0.282	150.0	42.3	63	87
	15.66	0.300	150.3	45.1	60	90
H_2^+	11.24	0.315	152.0	47.9	59	93
	7.4	0.342	153.0	52.3	60	93
	4.39	0.344	154.0	53.0	58	96
	Extrap	0.365	154.0		56	98
56 volt	23.13	0.241	157.0	37.8	59	98
	17.69	0.263	156.0	41.0	58	98
H^+	7.8	0.320	161.0	51.5	60	101
	3.64	0.328	160.0	52.5	57	103
	Extrap	0.360	160.0		57.7	102.3

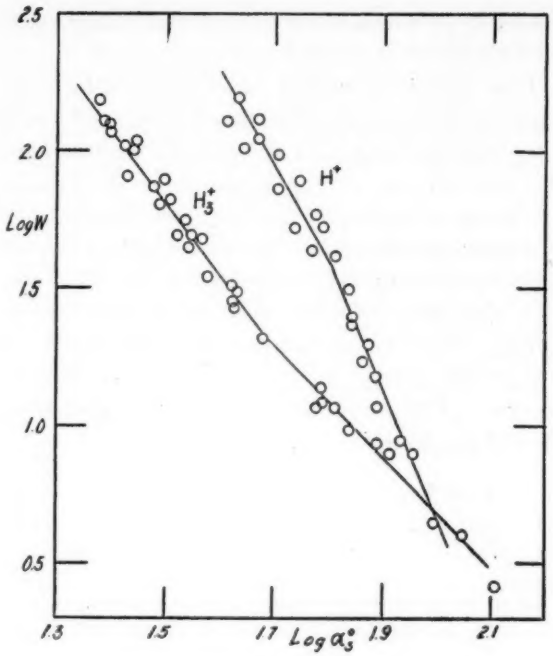

FIG. 5. H^+ and H_3^+ in methane.

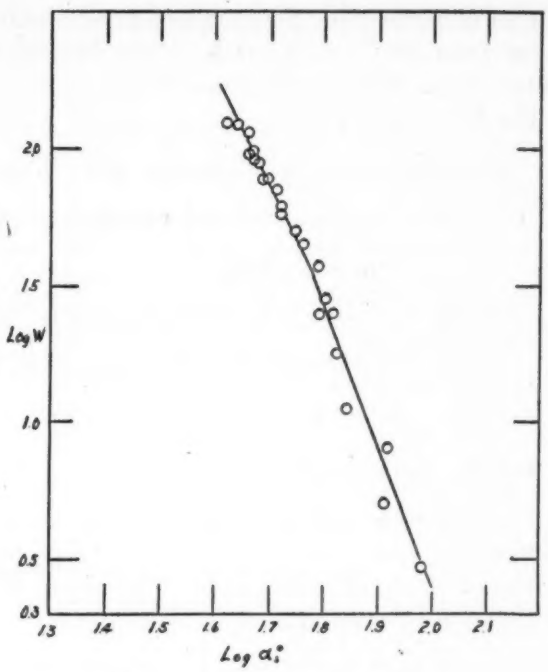

FIG. 6. H_2^+ scattered in methane.

and

$$\frac{(R_S^0/R_S)-1}{(R_T^0/R_T)-1}$$

is obviously the fraction of total scattering that is scattered elastically, a plot of this fraction against pressure at constant voltage should be extrapolatable to zero pressure and this extrapolated value used to obtain α_S^0 from α_T. Such a plot is shown in Fig. 4. In Table II the experimental values are given, and values of α_T and α_S, at constant voltage but at varying pressures are given. It is seen that α_T is practically independent of pressure. α_S decreases with pressure.

In collecting the experimental data for this study the large contribution of this pressure effect was not appreciated until much of the data had been collected and the pressure effect not experimentally determined at every voltage. In the following paper on the scattering of hydrogen ions in ethylene and propylene an effect of pressure on the total cross-sectional area is described. This was not experienced in this work, probably because of somewhat different experimental conditions and because the total amount of scattering was smaller. An analytical treatment is given in this following paper for the calculation of the cross section for elastic scattering corrected for the effect of pressure, α_S^0, which does not require measurements at a variety of pressures at the same velocity. We have used this method of calculating α_S^0. In Table II we compare these values with the value of α_S^0 obtained by extrapolating the experimental values to zero pressure. A satisfactory agreement is found.

The determination of a potential law from the elastic scattering curves for these experiments is less sure than for previous work for three reasons. Because of the greater total scattering power of methane, the pressure used in the scattering chamber is less and is thus determined with less precision. The electrical measurements are made with greater difficulty caused by the greater tendency to form carbonaceous films. The error arising from these two causes is of the order of 4 percent. In addition, the effect of pressure at constant voltage on the elastic scattering introduces some uncertainty.

In order to calculate potential laws for the elastic scattering, log α_S^0 is plotted against log W, where W is the velocity in volts. Figure 5 shows such plots for H^+ and H_3^+ and Fig. 6 for H_2^+. In these figures the straight lines are obtained by using values of the coordinates of the smooth

curves of α_S^0 in Figs. 1–3. The points are calculated from the experimental values. Potential laws calculated from these lines are as follows.

For H^+ in methane

$V=\frac{-7.0\times10^{-69}}{r^9}$ with K in volt cm^9 and r in cm between 5 and 40 volts (2.96A and 2.38A);

$V=\frac{-7.8\times10^{-54}}{r^7}$ with K in volt cm^7 and r in cm between 40 and 150 volts (2.38A and 1.97A).

For H_2^+ in methane

$V=\frac{-1.2\times10^{-76}}{r^{10}}$ with K in volt cm^{10} and r in cm between 5 and 40 volts (2.8A and 2.29A);

$V=\frac{-1.5\times10^{-61}}{r^8}$ with K in volt cm^8 and r in cm between 40 and 130 volts (2.29A and 1.97A).

For H_3^+ in methane

$*V=\frac{-2.8\times10^{-31}}{r^4}$ with K in volt cm^4 and r in cm between 5 and 22 volts (2.96A and 2.07A)

$V=\frac{-7.8\times10^{-39}}{r^5}$ with K in volt cm^5 and r in cm between 22 and 120 volts (2.07A and 1.5A).

The constants are not corrected for mass ratio as shown in previous work[1(f)] with the exception of the one which is starred.

This starred potential function may be compared to the potential function which would exist if a simple polarization force acted between the H_3^+ ion and the methane molecule. R. Sänger[2] has given a value for the dielectric constant of methane expressed as $(\epsilon-1)$, where ϵ is the dielectric constant, of 84.2×10^{-5} at 291.7A. From this, the polarizability may be calculated assuming only that methane obeys the ideal gas law at this temperature and at one atmosphere pressure. The potential function obtained from the polarizability is

$$V=\frac{-1.90\times10^{-31}}{r^4}$$ with K in volt cm^4 and r in cm.

This is in reasonable agreement with the experimental potential function given above expressing the interaction between H_3^+ and the methane molecule at large distances.

There are several interesting facts uncovered by these experiments: the exhibition of the neutralization phenomenon by H_3^+—this is the first case in which H_3^+ has undergone neutralization; and the large percentage of neutralization displayed by H^+ and H_2^+—about 70 percent of total scattering. This latter indicates a strong tendency on the part of methane readily to lose an electron forming the positively charged aggregate CH_4^+ in preference to attracting a positive ion to form the aggregates CH_5^+ and CH_6^+. The high values for the exponent in the potential laws are also of interest.

[2] R. Sänger, Physik. Zeits. **27**, 556 (1926).

The Elastic Scattering and Neutralization of Low Velocity Hydrogen Ions in Ethylene and Propylene

J. H. SIMONS AND L. G. UNGER
School of Chemistry and Physics, The Pennsylvania State College, State College, Pennsylvania

(Received February 16, 1945)

The low velocity scattering of H^+, H_2^+, and H_3^+ in both ethylene and propylene has been measured at ion velocities of less than 150 volts. Both elastic scattering and neutralization have been obtained over a velocity range. An effect of gas pressure at constant voltage on the total scattering was experienced. This is briefly discussed as is also the change of the relative amounts of elastic scattering and neutralization with pressure at constant voltage. The amount of neutralization compared to elastic scattering is large in all six cases. The elastic scattering in ethylene is somewhat similar to that in methane whereas that in propylene is somewhat greater.

IN a previous paper[1] experiments on the elastic scattering and neutralization of hydrogen ions in methane were reported. In exploring the possible use of this technique for organic chemical substances, the olefins ethylene and propylene were selected for the present study. The previously reported techniques were employed, and it was found possible to make satisfactory measurements.

EFFECT OF PRESSURE ON THE TOTAL CROSS-SECTIONAL AREA

Inability to check the total cross-sectional areas in experiments at different total gas pressures led to an investigation of the total cross-sectional area as a function of pressure. It was found that a plot of α_T (total cross-sectional area) against pressure at constant velocity gave approximately a straight line. At a lower velocity where α_T is larger, the variation of α_T with pressure is much greater. A quadratic relationship was found to hold between the slopes of the above-mentioned lines and the value of α_T extrapolated to zero pressure, α_T^0.

$$-d\alpha_T/dp = K(\alpha_T^0)^2. \quad (1)$$

Integrated between pressure limits, p and zero, this becomes

$$\alpha_T^0 = \alpha_T + K(\alpha_T^0)^2 p. \quad (2)$$

For convenience and without serious loss, $(\alpha_T^0)^2$ is replaced by α_T^2 to give

$$\alpha_T^0 = \alpha_T(1 + K\alpha_T p). \quad (3)$$

The value of K in Eq. (3) appeared to be approximately the same for the three different ions in both ethylene and propylene and also for some of the data previously reported on the scattering in water vapor,[2] when reexamined in the light of this effect. Perhaps, therefore, K is a property of the instrument and a function of the constants of the apparatus. The value of K thus found is 0.35.

In all previously reported work on low velocity ion scattering, except that of water, this correction is smaller than the experimental error. Its value depends upon the product $\alpha_T p$ and where this is small, the total cross section is independent of the pressure within the precision of the measurements. In the scattering in water vapor the value of $\alpha_T p$ is larger, but the total precision of the measurements is much less due to the difficulty of pressure measurements. This correction applied to the scattering in water vapor is probably not greater than the experimental error.

EFFECT OF PRESSURE ON THE FRACTIONAL AMOUNT OF THE TOTAL CROSS-SECTIONAL AREA TO BE CREDITED TO ELASTIC SCATTERING

A previous paper[1] described an effect of pressure at constant voltage on the effective cross-sectional area for elastic scattering. An ion in the beam in the scattering chamber is counted as not suffering a collision of any kind if it is caught in the collecting chamber. If it reaches the walls of the scattering chamber, it is initially recorded as

[1] J. H. Simons, and G. C. Fryburg, J. Chem. Phys. 11, 132 (1943).

[2] J. H. Simons, H. T. Francis, E. E. Muschlitz, Jr., and G. C. Fryburg, J. Chem. Phys. 11, 316 (1943).

suffering an elastic collision; and if its resultant of an electron exchange reaches the lid of this chamber under the influence of the retarding field, it is initially counted as having been neutralized. After the primary act of neutralization, a further electron exchange or elastic collision will not effect the determination. Also, after a primary act of elastic scattering, a further elastic scattering will effect the measurements only under the condition that this second collision diverts the ion either into the collecting chamber or to the lid. However, if after an initial elastic scattering, the ion suffers neutralization, the measurements will need correction as it will now be counted as neutralized rather than elastically scattered. For experiments where neutralization is relatively large this correction becomes appreciable.

If I_{Ns} is the amount of ion current which is scattered and subsequently neutralized, I_s is the total current scattered, I_s' is the uncorrected scattered current, x is the distance the scattered ion travels before neutralization, $\bar{d}$ is the average distance traveled by a scattered ion before reaching the scattering cylinder, and p is the pressure, then

$$dI_{Ns}=I_s\alpha_N{}^0 p dx, \tag{4}$$

$$I_s'=I_s-I_{Ns}, \tag{5}$$

by integration between 0 and $\bar{d}$.

$$\ln I_s/(I_s-I_{Ns})=p\alpha_N{}^0\bar{d}. \tag{6}$$

It can be seen that the ratio of the cross-sectional area for elastic to total scattering is now modified to

$$\alpha_s{}^0/\alpha_T{}^0=[(1/R_s-1)/(1/R_T-1)]I_s/I_s', \tag{7}$$

or

$$\log \alpha_s{}^0/\alpha_T{}^0=\log[(1/R_s-1)/(1/R_T-1)] + (\bar{d}/2.302)\alpha_N{}^0 p. \tag{8}$$

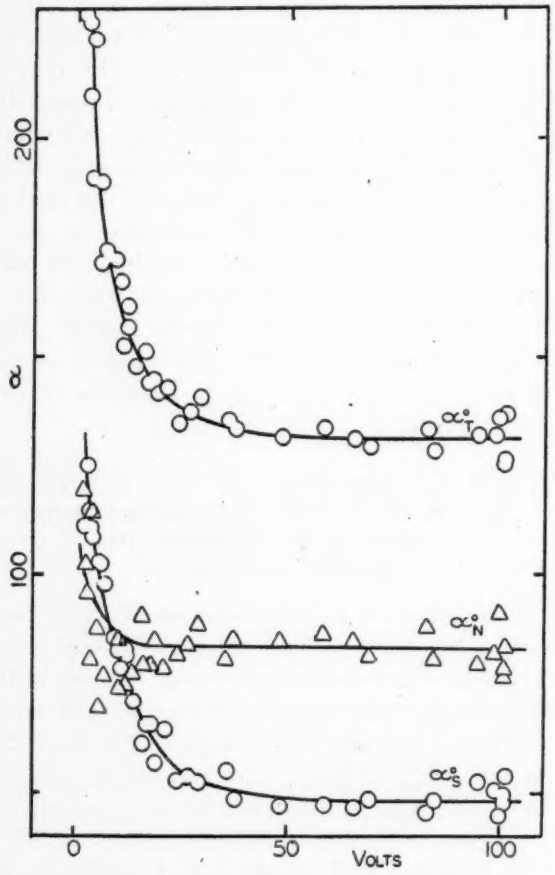

FIG. 1. Scattering of H^+ in ethylene.

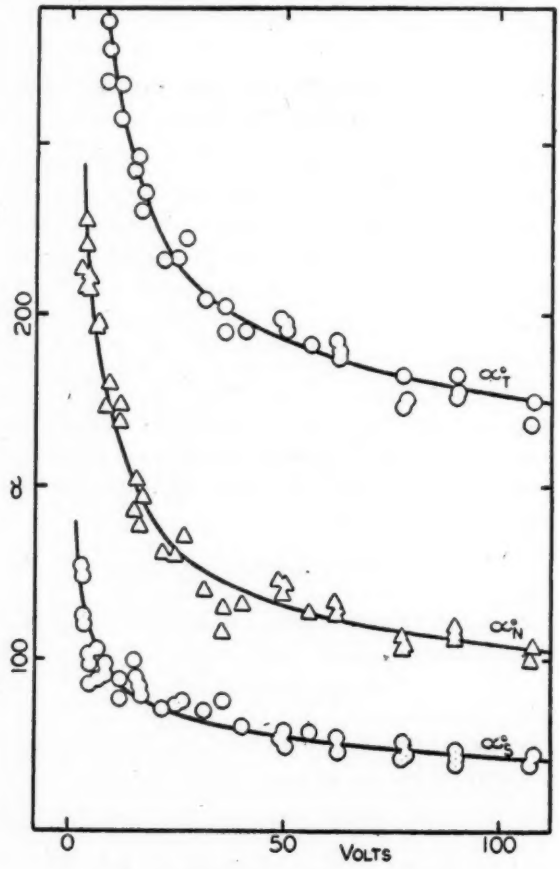

FIG. 2. Scattering of H_2^+ in ethylene.

TABLE I. Scattering of hydrogen ions in ethylene.

H^+					H_2^+					H_3^+				
Velocity in volts	α_T	α_T^0	α_s	α_s^0	Velocity in volts	α_T	α_T^0	α_s	α_s^0	Velocity in volts	α_T	α_T^0	α_s	α_s^0
100.5	129.1	137.3	42.7	53.9	116	160.9	168.1	56.2	66.1	138	62.5	63.5	40.2	41.6
100	122.3	125.8	42.8	47.6	108	164.0	175.3	56.2	72.1	116	58.2	59.1	36.1	37.4
100	120.4	126.4	41.5	49.7	107.5	154.0	168.6	48.9	69.4	108	66.7	68.5	40.4	42.3
99	125.2	136.1	31.3	45.0	90	174.1	182.7	61.4	73.3	107.5	68.3	69.5	42.4	44.0
98	126.1	132.3	42.4	50.8	90	171.5	176.7	62.2	69.5	107.5	65.6	68.3	36.7	41.2
94	125.0	132.2	42.5	52.5	90	166.9	177.3	57.3	71.8	94	64.3	66.9	37.0	40.7
84	122.7	128.6	40.4	48.2	78.5	160.0	175.8	50.2	72.4	93.5	65.2	66.4	39.7	41.5
82.5	125.3	133.6	35.1	45.7	77.5	170.3	182.5	58.5	75.7	93.5	62.8	66.8	34.0	39.9
69	123.4	129.4	40.2	48.4	77.5	162.7	173.5	60.5	71.0	93.5	63.2	65.0	38.1	40.5
65.5	123.0	131.2	35.7	46.5	62.5	181.5	187.4	64.9	73.0	82	67.6	70.4	36.9	40.6
58.5	125.8	133.8	37.5	47.3	62.5	177.7	189.5	60.5	77.0	78.5	73.7	76.0	41.8	45.0
48.5	122.9	131.5	36.6	46.9	62	182.8	192.7	63.5	77.0	78	67.3	68.5	42.0	43.8
38	124.4	133.3	36.1	48.5	56	178.5	191.7	64.0	78.7	78	75.7	77.2	45.9	48.2
36	128.8	135.2	46.1	55.0	50.4	190.0	195.7	66.0	74.3	63.5	73.1	75.4	42.3	45.7
29.5	129.7	140.6	37.8	52.4	50	187.8	197.7	65.4	79.0	63.5	74.7	76.3	43.2	45.3
27	129.6	137.2	43.2	53.5	49	190.9	199.0	65.5	76.7	63	71.8	77.1	36.9	44.7
24.5	126.3	134.4	41.7	52.8	40.5	186.3	195.6	67.0	80.2	63	73.8	76.3	40.8	45.7
21.5	134.0	142.7	51.8	64.3	36	184.0	202.4	61.8	88.0	46.5	79.7	82.8	44.4	48.9
19.5	130.4	141.5	41.5	56.8	36	186.5	195.0	75.5	87.7	46	79.4	81.3	44.1	46.8
18.7	132.8	144.5	48.5	65.4	31.5	192.3	204.3	68.0	84.8	45.1	75.0	79.5	40.7	47.3
17.6	135.0	144.0	52.5	65.6	27	215.3	222.4	77.0	87.2	41	88.7	90.8	51.6	54.5
16.3	141.2	151.3	47.1	61.1	25	206.7	216.2	73.4	86.4	37.7	92.7	94.8	52.3	55.5
14.2	137.2	147.8	55.0	70.5	22	205.0	216.0	69.8	85.4	26	93.2	99.2	53.2	61.5
12.7	147.0	161.3	60.2	81.4	17.2	228.3	235.8	79.2	89.4	22.5	101.3	104.5	59.2	63.0
12.6	146.4	156.9	66.9	82.5	16.6	216.0	230.1	72.5	92.0	22	103.1	108.2	52.5	61.4
11.3	143.9	152.3	66.3	78.6	15.8	234.7	246.0	78.8	94.2	21.5	98.4	106.2	51.8	63.1
10.8	156.1	167.3	62.4	82.3	15	226	242	76.7	99.4	17.8	111.4	119.6	59.5	71.4
9.8	159.2	172.4	65.5	85.2	11.9	248.8	267.3	69.8	93.9	17.6	107.2	112.9	59.3	68.9
7.2	159.8	174.3	76.2	97.8	11.8	244.8	257.1	72.5	88.2	17	108.0	111.6	65.4	70.4
6.25	160.8	171.6	86.6	102.3	9.0	260.5	277.7	75.5	98.1	13.9	140.6	145.3	90.4	96.4
6.0	176.1	190.3	81.8	102.9	8.7	251	268	72.5	95.1	13.7	138.8	145.7	89.0	98.0
4.5	209	223	81.2	108.5	8.7	276.5	286	86.2	98.4	12.7	128.2	139.0	76.1	91.0
4.3	178.0	191	91.4	110.7	6.85	282	291.5	82.2	93.8	12.2	126.1	134.0	82.0	92.4
3.7	195.0	210	84.1	114.5	6.7	278	298	77.5	102.6	12	129.0	134.1	94.5	100.4
3.1	204.0	227	90.0	125	4.95	292	309	77.0	98.4	11	127.3	136.2	84.5	95.7
2.4	211.5	229	85.0	111	4.65	288	299	78.4	92.4	9.5	191	204	127	143.7
					4.65	290	313	72.8	101.6	8.9	212	220	153	164.4
					3.75	305	330	78.3	110.0	8.9	178	185	127	135.9
					3.5	312	339	78.6	112.2	5.2	226	243	168	187.5
					3.3	317	331	105.5	124.0	3.5	231	250	172	193
					3.15	320	340	99.6	127	3.0	282	310	208	239

TABLE II. Scattering of hydrogen ions in propylene.

H^+					H_2^+					H_3^+				
Velocity in volts	α_T	α_T^0	α_s	α_s^0	Velocity in volts	α_T	α_T^0	α_s	α_s^0	Velocity in volts	α_T	α_T^0	α_s	α_s^0
118	202	210	50.2	59.5	114	212	229	64.4	87.0	116	103	107	51.0	56.7
61	201	213	54.1	68.7	60.5	224	234	76.3	90.4	60	126	132	53.8	62.2
61	194	202	55.2	64.7	60	219	233	75.7	91.3	60	108	116	49.6	60.6
60	204	212	53.5	63.5	59.5	233	254	68.1	94.8	31.5	135	146	56.5	73.6
32	214	227	60.0	76.8	31	245	257	79.2	95.9	30	145	152	68.2	77.5
31	213	223	64.5	74.2	30	251	269	76.7	100.6	29	149	152	75.9	80.4
30	222	232	58.4	70.0	21	265	279	87.7	106.3	21	168	177	77.0	89.7
21	230	240	61.5	74.0	20.5	271	294	73.5	101.9	16	186	194	81.3	93.2
21	222	232	64.0	77.0	15.5	286	304	73.9	97.7	10.3	208	221	86.2	108.5
15	233	244	66.4	80.8	15	300	313	90.8	107.2	9.8	222	234	86.6	102.8
10.7	262	282	65.5	90.0	14.9	281	297	78.2	98.3	9.3	248	257	94.0	106.4
10.3	272	282	73.6	86.3	10.2	304	317	84.0	100.4	6.6	258	272	101.4	121.2
7.1	310	323	76.3	91.9	9.7	313	335	75.2	102.6	4.5	308	327	116.3	144.3
3.7	461	490	57.8	80.0	6.3	337	366	77.7	105.4					
					4.0	374	394	75.5	105.8					

A corrected value of α_s can be obtained from Eq. (8) if $\log[(1/R_s-1)/(1/R_T-1)]$ is known at zero pressure. An extrapolated linear plot between these variables will give this for measurements at the same velocity but at different pressures. A value of $\bar{d}\alpha_N$ is obtained from the slope of this line. However, if $\bar{d}$ is known, α_s^0 may be obtained from a single measurement from Eq. (8) by means of successive approximations. From a large number of measurements an average value of $\bar{d}$ was found to be 2.0 cm. As this is about one-half the length of the scattering

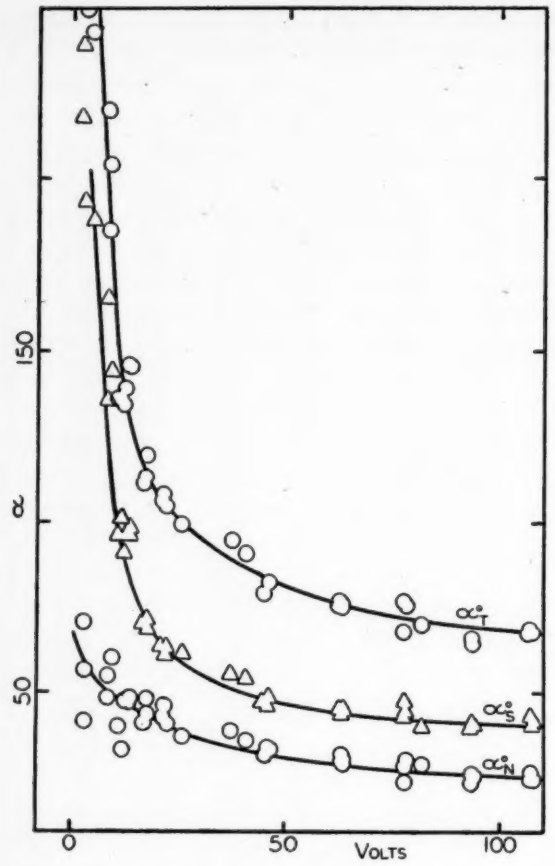

FIG. 3. Scattering of H_3^+ in ethylene.

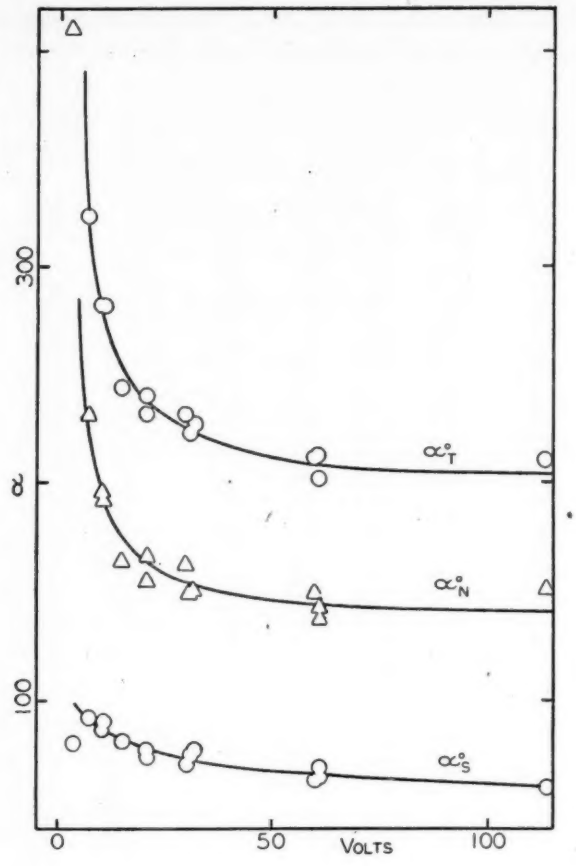

FIG. 4. Scattering of H^+ in propylene.

chamber, it is a reasonable value. The reported values of α_s^0 are obtained using this value of $\bar{d}$ and Eq. (8).

MATERIALS AND PROCEDURES

Both the ethylene and the propylene used were obtained from commercial cylinders and purified by repeated simple distillations. Check determinations were made with different samples. The experimental procedures used were the same as has been previously described.

RESULTS

The results of the experiments on the scattering of H^+, H_2^+, and H_3^+ in ethylene are given in Table I, and shown in Figs. 1, 2, and 3; and those for scattering in propylene are given in Table II and shown in Figs. 4, 5, and 6. Electrical measurements were made down to 0.5 volt, but below 2 volts the precision of measurement is questionable due to the pressure effects and errors in the pressure measurement. Gas pressures of the order of magnitude of 1×10^{-3} mm were used. Empty tube pressure was 2×10^{-5} or less. Temperature was 25 to 30°C. $\alpha_N^0=\alpha_T^0-\alpha_s^0$.

DISCUSSION

It was more difficult to obtain results of precision comparable to those obtained with hydrogen and helium. Although the use of hydrocarbon gas increased the experimental difficulties due to the formation of carbonaceous films, the chief reason for the lowered precision results from the fact that the total scattering is very much higher; and to make measurements in the same measuring tube, a lower pressure had to be employed. The poorer consistency of the measurements resulted from the difficulty of measuring this lower pressure.

The nature and the magnitude of the interaction of hydrogen ions with these olefins is a

matter of considerable interest. It is to be observed that a relatively large amount of neutralization was obtained. The elastic scattering is also found to be of considerable magnitude, that for ethylene being similar to that found previously for methane and that for propylene being somewhat higher. Despite the lower precision of the elastic scattering data, it was thought desirable to explore the force laws that could be evaluated. In Figs. 7, 8, and 9 are given the logarithmic plots for the evaluation of the force laws between ethylene and H^+, H_2^+, and H_3^+, respectively. The full lines shown in these plots are the lines used for the potential functions for these interactions, as shown in Table III.

A potential function based upon the interaction of a charge with a polarizable molecule contains the inverse fourth power of the distance. From the polarizability of the molecule, the constant and the function can be obtained. Debye[3] has given the polarization of ethylene as 9.4 cc per mol. The potential function based on this simple interaction with ethylene is

$$V = -26.8/r^4,$$

with K in volt (Angstroms)^4 and r in Angstroms. It is seen, when the straight lines that will give an inverse fourth-power law are drawn on Figs. 7, 8, and 9 and the constants corrected for mass ratios, that these constants found for H^+, H_2^+, and H_3^+ are 31.3, 21.8, and 56, respectively. The first two are in reasonable agreement with the theoretical polarizability law.

McAlpine and Smyth[4] have given the dipole moment of propylene to be 0.35 D and the polarization to be 15.7 cc per mole. The simple

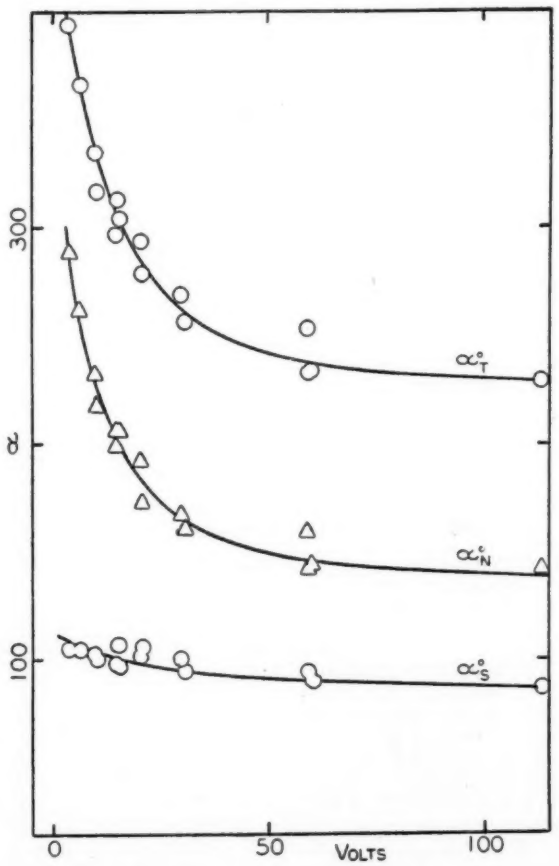

FIG. 5. Scattering of H_2^+ in propylene.

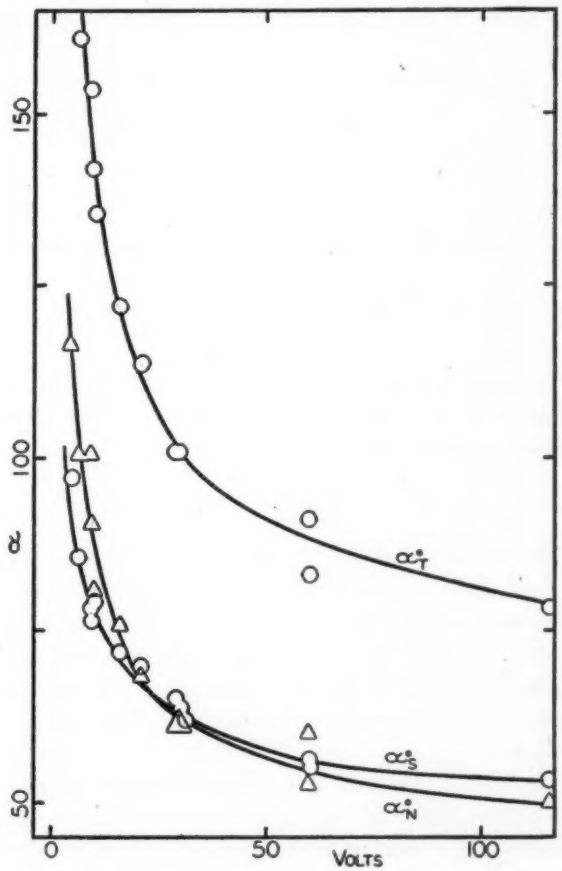

FIG. 6. Scattering of H_3^+ in propylene.

[3] Peter Debye, *Polar Molecules* (Chemical Publishing Company, Inc., New York, 1929).
[4] K. B. McAlpine and C. P. Smyth, J. Am. Chem. Soc., **55**, 453 (1933).

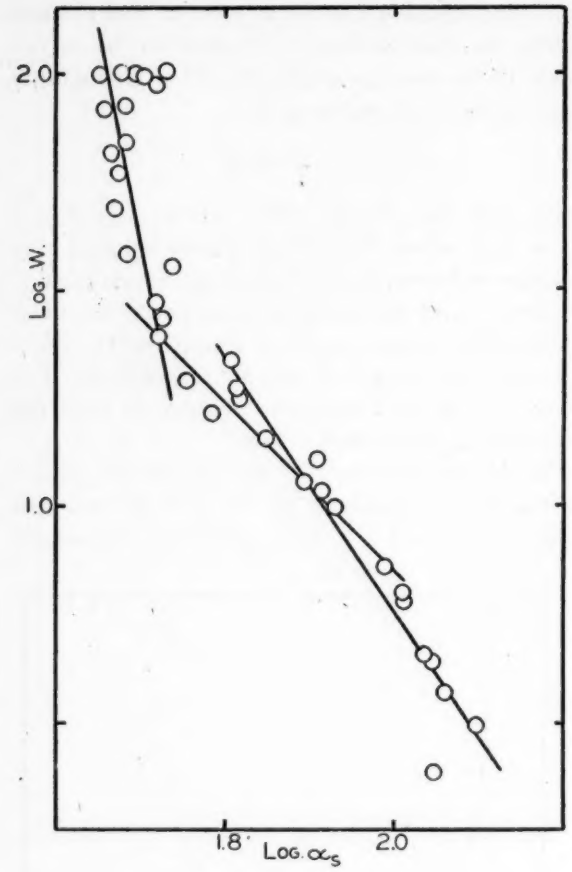

FIG. 7. H^+ in ethylene.

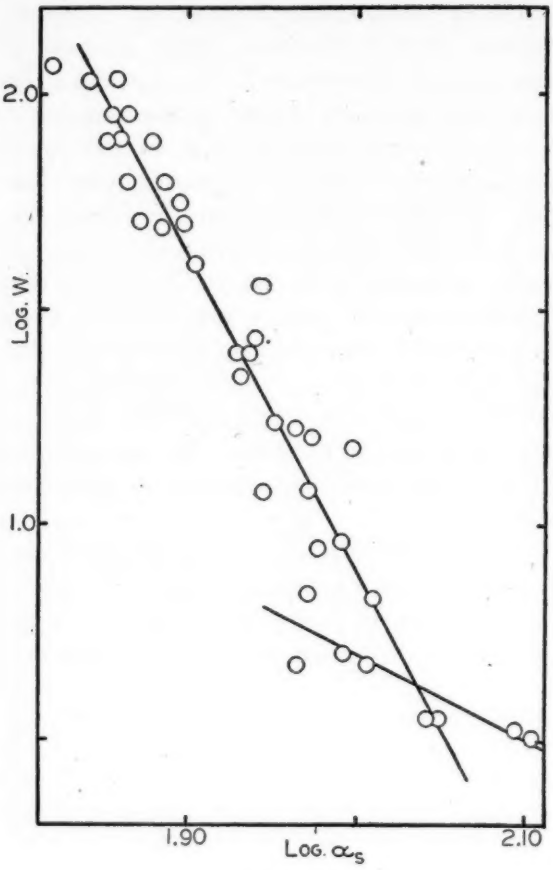

FIG. 8. H_2^+ in ethylene.

potential law based upon the interaction of a charge on a molecule of this polarizability and dipole moment is

$$V=-44.8/r^4-1.05/r^2.$$

The points in Figs. 10, 11, and 12 cannot be forced into a potential law of low exponent. However, a line has been drawn on these graphs which fits the above law and which crosses the path of the points. It is seen that the experimental evidence is hardly consistent with this simple theory.

In Figs. 7 and 9 the experimental points appear to follow an "*S*" type of curve. This is an interesting observation relative to the variation of the force law with distance between particles. If the distance decreases from relatively large values, the exponent in the attractive law of force would be expected to decrease. However, as the distance becomes smaller, repulsive forces will

TABLE III. Summary of potential functions.

Ion	Range	Potential function
	Ethylene	
	Theoretical interaction of charge and polarizable molecule.	$V=-26.8/r^4$
H^+	3–19 v (3.36–2.45A)	$V=-241/r^6$
	25–100 v (2.18–2.00A)	$V=-4.8\times10^6/r^{20}$
	6–25 v (3.08–2.18A)	$V=-38.2/r^4=[-31.3/r^4]^*$
H_2^+	Below 5 v (>3.00A)	$V=-26.8/r^4=[-21.8/r^4]^*$
	3–100 v (3.18–2.52A)	$V=-9.6\times10^7/r^{15}$
H_3^+	3–25 v (4.68–2.30A)	$V=-31.3/r^3$
	25–150 v (2.30–1.87A)	$V=-990/r^8$
	3–80 v (4.68–1.90A)	$V=-69/r^4$
	Propylene	
	Theoretical interaction of charge with polarizable molecule containing a dipole.	$V=-44.8/r^4-1.05/r^2$
H^+	6–120 v (2.92–2.12A)	$V=-10^5/r^{12}$
H_2^+	5–110 v (3.1–2.8A)	$V=-7.4\times10^{13}/r^{30}$
H_3^+	4–100 v (3.66–2.16A)	$V=-537/r^6$

r is given in angstrom units, and all values of K are uncorrected for mass ratio except those marked *. These are corrected by the method described in J. H. Simons, E. E. Muschlitz ,and L. G. Unger, J. Chem. Phys. 11, 322 (1943).

come into play and the laws expressing these have large values of the exponent. In these scattering measurements, attraction and repulsion are indistinguishable so that plots such as shown in Figs. 7 and 9 might be expected to form an "*S*" curve. These are the first cases showing an increasing value of the exponent "*n*" with decreasing distance. In most previous experiments the value of "*n*" decreased with decreasing distances, but these experiments were for molecules of much smaller size. If attempts were made to evaluate the energy of combination of, for example, H^+ and ethylene, it seems that the potential function with high values of the exponent at the smaller distances should not be employed, for if these are due to repulsion, they are recorded at greater distances than the equilibrium distance. These appear in the experimental results only from the statistical effect of the molecules being oriented at all angles in space. If, for example, in ethylene the equilibrium position of an added proton is between the two carbon atoms, the average effect of the repulsion of the ends of the molecule on the ion would be felt by an approaching proton at greater distances than the equilibrium distance. The reverse calculation of the above has been made in this case. Baughan, Evans, and Polanyi[5] have calculated the proton affinity of ethylene to be 174 Kcal. Using the sixth-power potential function, an equilibrium distance of 1.50A is obtained. This compares with 1.34A which is the distance the nucleus of the hydrogen atom of ethane is from the center of gravity of the molecule. It could be reasonably expected that the distances in the $C_2H_6^+$ ion might be greater than in the neutral molecular ethane.

If we picture an ion passing an unsymmetrical rotating molecule, we can anticipate two alternative situations to develop. If the interaction is dependent chiefly upon the electrostatic attrac-

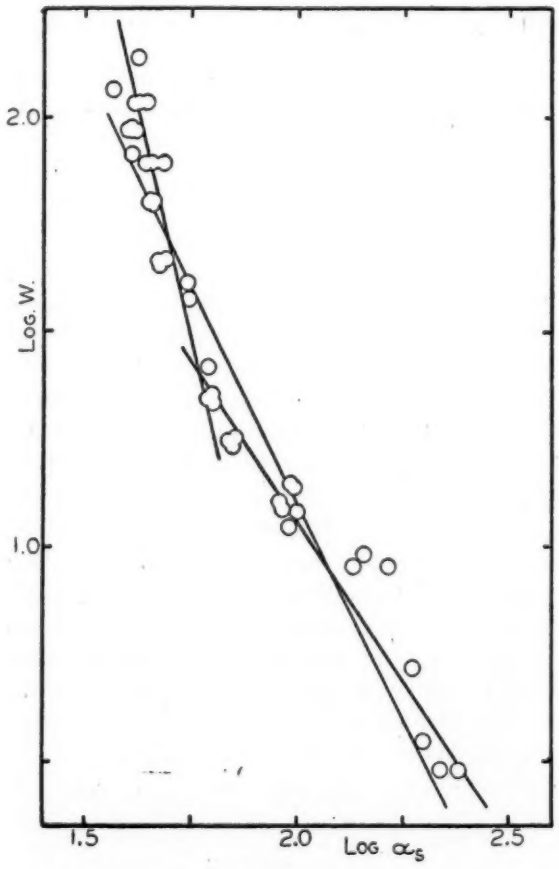

FIG. 9. H_2^+ in ethylene.

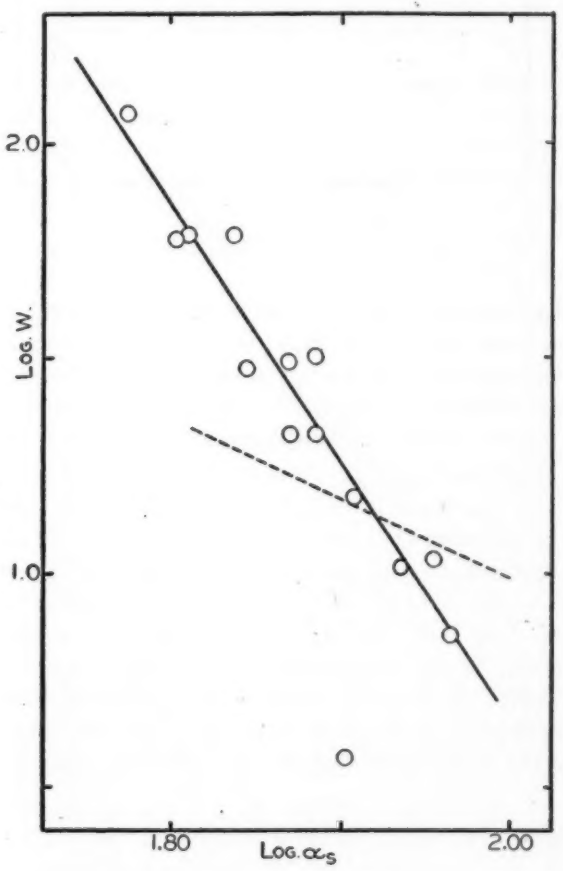

FIG. 10. H^+ in propylene.

[5] E. C. Baughan, M. P. Evans, and M. Polanyi, Trans. Faraday Soc. **37**, 377 (1941).

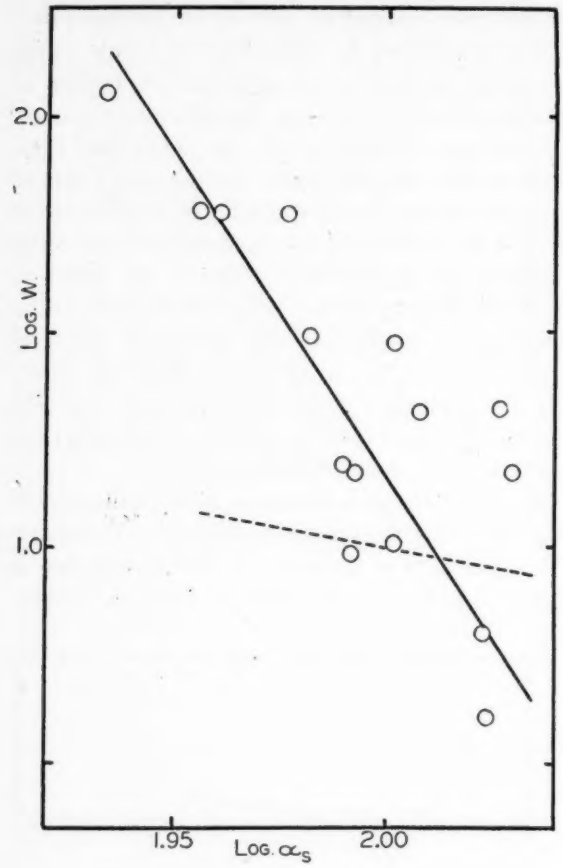

FIG. 11. H_2^+ in propylene.

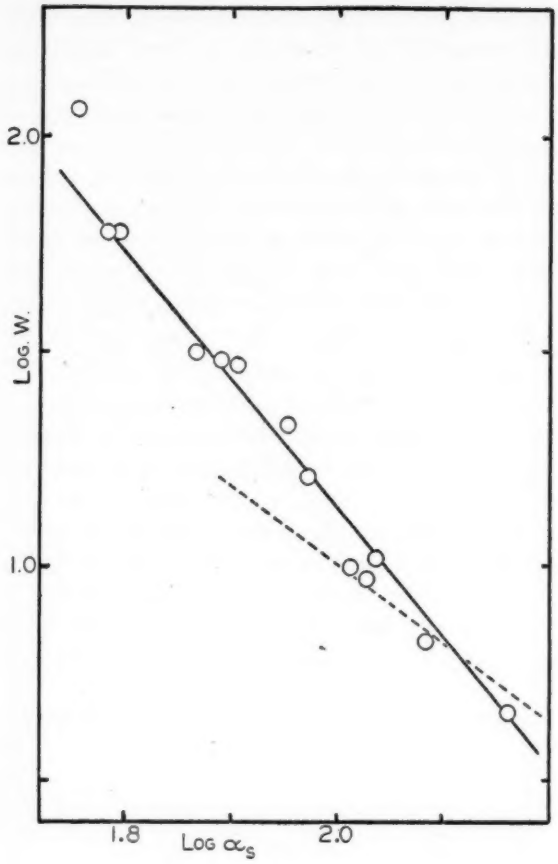

FIG. 12. H_3^+ in propylene.

tion between the charge of the ion and the induced dipole of the molecule and if the polarizability of the molecule is isotropic, the rotations should be unaffected and the repulsive forces experienced upon close approach should be felt on nearing the greatest radius of the molecule.

If, however, forces of attraction for the ion already present in the molecule or induced by its approach are not spherically symmetrical, such as would be expected for the chemical binding of the two particles, a different situation would result. As the ion approached the molecule more closely, the rotation would be converted into an oscillation of the same energy and that direction of the molecule having the greatest attraction for the ion would be uniformly presented to it. The distance of closest approach would not be a statistical effect but would be that distance given by the properties of the molecule along this direction.

If this argument is applied to the interaction of H^+ with C_2H_4, it would be expected that a small distance of close approach would be obtained before the potential law had a high value of the exponent. It might also be expected that the value of "n" would decrease to below 2 as was found in the interaction of H^+ with both H_2 and He. The results obtained indicate that this is not the nature of the interaction for H^+ with ethylene and propylene.

Multiple Adsorption from Solutions

JOHN E. WALTER
Palmer Physical Laboratory, Princeton University, Princeton, New Jersey
(Received March 15, 1945)

The general theory of the adsorption of solutes from solutions which are treated by a process similar to that employed in chromatography is presented. By assuming a chemical equilibrium between adsorbed material and the solution, the adsorption equations can be solved explicitly. A detailed discussion of the two-component problem is given; the many-component problem and the extension of the theory to more general adsorption isotherms are considered briefly.

INTRODUCTION

THE problem of the adsorption of solutes from a solution which is passed through a tube containing an adsorbing material has been considered from the theoretical viewpoint by several authors.[1–3] The equations which apply to this problem are the set of simultaneous partial differential equations

$$(\partial c_i/\partial l)+(\partial q_i/\partial v)=0, \quad i=1, 2, \cdots m, \quad (1)$$

where c_i is the concentration of the i'th solute in the solution at a distance l along the tube after a volume v has passed this point, q_i is the concentration of the corresponding component on the adsorbing material, and m is the number of solutes which are being adsorbed. Wilson[1] showed that in certain instances q_i may be a discontinuous function of l. DeVault[2] solved the problem for one solute completely, in terms of a general adsorption isotherm, and discussed the problem of multiple adsorption qualitatively. DeVault's investigation of the one-component problem showed that q will be a discontinuous function of l only if the solute is adsorbed strongly. Weiss[3] solved the one-component problem for several different types of adsorption isotherms, with results similar to those of DeVault.

In this article the general solution of the problem of multiple adsorption is given, assuming that the interaction between dissolved and adsorbed material is governed by the ordinary relations of chemical equilibrium. This assumption is probably valid for ionic adsorption; for example, in the replacement of the hydrogen ion of hydrogen zeolite by an alkali ion.[4] In addition, the solution of this particular problem will indicate the results to be expected if the adsorption is governed by more general adsorption isotherms, since the results depend primarily on the curvature of the isotherm and not on its exact analytical form. The effects of diffusion are not considered.

ONE COMPONENT

The equations in this section could be obtained from the general equation given by DeVault.[2] Because we are dealing here with a particular type of adsorption it will be convenient to state the results explicitly. The solution of the one-component problem is valuable as a guide to the more general solution. We will visualize the process as the replacement of the hydrogen ion of hydrogen zeolite by an alkali ion, although of course the results apply to any adsorption process which can be regarded as a chemical equilibrium. The reaction involved could be

$$\underset{(P-q)}{HZ} + \underset{(c)}{MX} \rightleftharpoons \underset{(q)}{MZ} + \underset{(c^0-c)}{HX} \quad (2)$$

where P is the total replaceable hydrogen per unit length of tube, c is the concentration of dissolved M, q is the concentration of adsorbed M, and c^0 is the original concentration of dissolved M. q and c will be functions of both l and v. We assume that the relation between q and c is given by the equilibrium equation

$$K=q(c^0-c)/c(P-q). \quad (3)$$

[1] J. N. Wilson, J. Am. Chem. Soc. **62**, 1583 (1940).
[2] D. DeVault, J. Am. Chem. Soc. **65**, 532 (1943).
[3] J. Weiss, J. Chem. Soc. London 297 (1943).
[4] Private communication from Dr. F. R. Duke, Frick Chemical Laboratory, Princeton University. An experimental article on this subject will be published by Dr. Duke in the J. Am. Chem. Soc.

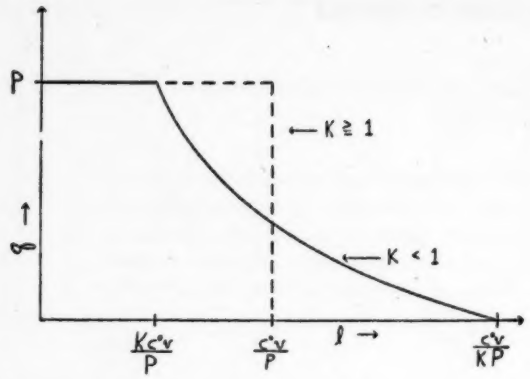

FIG. 1. Distribution of adsorbed material: one component.

Using (3) to eliminate c from Eq. (1), we obtain

$$KPc^0\frac{\partial q}{\partial l}+[KP+(1-K)q]^2\frac{\partial q}{\partial v}=0, \qquad (4)$$

as the differential equation which determines q as a function of l and v. This differential equation can be solved by the method of characteristics.[5] The general solution is

$$q=\varphi\{[KP+(1-K)q]^2l-KPc^0v\}, \qquad (5)$$

where φ is any arbitrary function of the argument in brackets. This general solution may be verified by direct substitution in Eq. (4). The boundary conditions for this problem are

$$q=P \quad \text{for} \quad l=0, \quad v>0; \qquad (6)$$

$$\lim_{v\to 0} q=0 \quad \text{for} \quad l>0. \qquad (7)$$

The first condition expresses the fact that the zeolite at the end of the tube must be saturated, since it is in equilibrium with solution containing M at a concentration c^0. The second condition states that there can be no adsorbed material a finite distance down the tube if only an infinitesimal volume v has entered the tube. The boundary condition for $v=0$, $l=0$ is undefined, since q changes discontinuously at $l=0$ when v passes through zero. There is an additional subsidiary condition

$$\int_0^\infty q\,dl=c^0v, \qquad (8)$$

which expresses the conservation of M.

[5] See, for example, E. B. Wilson, *Advanced Calculus* (Ginn and Company, New York, 1912), p. 268.

The boundary condition (6) tells us that we must take $q=P$ for all negative values of the argument in (5). Boundary condition (7) tells us that $q=0$ for all positive values of this argument. Placing the argument equal to zero gives an explicit equation for the variation of q between the limits P and zero. The desired solution is therefore

$$q=P; \quad l<\frac{Kc^0v}{P}, \qquad (9a)$$

$$q=\frac{1}{1-K}\left\{\left(\frac{KPc^0v}{l}\right)^{\frac{1}{2}}-KP\right\};$$

$$\frac{Kc^0v}{P}<l<\frac{c^0v}{KP}, \qquad (9b)$$

$$q=0; \quad l>\frac{c^0v}{KP}. \qquad (9c)$$

Figure 1 (calculated for $K=0.5$) illustrates the variation of q with l after a given volume v has passed completely through the tube. As K increases from zero toward one, the curved portion becomes more nearly vertical; for $K>1$, Eq. (9b) gives a curve with positive slope, and q becomes a triple-valued function of l. Since this would have no physical significance, we conclude that q is a discontinuous function of l for $K\geqq 1$. Equations (9) are valid for $K<1$; for $K\geqq 1$ we have

$$q=P; \quad l<c_0v/P, \qquad (10a)$$

$$q=0; \quad l>c_0v/P, \qquad (10b)$$

which gives the dotted curve in Figure 1. The solutions (9) and (10) satisfy the conservation boundary condition (8). It should be noted that the break in the q *versus* l curve comes at the point where a fraction K of the total original solute has been adsorbed.

TWO COMPONENTS

We assume that two substances are being adsorbed by equilibrium processes of the type

$$\begin{array}{cccccc} HZ & + & M_1X\rightleftharpoons M_1Z & + & HX, \\ (P-q_1-q_2) & & (c_1) \quad (q_1) & & (c_1^0+c_2^0-c_1-c_2), \\ HZ & + & M_2X\rightleftharpoons M_2Z & + & HX, \\ (P-q_1-q_2) & & (c_2) \quad (q_2) & & (c_1^0+c_2^0-c_1-c_2), \end{array} \qquad (11)$$

where the notation is the same as before. As a slight algebraic simplification, we make the substitutions

$$y_i=q_i/P;\quad n_i=c_i/(c_1^0+c_2^0);\qquad x=lP/(c_1^0+c_2^0), \tag{12}$$

that is, we measure adsorbed material as a fraction of the total capacity, dissolved material as a fraction of the total original dissolved material, and length in terms of the length required to adsorb completely the dissolved material in unit volume of the original solution. Equations (1) are then

$$\partial n_1/\partial x+\partial y_1/\partial v=0;\quad \partial n_2/\partial x+\partial y_2/\partial v=0, \tag{13}$$

and the equilibrium constants for reactions (11) are

$$K_1=\frac{y_1(1-n_1-n_2)}{n_1(1-y_1-y_2)},\quad K_2=\frac{y_2(1-n_1-n_2)}{n_2(1-y_1-y_2)}. \tag{14}$$

Eliminating the n's from Eqs. (13) by use of the equilibrium equations leads us to the following differential equations for the y's

$$[K_2+(1-K_2)y_2]\frac{\partial y_1}{\partial x}-(1-K_2)y_1\frac{\partial y_2}{\partial x}+\frac{\Delta^2}{K_1K_2}\frac{\partial y_1}{\partial v}=0, \tag{15a}$$

$$[K_1+(1-K_1)y_1]\frac{\partial y_2}{\partial x}-(1-K_1)y_2\frac{\partial y_1}{\partial x}+\frac{\Delta^2}{K_1K_2}\frac{\partial y_2}{\partial v}=0, \tag{15b}$$

where

$$\Delta=K_2K_1+K_2(1-K_1)y_1+K_1(1-K_2)y_2.$$

We need solutions of these simultaneous equations which will satisfy the boundary conditions and, in addition, reduce to the one-component equations for the special case $K_1=K_2$. This last requirement suggests that we should look for special solutions which are similar to those in Eqs. (9). As boundary conditions we will use (6) and (8), which become, for this problem

$$y_1=y_1^0\equiv\frac{K_1n_1^0}{K_1n_1^0+K_2n_2^0};\qquad y_2=y_2^0\equiv\frac{K_2n_2^0}{K_1n_1^0+K_2n_2^0}; \tag{16}$$

for $x=0$, $v>0$; and

$$\int_0^\infty y_1dx=n_1^0v;\quad \int_0^\infty y_2dx=n_2^0v, \tag{17}$$

where

$$n_1^0=\frac{c_1^0}{c_1^0+c_2^0};\quad n_2^0=\frac{c_2^0}{c_1^0+c_2^0}.$$

The solution $y_1=$constant, $y_2=$constant is obviously valid. Inspection of Eqs. (15) shows that a change in y_1 is accompanied by a change in y_2, and conversely, so that it is not possible to keep one y a constant (not including zero) and vary the other. If neither y is a constant, a possible solution is

$$y_1=\frac{y_1^0}{1-K_1}\left\{\left(\beta\frac{v}{x}\right)^{\frac{1}{2}}-K_1\right\}, \tag{18a}$$

$$y_2=\frac{y_2^0}{1-K_2}\left\{\left(\beta\frac{v}{x}\right)^{\frac{1}{2}}-K_2\right\}, \tag{18b}$$

where

$$\beta=K_1n_1^0+K_2n_2^0.$$

There are other special solutions of this form but none of them will satisfy the boundary conditions and reduce to (9b) for $K_1=K_2$. The boundary conditions show that both y's remain constant at their original values until a value of x is reached at which Eqs. (16) and (18) give the same value for the y's; the y's are given by Eqs. (18) beyond this point. The desired solution is thus (for $K_1<1$, $K_2<1$)

$$y_1=y_1^0,\quad y_2=y_2^0,\quad x<\beta v, \tag{19}$$

and the values given by Eqs. (18) for $x>\beta v$. At $x=\beta v$ a fraction K_1 of component 1 and a fraction K_2 of component 2 have been adsorbed. Let us now assume that $K_2>K_1$. The y's are given by Eqs. (18) until the point $x=\beta v/K_2^2$ is reached; at this point $y_2=0$ and component 2 has been adsorbed completely. We therefore have

$$y_2=0;\quad x>\beta v/K_2^2,\quad (K_2>K_1). \tag{20}$$

At this point y_2 is continuous but has a discontinuous derivative. There will therefore be at least a discontinuous derivative in the y_1 curve at this point. For $x>\beta v/K_2^2$, y_1 is determined by the differential equation obtained by placing $y_2\equiv0$ in Eq. (15a). This gives a one-component

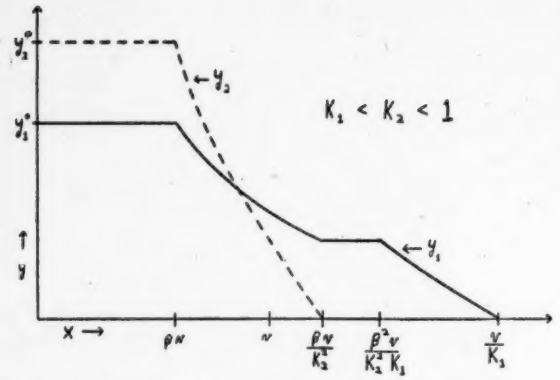

FIG. 2. Distribution of adsorbed material: both components weakly adsorbed.

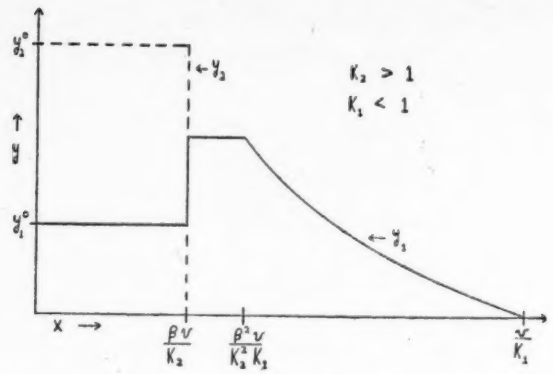

FIG. 3. Distribution of adsorbed material: one component strongly adsorbed, one component weakly adsorbed.

equation

$$K_1\frac{\partial y_1}{\partial x}+[K_1+(1-K_1)y_1]^2\frac{\partial y_1}{\partial v}=0, \quad (21)$$

with solutions $y_1=$constant or

$$y_1=\frac{1}{1-K_1}\left\{\left(K_1\frac{v}{x}\right)^{\frac{1}{2}}-K_1\right\}. \quad (22)$$

Boundary condition (17) shows that the y_1 curve becomes horizontal at the point where y_2 becomes zero, retains this value until it meets the sloping curve (22), and then follows that curve down to zero. We have

$$y_1=y_1{}^0\frac{K_2-K_1}{1-K_1}; \quad \beta v/K_2{}^2<x<\left(\frac{\beta}{K_2}\right)^2\frac{v}{K_1}, \quad (23)$$

$$y_1=\frac{1}{1-K_1}\left\{\left(K_1\frac{v}{x}\right)^{\frac{1}{2}}-K_1\right\}; \quad \left(\frac{\beta}{K_2}\right)^2\frac{v}{K_1}<x<\frac{v}{K_1}, \quad (24)$$

$$y_1=0; \quad x>v/K_1. \quad (25)$$

At this last point component 1 has been adsorbed completely. Figure 2 shows the variation of y_1 and y_2 with x after a given volume v has passed through the tube. (The actual curves are drawn for $n_1{}^0=n_2{}^0=0.5$, $K_2=0.7$, $K_1=0.5$.)

As K_2 increases the curved portion of the y_2 curve becomes more nearly vertical. Just as before, if $K_2\geqq 1$, the y_2 curve is discontinuous. The boundary condition (17) then shows that the desired solution for the problem $K_2>1$, $K_1<1$ is

$$y_2=y_2{}^0; \quad x<\beta v/K_2, \quad (25)$$

$$y_2=0; \quad x>\beta v/K_2, \quad (26)$$

$$y_1=y_1{}^0; \quad x<\beta v/K_2, \quad (27)$$

$$y_1=y_1{}^0\frac{K_2-K_1}{1-K_1}; \quad \beta v/K_2<x<\left(\frac{\beta}{K_2}\right)^2\frac{v}{K_1}, \quad (28)$$

$$y_1=\frac{1}{1-K_1}\left\{\left(K_1\frac{v}{x}\right)^{\frac{1}{2}}-K_1\right\}; \quad \left(\frac{\beta}{K_2}\right)^2\frac{v}{K_1}<x<\frac{v}{K_1}, \quad (29)$$

$$y_1=0; \quad x>\frac{v}{K_1}. \quad (30)$$

Equation (28) can be determined from the equilibrium conditions at the point $x=\beta v/K_2$, although the boundary condition (17) gives a unique solution. Equations (25) to (30) are illustrated by Fig. 3. (The actual curves are drawn for $n_1{}^0=n_2{}^0=0.5$, $K_2=1.5$, $K_1=0.5$.) Equations (28) and (29) must be modified if (K_2-K_1) is sufficiently large. The maximum value of y_1 is 1, therefore, if

$$y_1{}^0\frac{K_2-K_1}{1-K_1}>1, \quad (31)$$

Eqs. (28) and (29) must be replaced by

$$y_1=1; \quad \beta v/K_2<x<K_1v, \quad (32)$$

$$y_1=\frac{1}{1-K_1}\left\{\left(K_1\frac{v}{x}\right)^{\frac{1}{2}}-K_1\right\}; \quad K_1v<x<\frac{v}{K_1}. \quad (33)$$

For $n_1^0=n_2^0=0.5$, condition (31) becomes $K_2>K_1/(2K_1-1)$, which can be satisfied if $K_1>0.5$. This behavior is illustrated in Fig. 4 (drawn for $n_1^0=n_2^0=0.5$, $K_2=4.0$, $K_1=0.8$).

As K_1 increases, the last segment of the y_1 curve approaches the vertical, and for $K_1\geqq 1$ we have a discontinuity at $x=v$. For $K_2>K_1\geqq 1$, the solutions become

$$\begin{aligned} &y_1=y_1^0, \quad y_2=y_2^0; \quad x<\frac{\beta v}{K_2}, \\ &y_1=1, \quad y_2=0; \quad \frac{\beta v}{K_2}<x<v, \\ &y_1=0, \quad y_2=0; \quad x>v. \end{aligned} \tag{34}$$

MORE THAN TWO COMPONENTS

If we have m equilibria of the type (11), with equilibrium constants defined by

$$K_i=\frac{y_i(1-\sum_{i=1}^{m} n_i)}{n_i(1-\sum_{i=1}^{m} y_i)}; \quad i=1, 2, \cdots m, \tag{35}$$

the set of partial differential equations becomes

$$\Delta\frac{\partial y_i}{\partial x}-y_i\frac{\partial \Delta}{\partial x}+\frac{K_i\Delta^2}{K_1K_2\cdots K_m}\frac{\partial y_i}{\partial v}=0; \quad i=1, 2, \cdots m, \tag{36}$$

where

$$\Delta=(K_1K_2\cdots K_m)\left\{1+\sum_{i=1}^{m}\left(\frac{1-K_i}{K_i}\right)y_i\right\},$$

with the boundary conditions

$$y_i^0=\frac{K_in_i^0}{\sum_{i=1}^{m} K_in_i^0}, \quad \int_0^\infty y_i dx=n_i^0v, \quad i=1, 2, \cdots m. \tag{37}$$

Solutions of Eqs. (36) of the form (18) are

$$y_i=\frac{y_i^0}{1-K_i}\left\{\left[\left(\sum_{i=1}^{m} K_in_i^0\right)\frac{v}{x}\right]^{\frac{1}{K_i}}-K_i\right\}. \tag{38}$$

If all the K's are less than 1, the y's will remain constant at the values y_i^0 until the point

$$x=(\sum_{i=1}^{m} K_in_i^0)v$$

is reached. At this point a fraction K_i of each i'th component has been adsorbed. The y's would then follow Eqs. (38), giving curves similar to the first part of Fig. 2 but with m curves instead of two, until the component with the largest K has been adsorbed completely. The problem is then reduced to one of lower order and the same general type of variation is repeated, giving a succession of curves similar to those of Fig. 2. If some of the K's are greater than unity, the corresponding y's will be discontinuous, and we will have saturation of the adsorbing material up to the point at which all components with K's greater than unity have been completely adsorbed.

CONCLUSION

The above results apply to the original deposition of the adsorbed material. In the process of chromatography, the chromatogram is "developed" by pouring pure solvent down the tube. The region containing the adsorbed material is then displaced along the tube. For our particular problem, this process corresponds to pouring HX at concentration $(c_1^0+c_2^0)$ down the tube. The same equations apply to this problem, but they apply to both the front and rear boundaries of the adsorbed material. Equation (9b) has a positive slope for $K>1$, and therefore is meaningless when applied to the front boundary, but not when applied to the rear boundary. Therefore, for $K>1$, the front boundary is sharp during development but the rear boundary is not; for $K<1$ the rear boundary is sharp and the front boundary is not.[2,3] In developing a pattern such as that of Fig. 3 ($K_2>1$, $K_1<1$), the y_1 curve

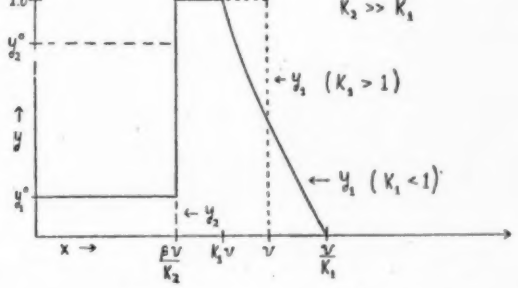

FIG. 4. Distribution of adsorbed material: both components strongly adsorbed.

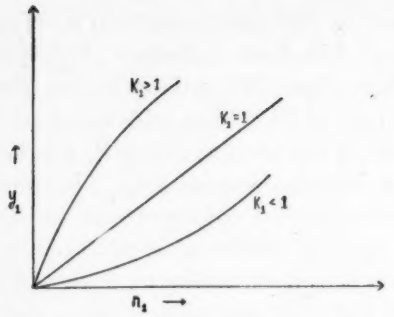

FIG. 5. Concentration of adsorbed material as a function of concentration of solute, illustrating type of curvature of the isotherms.

will have a sharp rear boundary, and the y_2 curve will develop a diffuse rear boundary. The region over which the two curves overlap shortens and eventually disappears. For the particular situation illustrated in Fig. 3, the solution during development which reaches the point at which y_2 becomes zero will have the same concentration as had the original solution, and this point will therefore move a distance $\beta V/K_2$, where V is the volume of solvent used in development. The rear boundary of y_1, which is sharp, will move a distance $\beta V/K_1$, since a volume V of solvent will remove $n_1^0 V$ units of component 1 from a region where the concentration of adsorbed material is $y_1^0=K_1 n_1^0/\beta$. The two components will therefore be separated completely when

$$\beta(V+v_0)/K_2=\beta V/K_1, \quad \text{or} \quad V=\frac{K_1}{K_2-K_1}v_0, \quad (39)$$

where v_0 is the volume of solution used in the original adsorption. If both K's are greater than one or both less than one, complete separation will be more difficult.

The explicit formulas for the amount of material adsorbed as a function of distance down the tube are of some interest. The total adsorbed material in a length L of the tube is

$$M_i=\int_0^L q_i dl. \quad (40)$$

Let $L=\alpha L_0$, where L_0 is the length required to adsorb all the solute in a volume v_0 of solution. For the one component problem, with $K<1$, we have $L_0=c^0 v_0/KP$. The *fraction* of the original solute adsorbed in a length L is then

$$\frac{\alpha}{K}; \qquad \alpha \leqq K^2, \quad (41)$$

$$\frac{2\alpha^{\frac{1}{2}}-\alpha-K}{1-K}; \quad K^2 \leqq \alpha \leqq 1. \quad (42)$$

Although the above algebraic relations apply only to a special type of adsorption, the results should have general qualitative validity. If Eq. (14) is solved for y_1, we have

$$y_1=K_1 n_1/[1-(1-K_1)n_1-(1-K_2)n_2]. \quad (43)$$

The behavior of this function for the region of small n_1 (holding n_2 constant) is shown in Fig. 5. $K_1=1$ gives the dividing line between substances which give a sharp front boundary and those which give a diffuse front boundary. As shown above, this criterion is independent of K_2. The important feature is not the actual slope of the y_1 *versus* n_1 curve, since this depends on $(1-K_2)n_2$ as well as on K_1, but the way in which the slope changes with increasing n_1. If the adsorption isotherm is represented by a more general equation than Eq. (43) we expect a diffuse front boundary if the slope of the y_1 *versus* n_1 curve increases with increasing n_1 for small n_1 and a sharp front boundary if the slope of the curve decreases with increasing n_1 in this region. This conclusion is in accord with the original suggestion of DeVault.[2] Of course, the exact shape of the diffuse boundary will depend on the particular adsorption isotherm.

This problem was suggested to the author by Dr. F. R. Duke. The author wishes to acknowledge his indebtedness to Dr. Duke for the formulation of the problem and for valuable discussions regarding the validity of the assumptions made and the results obtained.

Electron Microscopy of Catalysts

JOHN TURKEVICH
Frick Chemical Laboratory, Princeton University, Princeton, New Jersey
(Received March 16, 1945)

THE present paper is a survey of the appearance in the electron microscope of a number of important catalysts. Its purpose is to delineate the forms of catalytic materials and to serve as an introduction to further quantitative studies. Previous work on the subject has been reported in Germany by M. V. Ardenne and D. Beischer.[1] The electron micrographs were taken on the RCA B Electron Microscope at the RCA Research Laboratories at Princeton. The catalyst material was mounted for examination in the following way: The catalyst was triturated with a two percent solution of pyroxylin in amyl acetate. A drop of the suspension so obtained was placed on the clean surface of distilled water and allowed to spread freely to give a thin film about 200A thick. Two hundred mesh supporting nickel screens were then placed on the collodion, the film and screen picked up, dried, and examined in the microscope. The grinding with the pyroxylin solution seems to break up the secondary aggregates or clumps, and the spreading of the film on water often facilitates the separation of one particle from another.

The results obtained are presented in a series of electron micrographs. The scale is indicated on the side and it must be recalled that 1 micron is equal to 10,000A. Figure 1 represents platinum oxide prepared according to the directions of Adams.[2] It can be seen that there are flakes of material ranging in size from a tenth of a micron to two microns. In addition to these more obvious particles one should note that the whole background of the collodion membrane is filled with finely-divided, homogeneous material whose particle size is near the limit of the resolution of this micrograph (about 200A). This finely-divided material is interpreted to be the platinum oxide from which the platinum catalyst is to be made by reduction. This interpretation is to be confirmed by subsequent electron diffraction study.

Figure 2 represents the platinum catalyst obtained by the reduction of the previously described platinum oxide. The dark masses are the platinum particles. It is seen that they range in size from 200 to 10,000A. There is definite evidence from the straight sides on some of the platinum particles that they are crystalline. The micrograph shows several folds and holes in the supporting collodion membrane.

The next series of micrographs deals with the appearance of asbestos and platinized asbestos.

FIG. 1. Platinum oxide.

FIG. 2. Adams' platinum catalyst.

[1] M. V. Ardenne and D. Beischer, Angew. Chem. **53**, 103 (1940).

[2] Gilman, *Organic Syntheses* (John Wiley & Sons. Inc., New York, 1932), p. 53.

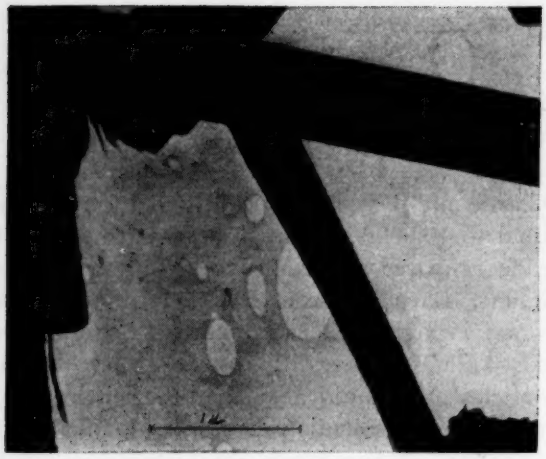

FIG. 3. Asbestos fibers.

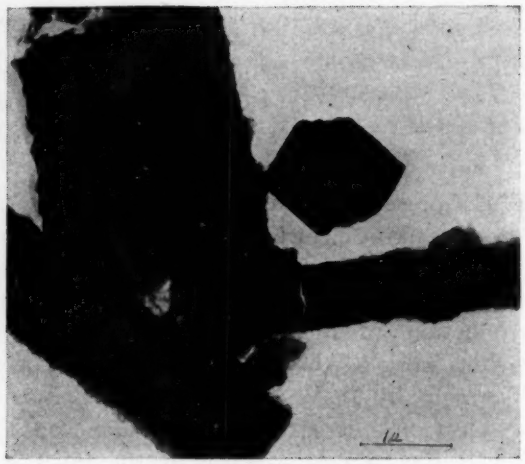

FIG. 4. Platinized asbestos.

Figure 3 represents a dispersion of asbestos fibers. The breadth of these fibers is 3000 and 6000A and their straight edge is particularly noteworthy. The ovals in the picture are merely holes in the supporting collodion membrane. Impregnation with chlorplatinic acid does not change the appearance of the fiber—the chlorplatinic acid seems to be very finely dispersed in the fiber.

Figure 4 presents the appearance of an active platinized asbestos catalyst. This particular preparation has had considerable use in catalyzing the hydrogen-oxygen reaction. The formerly clear asbestos fiber is thickly covered with material which is undoubtedly finely-divided platinum. A significant feature of this micrograph is the cubical crystal (one micron on side) of platinum which is attached to the fiber by one side and corroded at the two adjacent sides. Other micrographs indicate that the cubical shape and this type of attachment to the fiber, is typical of the platinum. Figure 5 is another electron micrograph of a platinized asbestos catalyst. The field here chosen represents very thin slivers of asbestos which are partially transparent to the electrons. The dense aggregates disclose the size and distribution of the platinum material on this support. One can detect in this micrograph particles very close to 50A in diameter, the very resolution limit of the microscope.

Figure 6 shows the appearance of the catalyst after it has been subjected to a sintering process of heating to 600°C. The appearance of this

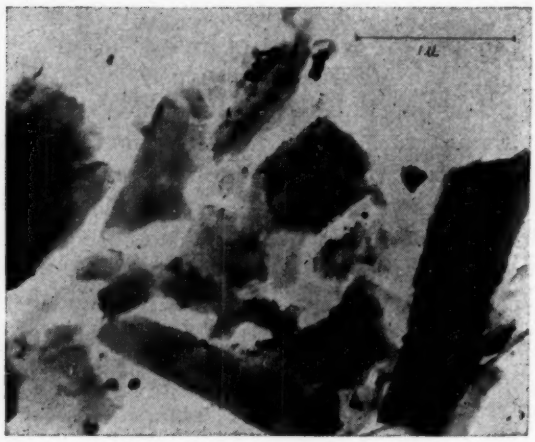

FIG. 5. Platinized asbestos.

inactive catalyst is in striking contrast to the previous platinum photographs. The edge of the asbestos is clean, the fine particles of platinum have disappeared and the main bulk of the catalyst has formed a swarm-like aggregate on the fiber. There is also some indication that the corners and edges of the material have rounded off.

Figure 7 represents ten-percent platinum on activated charcoal. The characteristic feature of this catalyst is the plate-like structure of the support which is particularly evident under and beside the large piece of charcoal. The plate form of charcoal is consistent with its large surface area of about 1000A per gram.[3] The platinum is

[3] P. Emmett, in *Advances of Colloid Science* (Interscience Publishing Corporation, New York, 1940) 1, 29.

so well dispersed that in spite of the fact that there is two percent of it on the charcoal, one can see the dense platinum aggregates only here and there on the field.

Figure 8 shows the appearance of Alorco activated alumina. It is seen that the product is homogeneous and consists of some particles of 100A and less. The surface of this material as determined by the Emmett-Brunauer gas adsorption method is equal to 270 sq. meters per gram. Steaming at 600°C for 40 hours reduces the surface to 13 sq. meters per gram. This product

FIG. 6. Sintered platinized asbestos.

FIG. 7. 10-percent platinum on charcoal.

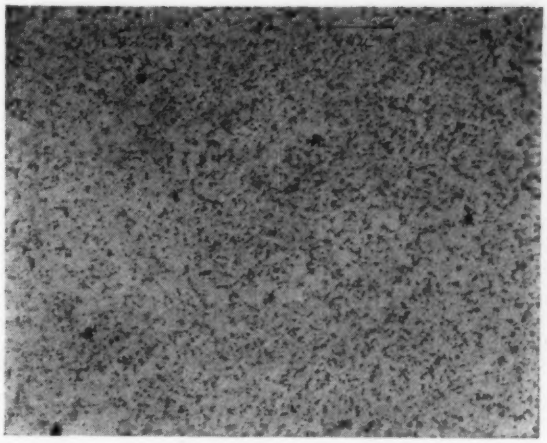

FIG. 8. Activated alumina.

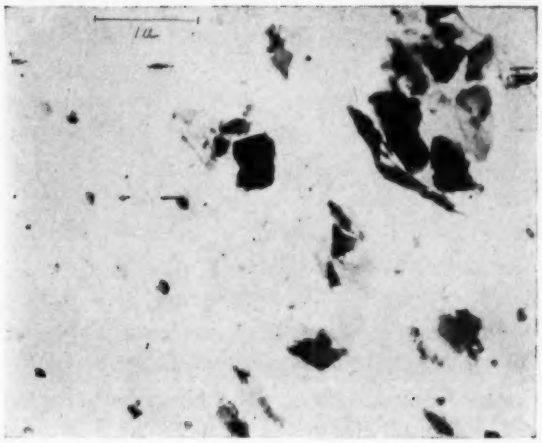

FIG. 9. Steamed alumina.

FIG. 10. Silica gel.

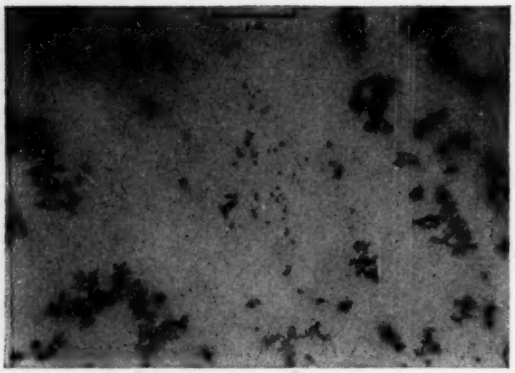

FIG. 11. Alumina silicate cracking catalyst.

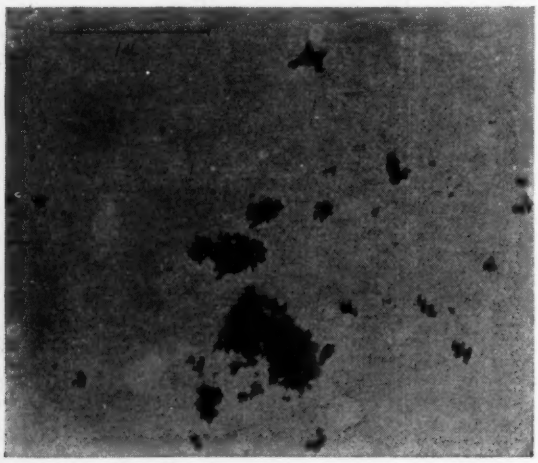

FIG. 12. Zinc oxide methanol catalyst.

is shown in Fig. 9. The particles are considerably larger and have a definite plate like structure.

Active silica gel is shown in Fig. 10. In addition to the larger clumps the field is full of very small particles whose diameter is of the order of 200A. This is consistent with the large specific area of the silica gel.

The electron micrograph of an alumina silicate catalyst used for catalytic cracking of petroleum is shown in Fig. 11. There is marked evidence for spheres of 200A-diameter and rod-like particles 1000A long and 300A wide.

The appearance of zinc oxide catalyst made by the decomposition of zinc oxalate and used for methanol synthesis is shown in Fig. 12. The particles are very finely divided having diameters which fall in the range of 100–200A. Their

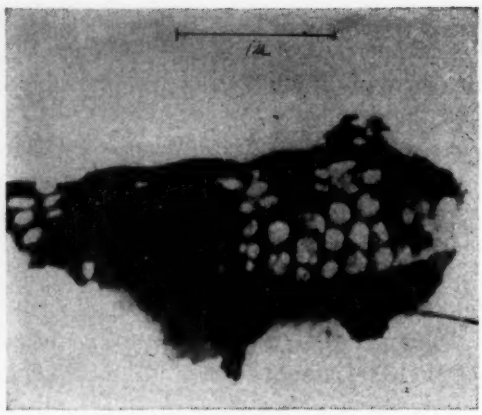

FIG. 13. Fischer synthin catalyst.

spherical shape may be due to the inability of the microscope to resolve the shape in this particular micrograph. The appearance of this zinc oxide catalyst is in marked contrast to the zinc oxide smoke which has the well-known needle like structure.

The last electron micrograph (Fig. 13) to be presented is that of the Fischer catalyst consisting of nickel-thoria supported on kieselguhr. This catalyst is used for the formation of petroleum hydrocarbons from carbon monoxide and hydrogen. The kieselguhr is seen to be composed of diatoms which are particles full of holes 1300A in diameter. These openings offer a large surface for the support of the nickel and thoria. It can be seen from the picture that some of these openings are completely filled while others are only partially filled.

The electron micrographs presented give a survey of the various ways large surfaces are produced by the art of the catalytic chemist. One method consists of using finely divided materials as in the case of active alumina, silica gel, etc.; the second available method is to take advantage of the rod-like nature of asbestos fiber as a support for metallic particles like platinum. Another method consists in using as a support the plate-like structure of materials such as active charcoal. Another way of attaining a large surface per unit weight is the use as a support of such porous material as the diatoms found in kieselguhr. Since catalytic activity is associated

with large surface area, the electron microscope is a powerful tool for the evaluation of a given material as a possible catalyst.

This investigation has been carried out in part at the RCA Research Laboratories at Princeton. We wish to thank Dr. V. K. Zworykin for the inspiring interest in this work and for the courtesies of the RCA Laboratories and Drs. J. Hillier and R. F. Baker for their unstinting help in the taking of these electron micrographs.

THE JOURNAL OF CHEMICAL PHYSICS VOLUME 13, NUMBER 6 JUNE, 1945

Molecular Constants and Chemical Theories

G. W. WHELAND
Department of Chemistry, University of Chicago, Chicago, Illinois

(Received January 29, 1945)

A few selected topics from four papers by Samuel on the theory of valence are critically examined. The conclusions are drawn that Samuel's bond-moments for molecules containing "pentacovalent nitrogen" are not as satisfactory as claimed, and provide no evidence in favor of the existence of pentacovalent nitrogen; that Samuel's eigenfunctions for structures with pentacovalent nitrogen are identical with the ones set up in the now conventional manner for structures without pentacovalent nitrogen but with semipolar double bonds instead; that the existence of antibonding orbitals seems to be theoretically necessary; and that several of Samuel's further conclusions are either based upon the use of words in unfamiliar senses, or else are erroneous.

IN a recent series of papers by the same name as the present one, Samuel[1] has come to conclusions which appear to be at variance with the present generally accepted theories of valence. He proposes that many of the features of modern theory be abandoned, and that a return be made to the corresponding features of classical theory.* For example, he considers that the semipolar double bond and the octet rule are without either experimental or theoretical proof and, indeed, that their acceptance makes more difficult the interpretation of a number of the physical properties of the substances concerned. In order to support his thesis, he advances two types of argument. First, on the basis of the classical structures, he establishes sets of constants, with the use of which, in his opinion, the molecular parachors, dipole moments, and the like can be calculated more satisfactorily than with the use of any other sets of analogous constants that have been derived hitherto on the basis of modern theory. And second, he points out several respects in which, in his opinion, the quantum-mechanical arguments that have been used to "prove" the modern theory are inconclusive, illogical, and contrary to spectroscopic evidence.

Since the significance of Samuel's papers may be somewhat obscure to the reader who is not particularly well acquainted with the field, I wish here to discuss critically, and in some detail, a selected few of the salient points which Samuel makes.

A

As has already been mentioned, Samuel is concerned to a considerable extent with the use of parachors, dipole moments, and the like, in the study of the finer details of molecular structure. He points out, quite correctly, that it is impossible, on the basis of such properties, to prove the existence of semipolar bonds, which he does not

[1] R. Samuel, J. Chem. Phys. **12**, 167, 180, 380, 521 (1944).

* For lack of better terms, the words "classical" and "modern" will be used throughout this paper to describe, respectively, the theories, structures, etc. which Samuel adopts, and the corresponding now generally accepted theories, structures, etc. which he rejects. The distinction between the classical and the modern points of view will become more apparent as we proceed. In the use of this terminology, no judgment regarding the relative merits of the two viewpoints is intended.

accept, to justify the octet rule, or to support any of several other features of modern valence theory. I wish here, however, to emphasize more strongly than Samuel does, that it is equally impossible, on the basis of these same properties, to establish the pentacovalence of nitrogen, which Samuel adopts, to disprove the octet rule, or to support the classical structures. The most that one can hope to do with the use of empirically obtained atomic parachors, bond-moments, and the like, is to make it seem probable that a given bond in a given molecule is (or is not, as the case may be) of the same type as a second bond in a second molecule. Whether the bond in question is double, semipolar double, hybrid, or whatnot cannot be decided in such a way, but only on the basis of theoretical arguments and with the use of a self-consistent set of definitions. This point will be elaborated further in the present section and in the following one.

Let us begin the discussion by considering Samuel's calculation of the dipole moments of several types of compound containing "pentacovalent nitrogen." With the assumption of the correctness of the classical structures, in which the covalence of nitrogen is permitted to be either three or five, as required, Samuel derives a set of bond-moments, which he considers to be constant from molecule to molecule. In tables (and also in the text and in diagrams illustrating the vector summation of bond-moments), he lists in his third paper a number of such values, of which the following ones will be important for our present purposes.

$H—C_{al}$	0.3 D	$N^{V}=O$	4.4 D	$N^{V}=C$	2.6 D
$H—C_{ar}$	0.4 D	$N^{V}—O$	1.4 D	$N^{V}—C$	1.0 D
$C_{al}—N^{III}$	0.5 D	$N^{V}\equiv N^{III}$	4.2 D	$C_{al}—C_{ar}$	0.6 D
$C_{ar}—N^{III}$	0.9 D	$N^{V}=N^{III}$	2.8 D		

In each case, the superscript designates the covalence of the nitrogen atom, and the subscripts "al" and "ar" mean "aliphatic" and "aromatic," respectively. The atom given at the *left* of each bond is considered to be at the *positive* end of the corresponding dipole. These values are apparently intended to be used in conjunction with the dipole moments measured in solution, rather than in the gas phase, since the gas-phase moments are not known for most of the compounds considered.

As Samuel shows, the above bond-moments permit the calculation of the molecular moments of a considerable number of different types of substance. The agreement between calculated and observed values, however, is not always as satisfactory as the reader might infer from Samuel's discussion. The following examples will illustrate the magnitudes of the discrepancies in the worst cases. The most serious of these discrepancies occurs with trimethylamine oxide, for which the calculated and observed[2] moments are 3.7 D and 5.0 D, respectively. Samuel does not discuss the moment of this substance. In some cases, the satisfactory agreement which Samuel obtains between calculated and observed moments appears to be due to numerical errors. For example, Samuel calculates the dipole moment of azoxybenzene to be 1.9 D, which is only 0.2 D greater than the observed value of 1.7 D. However, if the bond-moments and bond-angles are those given explicitly in his vector diagram, the resultant calculated moment is actually 2.3 D. The error is therefore three times as great as stated by Samuel. Furthermore, the calculated and observed moments of phenyl azide are 2.3 D and 1.55 D, respectively. For this substance, Samuel makes no calculation; instead, he merely states, without reference to specific data, that the moment of the azide group proper is 1.4 D to 1.6 D, as compared with the calculated value of 1.4 D. (Actually, in footnote 19 of his second paper,[1] Samuel refers to a paper[3] in which Sidgwick states that the moment of the azide group proper is "*ca.* 0.") And finally, Samuel gives 6.4 D and 1.4 D as the calculated moments of the α- and β-*N*-methyl-*p*-nitrobenzophenone oximes, respectively, as compared with the observed values of 6.6 D and 1.2 D, respectively. However, the correct calculated values,* obtained

[2] E. P. Linton, J. Am. Chem. Soc. **62**, 1945 (1940).
[3] N. V. Sidgwick, Chem. Rev. **19**, 183 (1936).
* According to a statement received from Dr. Samuel, the value of 132° given for the N—C—C bond angle in his diagram on page 387 is a misprint for 122°. Similarly, the value of 0.8 D for the moment of the bond between the nitro N and the phenyl C in the same diagram appears to be a misprint for 1.0 D. These corrected values are used in the calculations referred to above.

with the use of his bond-moments and bond-angles, are instead 6.0 D and 1.7 D, respectively.

Let us now return to Samuel's list of bond-moments. If we consider that all the moments which do not involve the "pentacovalent nitrogen atom," N^{v}, are correct, we are left with altogether six independent parameters, namely, the moments of the $N^{v}{=}O$, $N^{v}{-}O$, $N^{v}{\equiv}N^{III}$, $N^{v}{=}N^{III}$, $N^{v}{=}C$, and $N^{v}{-}C$ bonds. Consequently, Samuel should be able to calculate with no error the moments of six independent types of molecule, regardless of whether the bond-moments are even approximately constant or not. Actually, Samuel considers altogether nine types of molecule, namely, nitro compounds, methyl nitrate, nitrous oxide, azides, aliphatic diazo compounds, azoxybenzenes, iso-azoxybenzenes, and α- and β-N-methyl oximes; and he ignores a tenth type, namely trimethylamine oxide. It may be questioned whether the azoxybenzenes and the iso-azoxybenzenes are really independent of each other, since, being stereoisomers, they contain exactly the same kinds of bond and differ only in bond-angles. Similarly, and for the same reason, it may be questioned also whether the α- and the β-N-methyl oximes are independent. In any event, however, Samuel's method of calculation can be applied, at the very most, to only ten different types of molecule containing "pentacovalent nitrogen." Of the ten corresponding calculations, those for phenyl azide and for trimethylamine oxide are in error by 0.75 D and 1.3 D, respectively, as we have seen, and those for azoxybenzene and for α- and β-*N*-methyl-*p*-nitrobenzophenone oxime are, at best, not very good. It is evident, therefore, that Samuel's calculations are not sufficient to establish that the bond-moments which he has derived are more than very roughly constant from molecule to molecule. It is even more evident that these calculations provide no support for Samuel's belief that the bonds in question involve pentacovalent nitrogen.

Before leaving the present discussion, let us consider the modern interpretation of the above substances. Samuel's $N^{v}{=}O$ bond, for example, occurs in the nitro compounds, nitrous oxide, the azoxybenzenes, the N-methyl oximes, methyl nitrate, and trimethylamine oxide. For these molecules, Samuel writes the classical structures

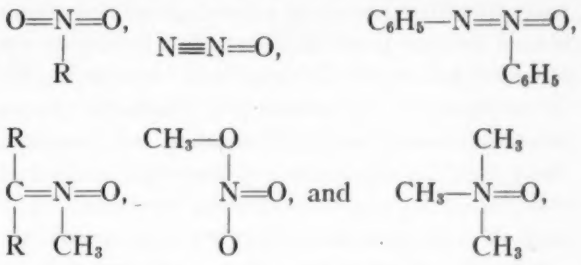

respectively. On the other hand, from the modern point of view, the structures must be written instead as

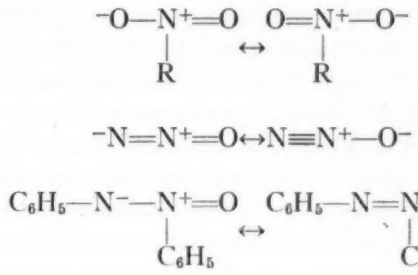

respectively.* The double-headed arrows here, as usual indicate that resonance occurs between the structures stated. In all of the first four molecules,

* Here, and throughout the remainder of the present paper, a semipolar double bond between two atoms A and B is represented as $A^{+}{-}B^{-}$, and not as A⇌B. The former mode of representation, which appears now to be quite generally adopted in this country, has the double advantage of being unambiguous and of suggesting correctly that the semipolar bond $A^{+}{-}B^{-}$ is an ordinary single covalent bond A—B plus an ionic bond $A^{+}B^{-}$; on the other hand, the latter mode of representation, which is employed by Samuel, could be confusing since it suggests erroneously that the bond A⇌B is a single bond A—B plus a singlet linkage A→B.

in which the resonance is between just two structures, the nitrogen-oxygen bond under discussion is seen to be of more or less similar, but of course not identical, type. Consequently, we can hardly be surprised if the moment of this bond proves to be sufficiently nearly constant to make possible the rather limited success of Samuel's method of calculation, since, as has already been seen, fairly large deviations from constancy would apparently not be inconsistent with the experimental data. In methyl nitrate and trimethylamine oxide, however, the situation is different, and the "N^{V}=O bonds" are not very closely analogous to those in the other molecules, since, in the former substance, the resonance includes *three* structures* and, in the latter, no resonance is presumed to occur at all. Consequently, the modern viewpoint might lead us to expect that here, if anywhere, relatively serious discrepancies between calculated and observed dipole moments would be found. With methyl nitrate, this expectation can be neither verified nor shown to be incorrect, since this substance is the only one considered by Samuel to contain the N^{V}—O *single* bond; consequently, perfect agreement between the calculated and observed moments can be obtained by suitable adjustment of this N^{V}—O bond-moment, no matter what values are assigned to the remaining bond-moments. With trimethylamine oxide, on the other hand, the expected discrepancy does indeed occur, as has already been noted.

In the present connection, mention may be made of the fact that the relative contributions of resonating structures are not as sensitive to the differences between their energies as is often supposed by people who are unfamiliar with the subject. In particular, no analogy exists with the way in which the position of equilibrium in a *tautomeric system* depends upon the difference in free energy between the isomers. For example, calculation shows that, if a molecule resonates between two structures that differ in energy by even as much as 100 kcal. per mole or more, there is no reason why the less stable structure might not make, say, half as great a contribution as does the more stable one. This is because the relative contributions of the structures are determined not only by the difference between their energies but also by the magnitude of their interaction integral (i.e., of the non-diagonal matrix element of the energy). In striking contrast, however, a similar difference of 100 kcal. per mole between the free energies of two tautomers would necessarily correspond to an equilibrium constant of about 10^{72}, so that at equilibrium the less stable form could be said not to be present at all. In his fourth paper,[1] in which he criticizes the modern interpretation of the moments of the above-mentioned substances, Samuel seems to overestimate both the importance of the variations in the relative contributions of the resonating structures, and also the success of his method of calculation.

* Actually, methyl nitrate may not be so different from the preceding substances after all, since the second of its above structures is doubtless relatively unstable on account of the unfavorable charge distribution. This fact does not affect the following discussion, however.

B

In this section we shall, like Samuel, consider whether the fundamental quantum-mechanical theory of valence permits a decision to be made between the classical and the modern structures. We shall find it necessary first, however, to examine rather carefully the exact meanings of the terms and symbols used.

Let us begin by considering what quantum-mechanical meaning is to be attributed to the statement that trimethylamine oxide, for example, has the classical structure I and not the modern one II (or *vice versa*). Obviously, it is not imagined that with a sufficiently powerful "γ-ray

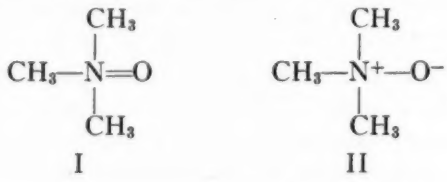

I II

microscope" one would actually be able to see the bonds, either as straight lines or as pairs of dots in the electronic representation. Neither, obviously, is it imagined that the distinction could be made on the basis of the chemical properties of the substance; actually, these would be even less useful for this purpose than the physical properties considered in section *A*. The view, which is probably shared by the majority of the people who have given recent critical thought to

the question, seems to be approximately the one developed in the remainder of this section.

The eigenfunction of a molecule, which defines the distribution of charge within it, provides the most precise and the most nearly complete description of the molecule permitted by quantum mechanics. Unfortunately, however, this eigenfunction cannot be determined exactly for such a complicated molecule, and, even if some well-disposed deity were kind enough to tell us what it is, the original problem would still be unsolved. The reason for this is that the correct eigenfunction would contain no recognizable feature which could be identified either as a double bond or as a semipolar double bond between the nitrogen and oxygen atoms. It would give the distribution of charge and, as corollaries, the geometry of the molecule, the magnitudes and directions of the restoring forces opposing the displacements of the atoms from their most stable positions, and so on, but it would say nothing about the *types of bond* present.

In order to obtain information about the types of bond, one must leave the rigorous quantum-mechanical procedure and must introduce approximations. Two different approximate methods have been adopted for effecting a correlation between quantum mechanics, on the one hand, and structure in the usual chemical sense, on the other. The first of these is known as the valence-bond, or pair-bond, or Heitler-London-Slater-Pauling (HLSP) method, and the second as the molecular-orbital or Hund-Mulliken (HM) method. In either method, a procedure exists by which an approximate eigenfunction can be set up to correspond to any given structure. If there is adequate reason to believe that an eigenfunction set up in either of these ways is a fair approximation to the correct, but unknown, eigenfunction of a given molecule, then, *by definition*, the molecule is said to have the corresponding structure. On the other hand, if there is reason to believe that a linear combination of two or more such functions should give a materially better approximation to the correct eigenfunction than any one of them alone, then, again by definition, the molecule is said to be a resonance hybrid of the two or more corresponding structures. It should be clear that, since no single approximate function which is set up in accordance with either of the two methods can be exactly correct, *every* molecule is, strictly, a resonance hybrid of a number of structures. In fact, it can be shown that a perfect representation of even the simplest molecule could be obtained only by consideration of resonance among *all the structures that can be imagined*, including an infinite number of them that cannot be represented by any of the conventional chemical symbols. However, it is a fundamental assumption of both the pair-bond and molecular-orbital treatments that any molecule can be described, with a precision that is sufficient for most chemical and spectroscopic purposes, by means of a single structure in the above sense, or, at worst, as a resonance hybrid of a small number of such structures. (In the interests of strict accuracy, the following qualifications should be noted. Some structures correspond to eigenfunctions which are identically equal to zero, as will be mentioned again later; and some turn out to be merely resonance hybrids of two or more other ones. Obviously, structures of the first type may always be ignored; and those of the second type may also be ignored if their various components have already been included in the treatment.)

From what has been said, it follows that the answer to the question whether trimethylamine oxide has the structure I or II, above, depends to a considerable extent upon the way in which structure and approximate eigenfunction are correlated. It is quite possible that two different people, approaching the problem from different angles, might relate a given function to two entirely different structures. As we shall see, this fact seems to be a major reason for the disagreement between Samuel's views and the modern ones, since Samuel essentially proposes a new way of correlating approximate eigenfunction and structure.

Let us now consider for a moment the way in which the pair-bond and molecular-orbital treatments deal with the structure of trimethylamine oxide. By either method, one can set up an approximate eigenfunction for each of the structures I and II, above. The functions for the two structures differ in the important respect that, whereas the ones for structure II make use of only K- and L-shell atomic orbitals, the ones for structure I require that also the M-shell orbitals

of the nitrogen atom be taken into account. Since the orbitals of the M-shell are much less stable than those of the K- and L-shells, the modern view is that structure I should be considerably less stable than II. Consequently, it is supposed that, although the resonance must to some extent, of course, include *both* structures, in addition to many others, nevertheless structure II gives much the best description of the molecule that any *single* structure can give.

In this connection, it will be instructive to consider the reason why the structure I, from either the pair-bond or molecular-orbital point of view, requires use of the M-shell orbitals on the nitrogen atom. By following the formal rules for setting up approximate eigenfunctions to represent specified structures, one can indeed write down an expression to represent I, in which only K- and L-shell orbitals are used. However, this expression, after it has been made antisymmetric as required by the Pauli exclusion principle, is expressible as a sum of terms, of which a number are identically equal to zero. If these vanishing terms are omitted from further consideration, the function which remains proves to be one corresponding to some modern structure, or to resonance among several modern structures, without any pentacovalent nitrogen atom. (Cf. the discussion, below, of the configurations of the excited nitric oxide and nitrogen molecules.) It is evident, therefore, that, with the restriction that only K- and L-shell orbitals be used, and within the limitations imposed by the definitions inherent in the pair-bond and molecular-orbital methods, the octet rule is not an added arbitrary assumption, but is a necessary consequence of quantum mechanics and of the exclusion principle. It cannot be violated even if the attempt is made to do so.*

Samuel, however, considers that structure I, with pentacovalent nitrogen, can be obtained even without use of the M-shell orbitals, and he shows how a non-vanishing approximate eigenfunction can be set up to represent that structure. We shall consider, first, the relation between his function and the ones which would be set up on the basis of the pair-bond and molecular orbital methods to represent the modern structure II; and, second, the significance of the statement that his function actually does represent the structure I.

Samuel explains, but does not write down explicitly, the configuration of an excited molecule of nitric oxide, which contains three unpaired electrons and so may be considered to be trivalent and capable of forming three covalent bonds to, for example, the three methyl carbon atoms in trimethylamine oxide. From his discussion,[4] and also from analogy with his configuration of an excited, divalent nitrogen molecule,[5] it is evident that the configuration under discussion can be expressed in his symbols as

$$\sigma^2(2s),\ \sigma^*(2s),\ \pi^4(2p),\ \sigma^2(2p),\ \pi^{*2}(2p),$$

where reference to the K-shell electrons is omitted as not being necessary for our purposes. (Actually, it makes no difference exactly what configuration is assumed here, since essentially the same discussion as the following could be based upon *any* reasonable configuration.) The three unpaired electrons include the one occupying the $\sigma^*(2s)$ orbital and the two occupying the two different $\pi^*(2p)$ orbitals. Since these electrons are to be used to form bonds to the *nitrogen* atom, the orbitals which they occupy must be, respectively, essentially $2s$ and $2p\pi$ atomic orbitals localized about the *nitrogen* atom; otherwise, the resulting bonds would involve the oxygen as well as the nitrogen or, in other words, would be resonance hybrids of nitrogen-carbon and oxygen-carbon bonds. Consequently, since Samuel restricts the consideration to the atomic orbitals of the K- and L-shells, we may replace the symbols $\sigma^*(2s)$ and $\pi^*(2p)$ by $2s_N$ and $2p\pi_N$, respectively. Moreover, it can be shown by application of the Pauli exclusion principle that the localization of the orbitals $\sigma^*(2s)$ and $\pi^*(2p)$ about the *nitrogen* atom requires the simultaneous localization of the further orbitals $\sigma(2s)$ and $\pi(2p)$ about the *oxygen*

* With phosphorus, sulfur, and any of the other atoms of the second row of the periodic table, the pair-bond and molecular-orbital treatments permit violations of the octet rule without the use of the orbitals of an outer valence shell. This is because, for these atoms, the valence shell, being the M-shell, contains $3d$, as well as $3s$ and $3p$, orbitals. Even though the $3d$ orbitals are relatively unstable, it is, in fact, decidedly questionable whether the octet rule is rigorously valid, even from the modern point of view, with such atoms. The situation is similar with the still heavier atoms of the third and subsequent rows.

[4] Page 385 of reference 1.
[5] Page 184 of reference 1.

atom.* These last orbitals can therefore be represented as $2s_O$ and $2p\pi_O$, respectively. Consequently, the above configuration assumes the form

$$2s_O^2,\ 2s_N,\ 2p\pi_O^4,\ \sigma^2(2p),\ 2p\pi_N^2,$$

in which only the orbital $\sigma(2p)$ is still a molecular one.

Now, Samuel considers that his configuration of the excited nitric oxide molecule corresponds to the structure III, so that, when bonds to three methyl groups are formed, the structure of the resulting amine oxide is indeed the classical one, I. However, inspection of the configuration in the

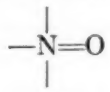

III

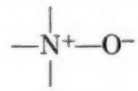

IV

second of its two above forms shows that it is exactly the configuration which would be set up, by a familiar method embodying some features of both the pair-bond and molecular-orbital treatments, to represent structure IV. On this basis, then, the resulting structure of the amine oxide is the modern one II. Consequently, it follows that, when Samuel shows how an eigenfunction can be set up to represent the classical structure I, he is not really contradicting the modern ideas of valence, nor is he adding anything essentially new to them; he is instead re-expressing the same ideas in different language and with a different symbol.

With nitrous oxide, and in general with the other molecules which, from the modern point of view, receive important contributions from two resonating structures, the situation is somewhat more complicated. In his third paper,[1] Samuel describes nitrous oxide as being formed from NO+N, that is, from the excited trivalent nitric oxide molecule discussed above, plus a normal nitrogen atom with its three unpaired electrons. If the nitric oxide is assigned Samuel's structure III, then the resulting nitrous oxide must be represented by the classical structure V. On the other hand, if the nitric oxide is assigned the structure IV instead, then the resulting nitrous oxide must be represented by the modern structure VI. This last structure is, of course,

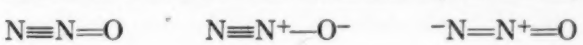

V VI VII

only one of the two structures between which the modern theory presumes resonance to occur. The second modern structure VII arises automatically, however, in the following way. In his second paper,[1] Samuel describes nitrous oxide as being formed from N_2+O, that is, from an excited, divalent nitrogen molecule plus a normal oxygen atom with its two unpaired electrons. Since Samuel considers the excited nitrogen molecule to have the structure VIII, he is of course again led to the same classical structure V as before for the nitrous oxide. However, this structure does not have the same meaning in terms of eigenfunctions as it did before. If Samuel's configuration of the

VIII IX

excited nitrogen molecule is examined in the manner employed above for that of the excited nitric oxide, it is found to correspond, from the modern point of view, to the structure IX, rather than VIII. Consequently, the resulting nitrous oxide must then be represented by the second modern structure VII. It is seen, therefore, that Samuel's method of setting up an eigenfunction for the classical structure V can lead to either one of two quite different functions, depending upon whether the molecule is regarded as formed from NO+N or from N_2+O. Moreover, these two different functions are just the ones which would have been set up to describe the two resonating modern structures VI and VII.

We come now to consider the sense in which Samuel's eigenfunction of excited nitric oxide, for example, can be said to correspond to structure III (as maintained by Samuel) rather than IV (as would follow from the modern theory). The point is that Samuel proposes a different way of correlating eigenfunction and structure. In particular, he denies the existence of antibonding orbitals (cf. section *C*, below) and maintains instead that any orbital is bonding to a greater or

* The proof of this statement, which is too long to be given here in detail, is based upon the fact that all the different molecular orbitals in the molecule must be mutually orthogonal; if they are *not* all orthogonal, the resulting antisymmetric eigenfunction for the molecule as a whole can be broken up into a sum of terms, of which one does involve only mutually orthogonal orbitals, and all the others are identically equal to zero.

less degree if it is occupied by a pair of electrons contributed by *different* atoms. In this way, although he apparently retains most of the essential features of the modern viewpoint, he uses a different procedure for counting the number of bonds, and so he arrives at different conclusions in regard to structure.

I shall not discuss in detail whether Samuel's position in this respect is, or is not, a tenable one, but I should like to point out that, in practice, it is not always unambiguous. For example, there are two equivalent ways of regarding a system which consists of two helium atoms. From the pair-bond point of view, we would assign two electrons to each atom; since each electron is therefore localized about a single atom, and no electrons are shared, Samuel's definition leads to the result that *no* bond exists. On the other hand, from the molecular-orbital point of view, we would assign two electrons to the lower (symmetric) molecular orbital and two to the higher (antisymmetric) molecular orbital; since each orbital contains electrons contributed by different atoms, each is bonding, according to Samuel, and so a *double* bond exists. The present discrepancy is not due to any inconsistency between the pair-bond and molecular-orbital treatments, because the two corresponding eigenfunctions prove to be *identical*. Consequently, if Samuel's definitions are adopted, the eigenfunction in question can be said to correspond to either zero or two bonds, depending entirely upon our mental attitude toward it. On the other hand, if we recognize that only the lower molecular orbital is bonding, whereas the higher is antibonding, then the discrepancy vanishes, since no bond exists from either point of view.

Let us now consider Samuel's configuration of the excited nitric oxide molecule. As we saw above, it can be written in the form

$$2s_O^2,\ 2s_N,\ 2p\pi_O^4,\ \sigma^2(2p),\ 2p\pi_N^2.$$

Of all the orbitals involved, only the one designated as $\sigma(2p)$ contains electrons contributed by different atoms. Consequently, *even when Samuel's own method of counting is used*, there is only a single bond between the nitrogen and oxygen atoms, and so the structure of the excited nitric oxide molecule is really IV, rather than III as assumed by Samuel. It follows therefore that no way has as yet been defined for setting up an approximate eigenfunction to represent a structure like III, and hence of a classical one like I or V, without the use of M-shell atomic orbitals.

In concluding this section, I should like to call attention to the fact that Samuel's arguments against the modern structures, which are based upon dipole moments, ionization potentials, and so on are irrelevant. No such experimental data can distinguish between two structures, one classical and one modern, which are merely two different ways of describing graphically the same eigenfunction. In particular, it may be noted that Samuel's eigenfunctions for the classical structures do not involve the configuration sp^4 of the neutral nitrogen atom as he states, but that instead, just like those for the modern structures, they involve the configuration sp^3 of the positive ion.

C

As was mentioned in section B, Samuel denies the existence of antibonding orbitals. To support this view, he brings forth spectroscopic evidence to show that a premoted[6] orbital is sometimes actually more strongly bonding than an unpremoted one. This argument is based upon the supposition that, in the molecular orbital theory of Mulliken *et al.*, all premoted orbitals are considered to be antibonding and all unpremoted orbitals to be bonding. As far as I know, however, no such view is held by any worker in the field at the present time.[7] The distinction between antibonding and bonding orbitals is based rather upon the presence or absence of nodes in the region between the two nuclei involved.[8] For example, let a and b be two atomic orbitals on different atoms, and let their signs be determined so that each is positive in the region where they overlap most strongly. Then, of the two molecular orbitals, ψ and ϕ, that are approximately representable as $a+b$ and $a-b$, respectively, the former has one less node between the nuclei than the latter. It is considered, then, that ψ is

[6] R. S. Mulliken, Phys. Rev. **41**, 49 (1932).

[7] See, for example, G. Herzberg, *Molecular Spectra and Molecular Structure* (Prentice-Hall, Inc., New York, 1939), page 398.

[8] F. Hund, Zeits. f. Physik **73**, 1 (1931); R. S. Mulliken, J. Chem. Phys. **1**, 492 (1933).

ordinarily bonding whereas ϕ is ordinarily antibonding.

The reasoning which leads to this supposition is as follows. An electron in the orbital ψ spends a larger part of its time in the region between the two nuclei than would one in either of the atomic orbitals a and b, whereas an electron in the orbital ϕ spends a smaller part of *its* time there. Consequently, the average force of electrostatic attraction between the electron and the *two* nuclei, which is the only force capable of leading to the formation of a bond, must be greater in ψ, but smaller in ϕ, than that in either a or b. In other words, an electron in ψ makes the approach of the two nuclei easier, but one in ϕ makes it more difficult, so that ψ is bonding whereas ϕ is antibonding.

The foregoing argument indicates that the existence of both bonding and antibonding orbitals is a necessary consequence of the respective distributions of electric charge. It also is of interest in connection with Samuel's further contention that the molecular-orbital treatment contains no theory of valence at all inasmuch as (according to Samuel) it ignores the factor responsible for the bonding forces, namely, the exchange degeneracy of a pair of electrons. It may be noted also that, even in the pair-bond treatment, in which the exchange degeneracy is considered, and which Samuel therefore regards as the only actual theory of valence, the distribution of charge is still the decisive factor. In a system consisting of two helium atoms, for example, exchange degeneracy still exists, but there is no bond-formation because the charge-distribution is such that the atoms actually repel each other strongly—more strongly, in fact, than if there were no exchange degeneracy. It appears, therefore, that the exchange degeneracy is important in the theory of valence only insofar as it affects the distribution of charge. If, as in the molecular-orbital treatment, a charge-distribution leading to attraction between the atoms can be arrived at without explicit consideration of the exchange degeneracy, the treatment loses none of its theoretical significance merely because it ignores this (for its purposes) irrelevant exchange degeneracy.

D

In this concluding section, I wish to mention two rather less fundamental matters which, however, underly much of Samuel's discussion of dipole moments.

The first of these questions is concerned with Samuel's calculation of the percent ionic characters of essentially covalent bonds[9] between dissimilar atoms. He treats hydrogen chloride, for example, in the following manner. The dipole moment of this molecule can be considered due to a displacement of the two electrons that produce the bond between the hydrogen and chlorine atoms. From the molecular orbital point of view, these electrons are in the same orbital, and so they must be displaced together. Now, the displacement of two electrons by the internuclear distance of 1.28A, as in Samuel's calculation, leads to a moment of $2\times4.8\times10^{-10}$ e.s.u.$\times1.28\times10^{-8}$ cm $=12.2$ D. Since the observed moment is only 1.03 D,* the percent ionic character is therefore $(1.03/12.2)\times100=8.5$ percent.

Let us consider the significance of this method of calculation employed by Samuel. The structure I may be written to represent an imaginary state of the hydrogen chloride molecule, in which the bond is a pure covalent one with zero dipole moment. The average position of the two valence electrons is therefore halfway between those of the nuclei, and so 0.64A from either. Structure

$H—Cl$	H^+Cl^-	H^-Cl^+
I	II	III

II, on the other hand, may be written to represent an equally imaginary state of the molecule, in which the bond is a pure ionic one, with a moment of 4.8×10^{-10} e.s.u.$\times1.28\times10^{-8}$ cm $=6.1$ D. Similarly, structure III may represent a second pure ionic structure, with a moment of 6.1 D in a direction opposite to that of structure II. Now, the displacement of *two* electrons by the *whole* distance, giving rise to a moment of 12.2 D, would lead to the structure II only if one starts with III, and not if one starts with I. In order to go from II to I, one must instead displace the pair of electrons by only *half* the internuclear

[9] Pages 182 and 183 of reference 1.

* Actually, Samuel uses an incorrect value of 1.28 D for this moment, so that he ends up with about 10 percent ionic character, instead of 8.5 percent.

distance, that is, by 0.64A. The resulting moment is then, of course, again only 6.1 D, instead of 12.2 D. Samuel's method of calculation makes it appear as if he is under the obviously erroneous impression that III, rather than I, represents the pure covalent bond with zero dipole moment.

The only way in which Samuel's calculation can be given a self-consistent interpretation seems to be the following. If the three structures I, II, and III make contributions of X percent, Y percent, and Z percent, respectively, to the dipole moment, and if W is the mean of Y and Z, then $Y=W+8.5$ and $Z=W-8.5$. The figure 8.5 is then taken as the percent ionic character. It would seem both simpler and more logical to follow Pauling,[10] and to consider, as an extremely rough first approximation, that resonance with III may be ignored (i.e., that $Z=0$), and that, furthermore, the percent ionic character is given simply by Y, which is then equal to $8.5+8.5=17.0$. It should be apparent that this same value of 17 percent ionic character is obtained, whether one employs the molecular-orbital treatment, as Samuel does, and considers the displacement of both electrons by only half the internuclear distance, or employs the valence-bond treatment, as Pauling does, and considers the displacement of only one electron by the whole distance. It follows, therefore, that the discrepancy between Samuel's and Pauling's values, which Samuel considers a very important one resulting from a fundamental difference between the molecular-orbital and pair-bond treatments, is due merely to a difference in definition. Samuel's percent ionic character is *defined* in such a way that it is always exactly half as great as Pauling's.

The second point to be discussed here is concerned with the fact that the moment of the $N^{III}=O$ bond, which is very nearly equal to zero in nitric oxide, is equal instead to about 2.0 D in a nitroso compound. Samuel's explanation[11] of the variation is that the nitrogen atom has a single unpaired electron in nitric oxide, which it shares with a carbon atom, and which it therefore loses control of to some extent, in the nitroso compound. Consequently, a positive charge is produced on the nitrogen, and a dipole moment results. This explanation, which is used without essential change with several further types of molecule, ignores the following facts. First, the nitrogen atom, when it *loses to* the carbon atom a share of the electron which it formerly possessed, also *gains from* the carbon atom a share of an electron which the latter formerly possessed. If the sharing of these two electrons is equal, no dipole is produced. Second, any moment arising in the above manner would belong to the carbon-nitrogen, and not to the nitrogen-oxygen, bond. And finally, if, as a result of an inequality in sharing, the nitrogen atom does gain a positive charge, the resulting moment would be in the wrong direction; Samuel fails to realize this fact because he attributes the moment to the wrong bond.

ACKNOWLEDGMENT

I wish to express my appreciation to Professors R. S. Mulliken and T. F. Young for the benefit of helpful discussions and of advice in the preparation of this paper.

[10] L. Pauling, *The Nature of the Chemical Bond* (Cornell University Press, Ithaca, New York, 1939), first edition, p. 46.

[11] Page 190 of reference 1.

Letters to the Editor

THIS section will accept reports of new work, provided these are terse and contain few figures, and especially few halftone cuts. The Editorial Board will not hold itself responsible for opinions expressed by the correspondents. Contributions to this section should not exceed 600 words in length and must reach the office of the Managing Editor not later than the 15th of the month preceding that of the issue in which the letter is to appear. No proof will be sent to the authors. The usual publication charge ($3.00 per page) will not be made and no reprints will be furnished free.

On the Possibility of Estimating the Average Surface Area of Solid Particles

Hans M. Cassel
General Ceramics and Steatite Corporation, Keasbey, New Jersey
April 14, 1945

IT would be easy to derive the average surface area of crystalline powders from the thermal effects caused by submersion into a suitable liquid if the heat of emersion per unit area were known. Since this is not the case it appears as a very ingenious idea to coat the crystalline particles with the adsorbed film of a liquid whose surface energy can be independently determined.

No objection shall here be raised against the principle of this method, but, unfortunately, the experimental procedure described by Harkins and Jura[1] implies a source of error which invalidates the reported results.

With the objective of surface conditioning single crystallites, the contiguous mass of the powder is exposed to the saturated vapor of a liquid and the entire system (presumably) allowed to attain thermal equilibrium. The powder treated in this way is then plunged into a body of the same liquid and the thermal effect observed.

In evaluating the measurements, it is assumed that the contact angle at the liquid-crystal-vapor boundary is zero. However, the point has been overlooked that under this very condition capillary condensation between the contracting crystals is inevitable. Consequently, in a thus treated powder, groups of particles may stick together, held by the capillary forces of the liquid. However, even the immediate cohesion of adjacent crystals may cause inseparable clusters to form.

Effects of this kind have been repeatedly investigated. Tomlinson[2] measured the adhesion between quartz filaments and concluded that the magnitude of the forces appears altogether too large for an explanation depending on the surface tension of a liquid film. Stone[3] found that glass beads would not adhere unless the humidity is close to saturation, but once sticking together cannot be separated by passing dry air to remove the moisture. In the work of Bloomquist and Shutt[4] it has been shown that microscopic glass spheres suspended in organic liquids are flocculated on increasing the amount of dissolved water. The coalescence is correlated to the magnitude of the interfacial tension at the organic liquid-water film boundary. Bradley[5] demonstrated a striking increase in the surface tension of concentrated suspensions caused by the mutual attraction of neighboring solid particles.

Taking all this into consideration, in the described procedure an indefinite reduction of the immersed film area has to be expected.

On the other hand, if capillary condensation is not accomplished the assumption of perfect wettability cannot be true. In that case, the heat of emersion per unit area would be smaller than anticipated and, again, the surface area would be underestimated.

Of course, such troubles would be avoided if it were possible to measure the thermal effects of particles individually coated and individually dropped into a liquid.

[1] William D. Harkins and George Jura, J. Am. Chem. Soc. **66**, 1362 (1944).
[2] G. A. Tomlinson, Phil. Mag. **6**, 695 (1928).
[3] William Stone, Phil. Mag. **9**, 610 (1930).
[4] C. R. Bloomquist and R. S. Shutt, Ind. Eng. Chem. **32**, 827 (1940).
[5] S. R. Bradley, J. Phys. Chem. **43**, 663 (1939).

Ion-Migration Phenomena Observed with the Electron Microscope

Helmut Thielsch
University of Michigan, Ann Arbor, Michigan
April 30, 1945

A DROPLET of water containing dissolved KCl (5 g per liter) was placed on a collodion film and then included into a vacuum system which was pumped down to 10^{-3} mm Hg within 30 seconds. Viewing the result in the electron microscope three rather curious types of structures are apparent, a regular cubic crystal structure (Fig. 1), a regular linear dendritic system (Fig. 1), and an irregular branch structure (Fig. 2). Obviously, the differences are due to the rate of nucleus formation and growth, depending, of course, upon the variation of local ion concentration within the droplet of water during the process of evaporation.

The first mentioned type of crystal (the cubes shown in Fig. 1) results from a relatively slow rate of growth; the second linear type will be produced by a somewhat faster rate (its closeness to the more stable cubic crystals signi-

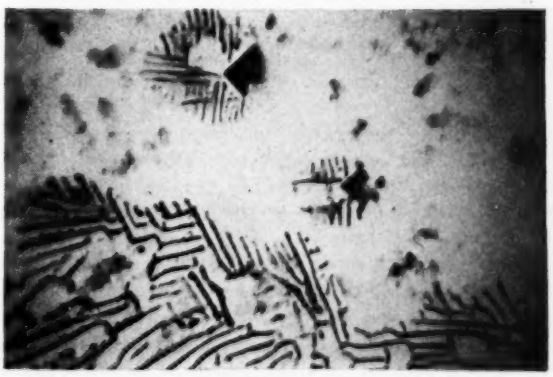

Fig. 1.

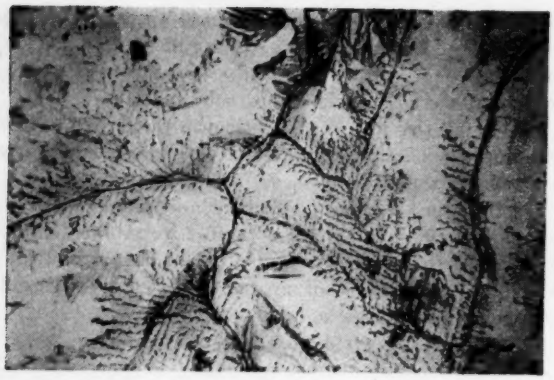

FIG. 2.

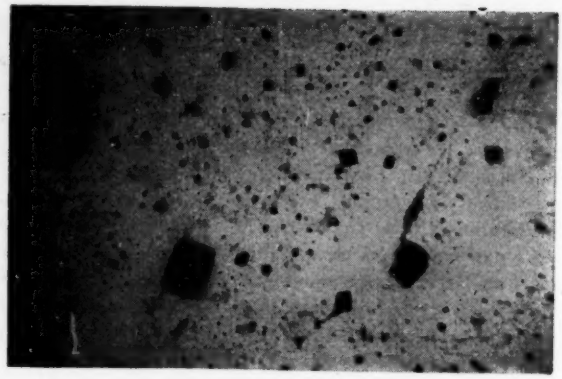

FIG. 5.

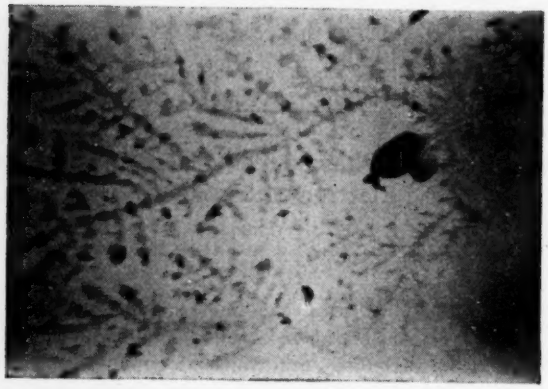

FIG. 3.

FIG. 6.

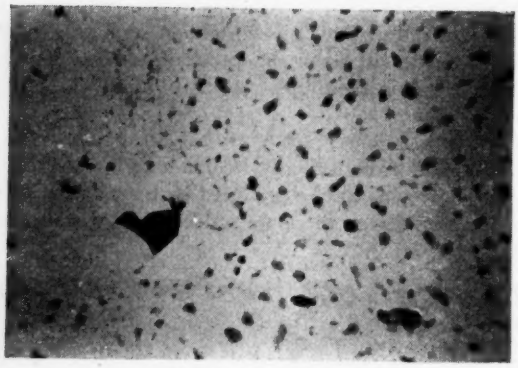

FIG. 4.

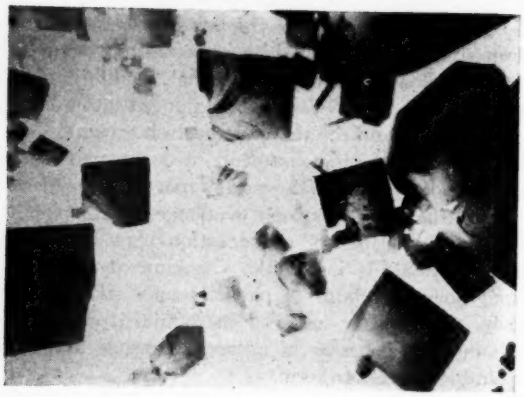

FIG. 7

fies that), and the irregular dendritic branch structure requires a still faster rate.

The two dendritic structures are unstable in atmospheric conditions, since upon standing for 6 hours in the atmosphere (Figs. 3 and 4), or merely breathing upon the sample (Figs. 5 and 6) will cause migration. In the last two figures outlines of the previous structure are still visible.

Whether or not the streaks or schlieren which appear in regularly grown crystals (Fig. 7) are identical with the linear dendrites observed or are due to electric surface charges,* further investigations will have to bring out.

A detailed discussion of this will follow in the near future.

* H. Seemann, "Die wandernden Schlieren in elektronenoptischen Bildern von Einkristallen, insbesondere Molybdanoxyd," Naturwiss. **31**, 415–416 (1943).

The Effect of Temperature on Molecular Parachors*

THOMAS S. GARDNER
Tennessee Eastman Corporation, Kingsport, Tennessee
April 26, 1945

THE effect of temperature on molecular parachors was not included in Professor Samuel's discussion. The temperature effect is of sufficient magnitude to invalidate the use of molecular parachors for structural determinations for many organic compounds.[1]

In order to use molecular parachor constants for structural work, it would be necessary to standardize all data on a constant temperature basis. It was found[1] in the case of the organic compounds investigated that nearly all of them exhibited an increase in molecular parachor with temperature. This was interpreted as being due to dissociation with increasing temperature. In the case of ortho, meta, and para isomers of compounds able to form chelated rings in the ortho form, the meta and para isomers gave the familiar effect of increasing parachor with increasing temperature, while the ortho isomer yielded almost constant molecular parachors.

We are in substantial agreement with Professor Samuel on the impossibility of assigning a parachor value to the coordinate covalent double bond.

The difficulty of determining parachor values for structural work is illustrated in Table I by the comparison of a few values obtained by both investigators.

TABLE I

	Samuel's Values (P) Calculated[b]	Samuel's Values (P) Observed	Buehler, Gardner, et al[a] (P) Calculated[c]	Buehler, Gardner, et al[a] Observed T(corr.)	Buehler, Gardner, et al[a] Observed (P)
Sulfuryl Chloride	195.3		196.8	30.0	196.2
				40.0	196.7
				50.1	198.6
Ethyl Sulfite	297.1	299.7	298.4	40.0	297.3
				70.3	299.7
				100.9	301.2
				130.4	301.5
Diphenyl Sulfone	466.9	465.7	468.2[d]	150.4	473.9[e]
				174.8	473.1
				191.6	473.8
Ethyl Nitrate	190.1	189.6	190.8[d]	30.0	189.6
				40.0	189.5
				50.1	190.6
				60.2	190.8
p-Toluene Sulfonyl Chloride	370.0	367.8	371.5[d]	100.9	371.0
				130.4	372.0
				150.4	373.2
				174.8	375.5

[a] See reference 1.
[b] Calculated by Samuel using parachor values for different valences.
[c] Calculated using Sugden's values for the parachor constants except that Sugden's value of −1.6 for the coordinate bond has not been included.
[d] Samuel's calculated Sugden values allowed Sugden's value for the coordinate bond.
[e] Results for diphenyl sulfone were unpublished[a] because of the unexplainable, high anomaly. The analysis of the material was: melting point (literature) 128–129°C; found 127.5–127.9°C. Percent S: calculated 14.70; found 14.90 and 14.94. The constancy of the parachor values for different temperatures is interesting. Unpublished data used in determining the observed parachors are as follows:

T(corr.)	D	γ
150.4	1.1434	38.08
174.8	1.1256	35.54
191.6	1.1139	34.27

It is evident that Professor Samuel's uses of parachor values for different valence states cannot compensate for the temperature effects of the parachors of associated organic compounds.

* An addendum to Professor R. Samuel's discussion (J. Chem. Phys. 12, 167 (1944)).
[1] C. A. Buehler, T. S. Gardner, and M. L. Clemens, J. Org. Chem. 2, 167 (1937).

Comments on "The Effect of Temperature on Molecular Parachors"*

R. SAMUEL
154 Nassau Street, New York, New York
May 10, 1945

THE parachor is indeed not entirely independent of temperature. Other molecular constants which are less sensitive to geometrical factors behave, however, in a similar manner, and this effect therefore cannot be ascribed entirely to association. For instance, the increased population of higher vibrational levels will probably be found among its causes. The various modes of vibration will be differently affected according to their different energies, which may result in a deformation of the molecule and may influence the intermolecular potentials.

However, for reasons which are discussed in a forthcoming publication, no rigorous additivity can exist for any of the so-called additive molecular constants, and an additivity in first-approximation is all what can be expected. Dr. Gardner's figures show that with decreasing temperature the parachors indeed converge towards those values for which this first-order additivity has been established. It is very interesting to see that such values are already obtained at temperatures midway between melting and boiling points.

The atomic parachors of course have been calculated for such values only, and these are, therefore, the only ones which can be used for structural work.

* Preceding letter by Thomas S. Gardner.

Remark to Dr. Wheland's Article

R. SAMUEL
154 Nassau Street, New York, New York
May 19, 1945

THE article of Dr. Wheland appearing in this issue of this journal cannot be answered without detailed considerations of experimental evidence, the meaning of additivity, and so forth. As such a detailed answer could not be prepared in time for this issue for outside reasons, it will be found in a forthcoming paper.

In this moment attention should be drawn only to the main point, namely, Dr. Wheland's theoretical argument. The wave function he uses is that of a diatomic and not that of a polyatomic molecule with its increased number of orbitals. It has no bearing on the problem of pentacovalent nitrogen.